

# University of Florida Swamp Launch Rocket Team: Project “See Ya’ Later, Alligator!”

Team 120 Project Technical Report to the 2023 Spaceport America Cup

Megan M. Wnek<sup>1</sup> and Dustin T. Faulkenberry<sup>2</sup>  
*University of Florida, Gainesville, FL, 32611, United States*

Nurettin K. Aslan<sup>3</sup> and Colton T. Shepard<sup>4</sup>  
*University of Florida, Gainesville, FL, 32611, United States*

Elizavetta A. Stetsenko<sup>5</sup> and Jason M. Rosenblum<sup>6</sup>  
*University of Florida, Gainesville, FL, 32611, United States*

Joseph A. Pinkston Jr.<sup>7</sup> and Maya R. Greene<sup>8</sup>  
*University of Florida, Gainesville, FL, 32611, United States*

“See Ya’ Later, Alligator!” is the University of Florida Swamp Launch Rocket Team’s project for competition in the 10,000 ft COTS category in the 2023 Spaceport America Cup: Intercollegiate Rocket Engineering Competition. The rocket’s mission is to carry a 9.2 lb payload to an apogee of 10,000 ft and descend safely under a 36 in drogue and a 96 in main parachute. The launch vehicle is constructed from SRAD carbon fiber airframe and utilizes 4 fiberglass fins mounted through the airframe wall and secured using epoxy. The recovery system is a dual-deploy flight computer system using COTS flight computers and a SRAD CO2 ejection system. The payload, “In a While, Crocodile!”, is an autonomous quadcopter made from SRAD carbon fiber and flown by a SRAD control system. The payload’s mission is to autonomously detect the different stages of launch, deploy itself from its retention system, autonomously stabilize, and capture images of the launch vehicle’s landing site. Images of the launch vehicles landing site provide the ground station with the launch vehicle’s status, orientation, and final location. This verification system could be utilized to verify a rover or other payload system has properly landed on another celestial body.

## I. Nomenclature

$A$	= Area
$a$	= speed of sound
$AR$	= Aspect ratio
$c$	= Root chord

---

<sup>1</sup> Project Manager and Chief Engineer, Swamp Launch IREC team, 939 Center Dr, Gainesville, FL 32611

<sup>2</sup> Structural Design Lead, Swamp Launch IREC team, 939 Center Dr, Gainesville, FL 32611

<sup>3</sup> Avionics and Recovery Lead, Swamp Launch IREC team, 939 Center Dr, Gainesville, FL 32611

<sup>4</sup> Flight Dynamics Lead, Swamp Launch IREC team, 939 Center Dr, Gainesville, FL 32611

<sup>5</sup> Payload Electronics Lead, Swamp Launch IREC team, 939 Center Dr, Gainesville, FL 32611

<sup>6</sup> Payload Software Lead, Swamp Launch IREC team, 939 Center Dr, Gainesville, FL 32611

<sup>7</sup> Payload Mechanical Lead, Swamp Launch IREC team, 939 Center Dr, Gainesville, FL 32611

<sup>8</sup> Manufacturing Lead, Swamp Launch IREC team, 939 Center Dr, Gainesville, FL 32611

$C_d$	=	Coefficient of drag
$\delta$	=	Tip deflection of a cantilever beam
$\Delta x$	=	Displacement
$E$	=	Modulus of Elasticity
$F$	=	Force
$g$	=	Gravity
$G$	=	Shear modulus
$I$	=	Moment of inertia
$k$	=	Spring constant
$l$	=	Length
$\lambda$	=	Ratio of tip chord to root chord
$m$	=	Mass
$M_x$	=	Motor command for motor number x
$\rho$	=	Air density
$P$	=	Pressure
$P_{throttle}$	=	Pitch throttle command
$R_{throttle}$	=	Roll throttle command
$T_{throttle}$	=	Thrust throttle command
$R$	=	Gas constant
$t$	=	Fin thickness
$T$	=	Atmospheric temperature
$V$	=	Descent speed
$\Psi$	=	Airframe volume
$Y_{throttle}$	=	Yaw throttle command

## II. Introduction

The University of Florida’s Swamp Launch Rocket Team is a design team within the Department of Mechanical and Aerospace Engineering (MAE) in the Herbert Wertheim College of Engineering. The team includes members from many departments across the College, including the Department of Electrical and Computer Engineering (ECE) and the Department of Computer and Information Science and Engineering (CISE), in order to form a well-rounded engineering environment for participation in the Spaceport America Cup. The team is supported by an academic advisor within MAE, Dr. Sean Niemi, who oversees the team’s project and provides space for the team to work. This year, the team is competing in the 10,000 ft Commercial off the Shelf (COTS) category with a launch vehicle project titled “See Ya’ Later, Alligator!” accompanied by a payload project titled “In a While, Crocodile!”.

The team is funded in part by the UF MAE department as well as external sponsors. The MAE department provides the team with monetary support as well as additional travel scholarships. In addition to this, the department provides the team with two facilities out of which the team can operate and manufacture: The Mechanical Design Laboratory and the Student Design Center. The team is also funded by four external sponsors: Blue Origin, Aerojet Rocketdyne, Autodesk, and Hands-On Gainesville, who all provide the team monetary support.

The team is structured into four sections: Managerial, Vehicle Design, Payload Design, and Manufacturing Support (Fig. 1).

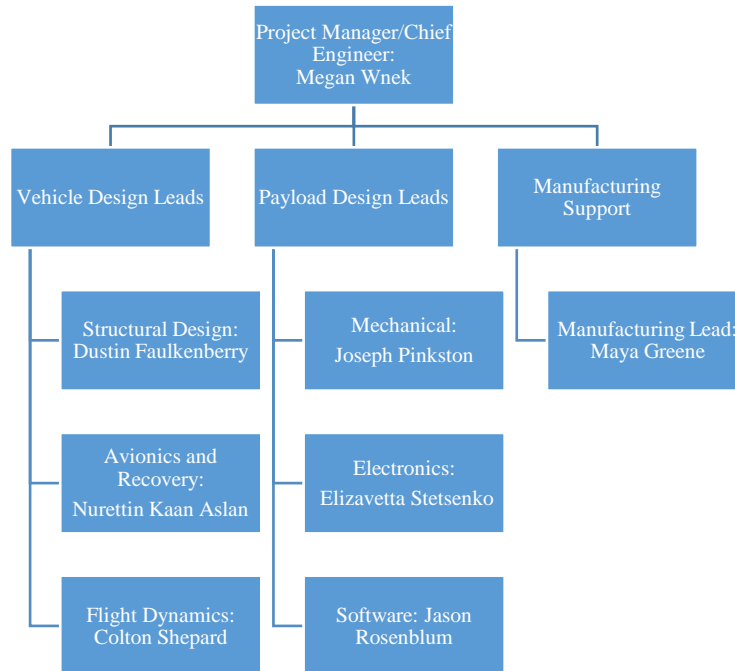


**Fig. 1 Swamp Launch Rocket Team Organizational Chart.**

The Project Manager role oversees the team by maintaining the schedule, setting the budget, fulfilling purchases, interfacing with the competition organizers, interfacing with the team’s executive board, and supervising the completion of required documents for competition. The Chief Engineer oversees the technical project for the team by meeting with the technical leads, verifying and approving final designs, integrating designs across all subteams, and assisting in design choices and manufacturing. The technical leads for the team are each responsible for designing and manufacturing their subsystems, and each runs a subteam of student members who assist them in their work. Manufacturing support leads are responsible for assisting and supervising manufacturing across all subteams as necessary.

The team operated on a master schedule set forth by the Project Manager at the start of the 2022-2023 academic year, which outlined the team’s required progress each month up to competition (Fig. 2). Technical Design Reviews were internal reviews done by the team to the general body that encouraged timeliness in completing the competition design. In general, the months of August to December were utilized for design and analysis and the months of January to May were for manufacturing and testing. The team incorporated plans for when to purchase materials so

manufacturing could begin in a timely manner, and also included backup dates for key milestones like the project test flight.

**Table 1: Team-defined Schedule**

August	Initial team meeting
	Overview of Documentation
	Initial concepts for project
September	Technical subteam meetings begin
	First Design Review: Preliminary Design Review
October	Competition Entry Form
	Second Design Review: Critical Design Review
November	Materials ordered
	Overall designs finalized
December	First Progress Report
	Composites manufacturing/testing begun
January	Third Design Review: Manufacturing and Testing Plans
	Prototype testing begun
	Full scale manufacturing begun
February	Second Progress Report
	Recovery test flight
	Full-scale manufacturing
March	Full-scale manufacturing and testing
	First full-scale launch attempt
April	Third Progress Report
	Backup full-scale launch attempt
	Travel organized
May	Project Technical Report and Podium Materials
	Video Conference Review
	Design corrections and additional testing as required
June	Competition attendance

With the assistance of the executive board, the team Project Manager also set forth a budget based on team funding at the beginning of the year to account for all costs and ensure the team's success and ability to attend the competition. At the start of the year, the team was allocated \$9300 for the construction of the launch vehicle and payload. Additional funding through scholarships and sponsorships was provided to assist in covering travel costs. The budget was updated throughout the year to incorporate this additional funding and account for updates to the project design. A breakdown of final overall costs was formed in order to establish precedence for future use (Fig. 2, Table 2). The final cost of the project construction fell within the initial planned budget.

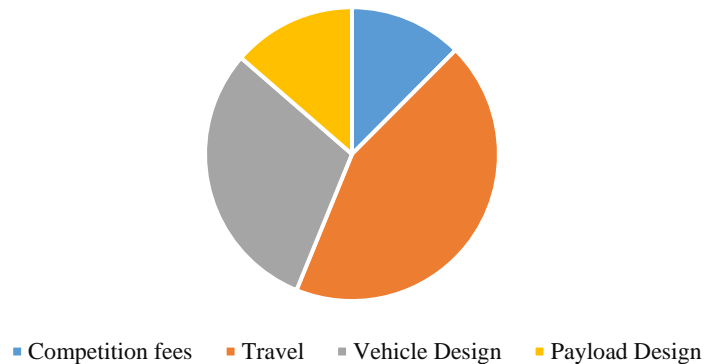


**Fig. 2 Project budget breakdown.**

**Table 2: Project cost breakdown**

Competition fees	\$1825
Travel	\$6398
Vehicle Design	\$4423
Payload Design	\$1993
Total	\$14,638

### III. System Architecture Review

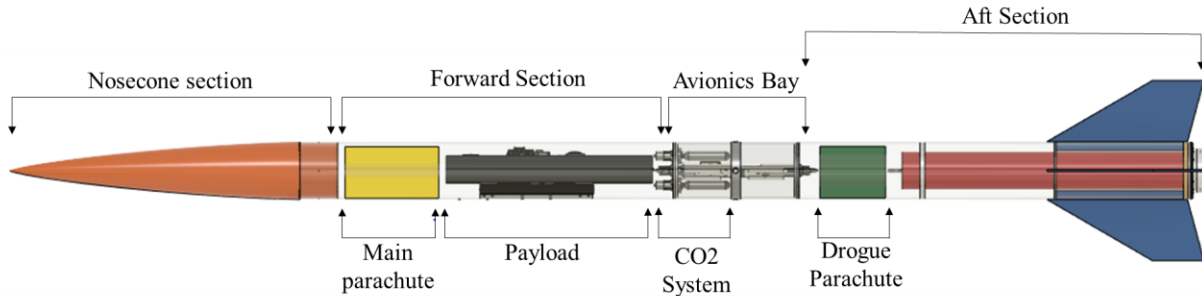


**Fig. 3 Project cutaway view.**

“See Ya Later, Alligator!” is a 6.14 in diameter, 11 ft tall launch vehicle that is propelled by an Aerotech M2500 motor to carry and deploy a 9.2 lb payload. The launch vehicle ascends to an apogee of 9996 ft before descending under a COTS 36 in drogue parachute and a COTS 96 in main parachute. The launch vehicle airframes are student research and developed (SRAD) made from carbon fiber designed to be lightweight while withstanding the forces of launch and recovery. The recovery system design employs two COTS flight computers, a StratoLogger SL100 and a StratoLogger CF, along with an SRAD CO<sub>2</sub> ejection system for the main parachute and payload deployment and black powder ejections for the drogue parachute ejection. The drogue parachute deploys at apogee, slowing the rocket to a deployment velocity of 89.3 ft/s for main parachute and payload deployment, which occurs at 800 ft. The launch vehicle will touch down with a ground-hit velocity of 19.4 ft/s. Simulations were performed using OpenRocket software and SRAD flight simulations written in MATLAB. The payload system, “In a While, Crocodile!” is an autonomous quadcopter designed to capture an image of the launch vehicle’s landing location and safely touch down upon mission completion. The quadcopter structure is made from SRAD carbon fiber and controlled by SRAD flight software. The electronics of the payload are mounted to a SRAD PCB. The payload is integrated into the launch vehicle by folding the quadcopter arms in and housing it inside a steel sheet metal container tethered to the main recovery harness. Throughout the ascent of the rocket and descent under drogue, the payload remains retained inside the forward airframe on an airframe concentric retention system. Upon its ejection, the payload descends another 200 ft before deploying from the container under a 36 in parachute. After performing system checks and verifying flight capabilities, the drone deploys from its parachute at approximately 400 ft to complete its mission, allowing the parachute to descend under ballast weight. The drone then touches down at a GPS location 20 ft from the landing location of the launch vehicle.

#### A. Propulsion Subsystems

The propulsion system of the rocket is central to the flight of the launch vehicle. A motor needed to be chosen that propelled the launch vehicle to an apogee of 10,000 ft and met the requirements for a minimum static margin of 1.5 and a velocity off the rail of 100 ft/s. With these characteristics in mind, a model of the launch vehicle was created in OpenRocket which matched estimates of the parameters of the rocket. The model was updated to employ as built weights and sizes as manufacturing progressed (Fig. 4).

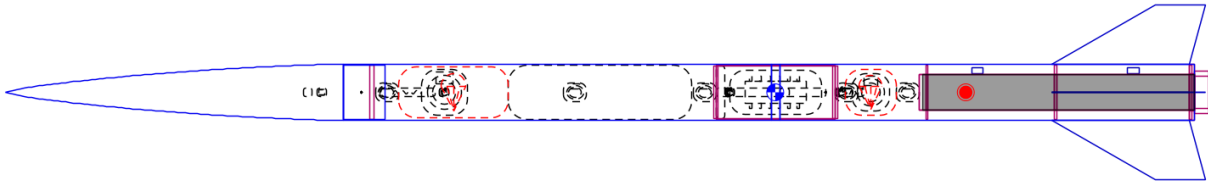


**Fig. 4 As-built OpenRocket model.**

The Aerotech M2500 was the motor that, when simulated, best met the above conditions. Plotting the stability vs. time, the minimum static margin was found to be 1.875 when a ballast weight of 2 lbs was applied (Fig. 5).

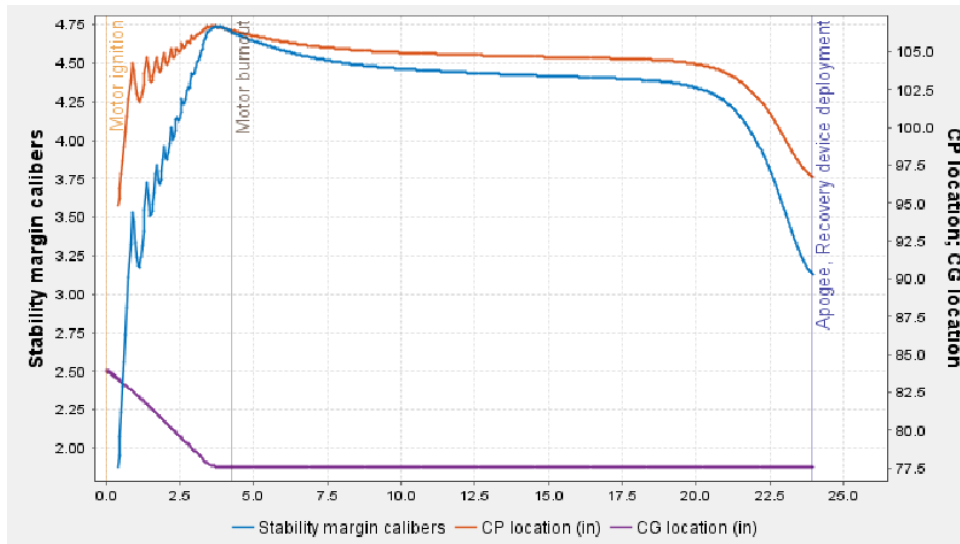


**Fig. 5 As-built simulated stability vs. time plot.**

Additionally, the altitude and velocity off the rail requirements were also met by an as-built simulated apogee of 9996 ft and a rail exit velocity of 104 ft/s (Fig. 6).

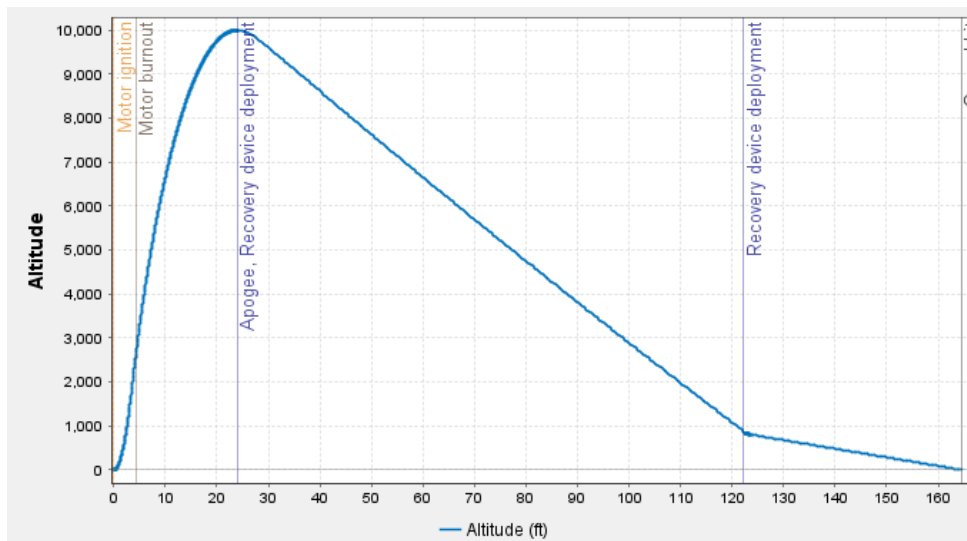


**Fig. 6 As-built simulated altitude vs. time plot.**

Another requirement for the simulation was to confirm that the fins would not experience any flutter. An analysis was performed using the SRAD MATLAB simulator, which was based on Ref. [3] and employed Eq. (1). The fin flutter velocity took into account the design of the fins, which are discussed in the Aero-structures section, and was calculated to be 1366 ft/s. The as-built simulated results yielded a maximum velocity of 1010 ft/s, thus confirming the fin design would not experience flutter (Fig. 7). The rest of the results of the OpenRocket simulations are shown in Appendix I, along with the M2500 manufacturer specifications.

$$V_f = a \sqrt{\frac{G}{\frac{1.337AR^3P(\lambda + 1)}{2(AR + 2)\left(\frac{t}{c}\right)^3}}} \quad (1)$$

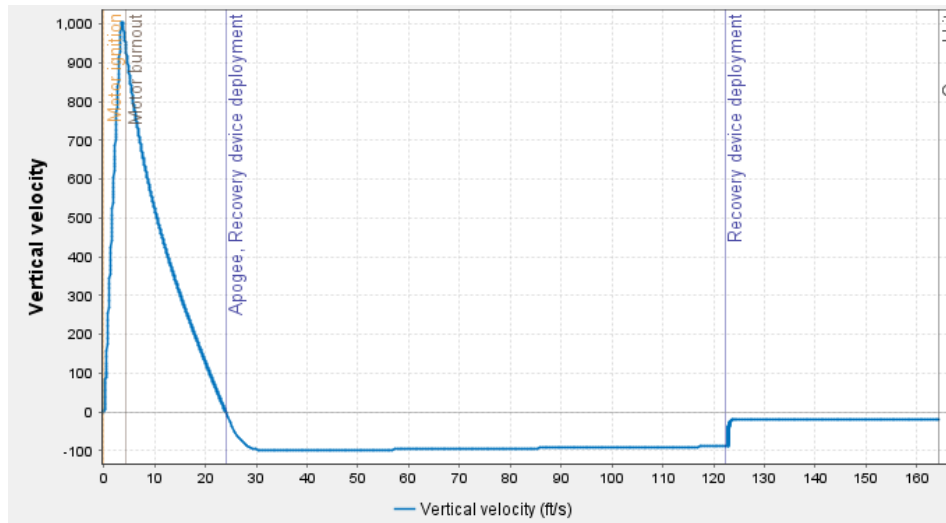


**Fig. 7 As-built simulated vertical velocity vs. time plot.**

The selected motor required specific components for motor retention and assembly which were integrated into the internal structural design of the launch vehicle. The majority of motor hardware was selected to be COTS due to the complexity of the parts and their critical nature to the safety and success of the flight (Table 3).

**Table 3: COTS Motor Hardware**

Casing	AeroTech RMS-98 98/10240 N-sec aluminum motor case - 9810C
Forward closure	AeroTech RMS-98 98/10240 forward closure
Aft closure	AeroTech RMS-98 98/10240 aft closure
Forward seal disk (comes with motor casing)	AeroTech RMS-98 98/10240 forward seal disk
Retainer	Aero Pack 98mm Retainer (Flanged)

### B. Aero-structures Subsystems

The primary goals of the aero-structures subsystems are to retain all other subsystems during vehicle flight and achieve acceptable aerodynamic performance during ascent, all while remaining within safe ranges of stress and loading to prevent mechanical failure. This is achieved through the use of an SRAD carbon fiber airframe, manufactured by performing a three-ply wet layup consisting of a layer of 3K biaxial carbon fiber sleeving, a layer of 12K uniaxial carbon fiber sleeving, and finally a second layer of 3K biaxial carbon fiber sleeving. This particular layup was chosen for its high strength in axial compression and moderate flexibility in the radial direction. The former prevents the airframe from failing under the sustained load produced by the motor as force is transmitted through the thrust plate, while the latter mitigates the risk of material failure due to pressurization during ejection. The layup was performed on a 6 in. diameter polycarbonate mandrel, wetting out each layer with Soller Composites 820 epoxy system, which was selected for its wet-out characteristics, high strength, and slow cure time. After wet-out, the layup was wrapped helically with PET flash tape, which has a silicone-based adhesive and therefore does not adhere to the

epoxy (Fig. 8). The function of the tape wrap was to force out excess epoxy from the layup, resulting in a superior fiber-volume fraction. Curing of the layup was conducted over three days using an insulated curing chamber and heat lamp. An SRAD three-ply carbon airframe was selected over a COTS G12 fiberglass airframe due to superior specific strength and significant weight savings, offering a 62.5% reduction in weight-per-inch while incurring only a 12.9% reduction in maximum load at failure. Despite the reduction in maximum load, the airframe was found to comply with a 2.5 factor of safety in a compression test, placing it well within acceptable parameters for expected loading conditions during flight. Furthermore, the SRAD carbon airframes were successfully flown on a test flight and found to be suitable for use.



**Fig. 8 Layup after tape wrapping on polycarbonate mandrel.**

It is critical that the structural components of the launch vehicle are not designed in such a way as to compromise the integrity or operation of the payload, recovery subsystems, or propulsion subsystems. For this reason, a COTS G12 fiberglass nose cone was selected. A carbon fiber nose cone was not considered due to cost and complex manufacturing. Additionally, the G12 nosecone eliminated the risk of attenuation of a radio signal and allowed the GPS to be situated inside. A 5:1 Von Karman nose cone shape was selected for optimal aerodynamic performance in the predicted operational flight regime of the launch vehicle. A metal-tipped nose cone was selected for superior strength and an improved stability margin. The nose cone was successfully employed during a test flight and found to be suitable for use.

To meet the aerodynamic requirements of the launch vehicle, a four-fin design was selected, which offered a higher stability margin than a three-fin design at minimal additional weight cost. Epoxyglass was chosen as the material of choice for manufacture of the fins due to high torsional stiffness – mitigating risk of flutter – and low weight. Epoxyglass was selected over carbon fiber due to considerably lower material costs and manufacturing time. A low fin span was chosen to further reduce the risk of flutter, while a high sweep was chosen to improve the stability margin. These mitigating factors resulted in a fin flutter velocity of 1366 ft/sec, considerably higher than the simulated maximum velocity of 1010 ft/sec. These fins were successfully employed during a test flight and found to be suitable for use.

The SRAD thrust plate was manufactured from 6061 aluminum and served to transmit thrust from the motor into the airframe of the vehicle. The thrust plate was machined via a combination of cutting on an abrasive water jet and CNC milling to produce the complex geometry of the component. A ½ in thickness was selected for the thrust plate to ensure high strength under motor load, and weight-reducing pockets were included to reduce resulting weight cost. A center pocket was also included to improve ease of assembly by aligning the COTS aluminum motor retainer with the body axis of the launch vehicle. The thrust plate was designed to fasten to the motor retainer via 12 stainless steel buttonhead cap screws. The SRAD aluminum thrust plate was successfully employed during a test flight and found to be suitable for use.



To retain the propulsion subsystems, a fully modular aluminum aft system was designed (Fig. 9). The goal of this design was to allow the removal and replacement of fins in the event that they were damaged or required modification. This factor, along with the ability to reuse components in future projects, were the two major advantages of the proposed design over a traditional high powered rocketry (HPR) aft secured via epoxy. The design operates by replacing exterior epoxy fillets with exterior SRAD 6061 aluminum brackets, machined via CNC milling from bar stock. These brackets fastened to one another through holes in the fins themselves, and into the centering rings via black oxide alloy steel fasteners. The centering rings were manufactured using a combination of cutting on an abrasive water jet and manual milling and were designed to minimize weight. Weight reduction was a key design goal due to the high weight cost of designing an aluminum aft system, especially as compared to traditional HPR materials such as wood and fiberglass. The centering rings were also designed with press-fit slots to accommodate fin tabs and allow for through-the-wall fin tabs, with the aim of minimizing failure risk of the fins. The aftmost centering ring was designed to fasten via four stainless steel fasteners to the thrust plate, securing the thrust plate and motor retainer to the larger aft assembly. 6061 aluminum was selected for both the brackets and centering rings for its machinability and low weight relative to steel.

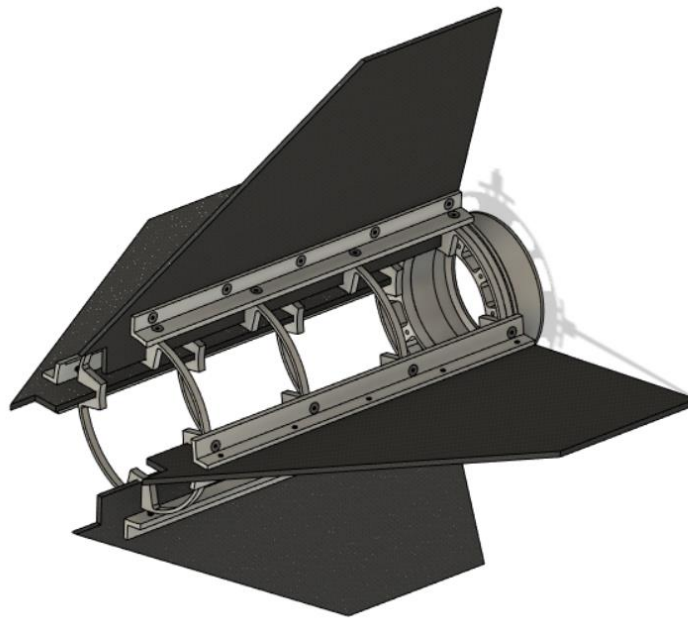


**Fig. 9 The modular aft in its fully assembled configuration (airframe and motor casing not shown).**

During test launch, the aluminum centering rings experienced catastrophic material failure, primarily consisting of shearing at the fillet joining the slot to the outer ring. The most probable cause of this failure is the load produced by the aerodynamic forces on the fin during ascent, resulting in failure of the foremost centering ring. This in turn placed a greater load on the remaining centering rings, leading the fin to progressively detach until separating completely from the airframe on landing. It is also believed that the introduction of fin slots to the centering rings and airframe compromised the overall integrity of the structure, and in particular weakened the centering rings to bending stresses.

Due to this failure, the initial modular aft design was modified to a more traditional epoxy-secured aft. The primary goal of the revised design was to reduce manufacturing costs – in terms of both finances and manufacturing time – while still maintaining the aerodynamic characteristics of the previous launch vehicle. The revised design omits the aluminum centering rings and fin brackets in favor of 2 epoxyglass centering rings and epoxy fillets, chosen for their lightweight characteristics and ease of manufacturing. The aftmost centering ring, damaged during the test flight, was replaced with a ½ in thick wood ring to accommodate fastening to the existing thrust plate. An additional feature introduced into the revised design is a 4 in diameter fiberglass motor tube, which provides a point to secure the centering rings via epoxy. This approach to constructing and securing the aft components of a high-powered rocket has been extensively tested through previous flights and has historically proven to be a highly effective method of retaining the fins and propulsion systems.

### C. Avionics and Recovery Subsystem

The Avionics and Recovery subsystem is responsible for the integration of a parachute configuration and a parachute deployment system to track and retrieve the launch vehicle without sustaining damage after the flight. The recovery mission of the launch vehicle follows a standard dual-deploy configuration in which a drogue and a main parachute are used to decelerate the vehicle. The chosen COTS altimeters record altitude data utilized to deploy the drogue parachute at apogee via ignition of a black powder charge and the main parachute, along with the payload, at 800 ft via puncture of a CO2 cartridge. The altimeters and their circuitry are stored inside the fiberglass avionics bay coupler which serves as a joint between the forward and aft airframe.

The avionics bay coupler is sealed from ejection gases on both sides with aluminum bulkheads to protect the altimeters from false pressure readings and hot gases. The bulkheads also serve as a mount for the SRAD CO2 ejection system and the eyebolts (Fig. 10). Throughout the flight, the location of the launch vehicle is tracked through radio signals coming from a COTS GPS that is mounted inside the nosecone. The radio signal is received from the ground station using a Tele Dongle Antenna that is connected to a laptop. The design of the Avionics and Recovery subsystem can be broken into four subsections: the recovery layout design, avionics bay structural design, avionics bay electrical design, and CO2 ejection system design.

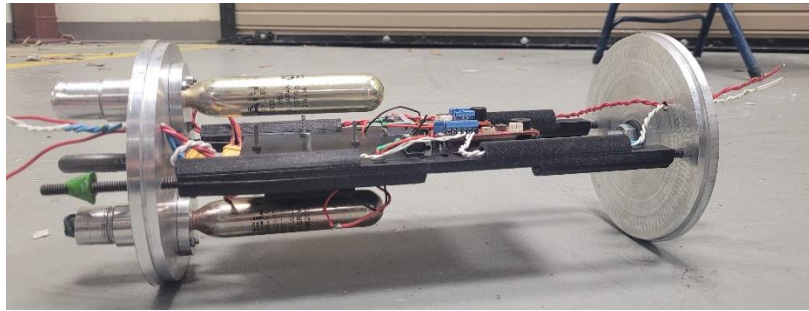


**Fig. 10 Avionics Bay Assembly without the Coupler.**

The components of the recovery layout are chosen to withstand the deployment forces and decelerate the launch vehicle's weight to safe landing speeds while minimizing the drift radius for easy retrieval. The dual-deployment method is chosen as the operation concept to meet the competition requirements and minimize the drift radius. The first deployment event takes place at apogee, where a smaller drogue parachute is deployed to decelerate the launch vehicle for a successful main parachute deployment while minimizing vehicle drift due to wind. The second event takes place when the launch vehicle has descended to 800 ft. This is when the main parachute and payload are deployed for the payload to start its mission and the launch vehicle to decelerate to a safe landing speed. The first consideration when choosing the parachutes for the mission is determining what safe landing speeds are and the weight of the launch vehicle after burnout. The safe descent speed under the parachutes is outlined by the competition as 75-150 ft/sec for the drogue parachute and <30 ft/sec for the main parachute. The weight of the launch vehicle after motor burnout was found to be 48 lbs. Multiplying the gravitational acceleration with mass of the launch vehicle gives the force necessary for the parachute to balance out. Equation (2) is used to calculate the descent speed,  $V$  by isolating it from the equation and filling in air density,  $\rho$ , parachute area,  $A$ , coefficient of drag of the parachute,  $C_d$  values. A 36 in and a 48 in Rocketman Standard Parachute were evaluated first since they were already in the team's inventory.

$$V = \sqrt{\frac{2F}{\rho A C_d}} \quad (2)$$

**Table 4: Drogue Parachute Evaluation**

Parachutes	Coefficient of Drag, $C_d$	Parachute Area, $A$ (ft <sup>2</sup> )	Descent Speed, $V$ (ft/sec)
36" Rocketman Standard Parachute	0.98	7.07	79 ft/sec
48" Rocketman Standard Parachute	0.98	12.57	59 ft/sec

The 48" Rocketman Standard Parachute resulted in a descent speed that was outside of the design requirements, so the 36" Rocketman Standard Parachute was chosen as the drogue parachute due to its desirable descent speed.

Choosing the main parachute followed a similar decision-making process. However, in addition to the main parachute’s drag force, the drogue parachute drag force also needed to be accounted for when using Eq. (2) to find the descent rate under the main parachute. This was done by adding the parachutes individual product of parachute area,  $A$ , and coefficient of drag,  $C_d$ . The first parachute evaluated for the main parachute was the 96” Iris Ultra–Standard Parachute, which fit the design requirements for the descent speed (Table 5). Since it was already in the team’s inventory, it was chosen as the main parachute.

**Table 5: Main Parachute Evaluation**

Parachutes	Coefficient of Drag, $C_d$	Parachute Area, $A$ (ft <sup>2</sup> )	Descent Speed, $V$ (ft/sec)
96” Iris-ultra–Standard Parachute	2.2	50.3	20 ft/sec

The components of the recovery layout are chosen to withstand the highest load expected. This happens before the forces balance out instantaneously when the parachute deploys. The drag force from the parachute and the weight of the launch vehicle act in opposite directions. So, the maximum force experienced through the recovery hardware can be found by adding the drag force and the weight of the rocket. The velocity,  $V$ , is equal to the velocity of the launch vehicle at deployment.

$$F = \frac{1}{2}V^2\rho AC_d + mg \quad (3)$$

Equation (3) results in 156 lbs of load at drogue parachute deployment and 875 lbs of load at main parachute deployment. The factor of safety of the recovery hardware can be seen below (Table 6).

**Table 6: Recovery Hardware Safety Ratings**

Component	Maximum Load Rating (lbs)	Factor of Safety
½” Kevlar Shock cord	6000	6.85
3/8” Steel Eyebolt	1400	1.6
5/16” Steel D-Links	1000	1.14
Steel Swivels	3000	3.43
¼ Steel Threaded Rods	7370	8.43

The forward recovery harness connects the nosecone eyebolt to the forward avionics bay eyebolt. The connection between the recovery harness and eyebolts is done using D-links to make disconnecting the recovery harness easy. The parachute protector is tied at 2/3 of the length of the recovery harness starting from the nosecone eyebolt connection. The payload recovery harness is tethered to the forward recovery harness 2 ft below the parachute protector to prevent it from wrapping around the protector. The main parachute is connected to the recovery harness at 1/3 of the recovery harness’ length starting from the nosecone connection to avoid entanglement with the parachute protector, nosecone, and forward airframe. The parachute is attached to the layout by attaching the main parachute’s swivel to the recovery harness through an additional D-link. The aft recovery harness follows a very similar layout where the recovery harness attaches the aft avionics bay eyebolt to the motor casing eyebolt using D-links. The drogue parachute and its swivel are connected at 1/3 of the aft recovery harness length starting from the avionics bay connection using a D-link. The drogue parachute protector is tied at 2/3 of the length of the aft recovery harness from the avionics bay connection to provide distance between the parachute and parachute protector. The length of the recovery harness is important to prevent sections of the launch vehicle from bouncing back towards each other after a powerful separation event. The length of the recovery harness is chosen to be 40 ft for the forward recovery harness and 40 ft for the aft recovery harness, which is approximately 3 times the length of the launch vehicle and is common rocketry practice. All the recovery hardware and parachutes were tested during the test flight. They were able to withstand all the forces and provide a safe landing for the launch vehicle.

The avionics bay houses the flight computers responsible for recording flight data and initiating the parachute deployment events inside a 13 in long fiberglass coupler, designed to meet the requirements of coupler length due to airframe diameter. This coupler also acts as a joint to connect the forward and aft airframes together. A 1 in long carbon fiber switch band was epoxied halfway along the couplers length to allow avionics bay access from outside while keeping the launch vehicle structure continuous. The band has 4 pressure port holes drilled around its circumference that are positioned 90 deg from each other, per flight computer manufacturer specifications. These

holes allow air to circulate inside the avionics bay, which allows the altimeters to collect barometric data during flight. The coupler can be seen in Fig. 11. The coupler is sealed from the ejection gases produced inside the airframe with two aluminum bulkheads located on its sides. They also serve as the mounts for eyebolts and the CO<sub>2</sub> ejection system. The bulkheads are fixed in place at the ends of the coupler with 4 nuts fastened on 2 threaded rods that go through both bulkheads along their diameters. The threaded rods also serve as the structure to support the avionics sled inside the avionics bay. The structure of the avionics bay is designed to withstand the parachute deployment forces as well as the recovery hardware since the recovery harnesses are attached to the eyebolts mounted on the avionics bay bulkheads. The force is divided between the two threaded rods. The factor of safety for the threaded rods can be seen in Table 6. The ability of the avionics bay's structure to withstand flight conditions was proved during the test flight.



**Fig. 11 Avionics Bay coupler with the Switch band epoxied in place.**

Two independent flight computers that are powered by independent batteries were implemented into the avionics bay design to ensure redundancy in the system and to meet competition requirements. Reliability and cost were the prominent factors that affected the recovery design choices. So, the flight computers were chosen based on team inventory and testing with various models' reliability. A COTS StratoLogger SL100 has been used as the primary altimeter by the team for more than five flights and has reliably collected flight data and fired ejection charges for all the flights. Since it has been reliable in the past and was available in the team's inventory, it was chosen as the primary flight computer for this design. The redundant altimeter is chosen based upon similar criteria. However, the redundant altimeter cannot be identical to the primary altimeter to account for similar failure points. So, a different altimeter was sought after. An additional altimeter that the team has flown on numerous occasions with reliable performance is a StratoLogger CF. Since reliability and the team's familiarity with the device were the main considerations, the StratoLogger CF was chosen as the redundant flight computer. Both the primary and redundant altimeter are powered by individual 9 V batteries. They are disarmed before flight and armed at the launch pad using two SS-5 micro switches. These switches are mounted on a 3D printed switch mount to create a pin plunger arming mechanism. The system is open (disarmed) when the pin is inserted into the mount and closed (armed) when the pin is removed. The switch mounts are accessible from the outside of the avionics bay since they are aligned with the pressure port holes on the switch band. The wiring diagram for the altimeters can be seen in Fig. 12.

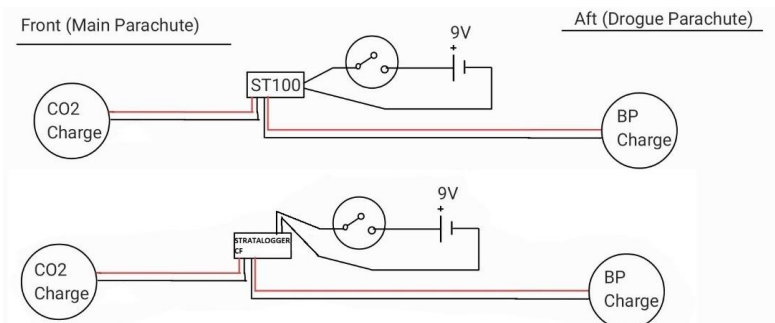


**Fig. 12 The wiring diagram for the Primary (top) and Redundant (bottom) Altimeters.**

The altimeters, batteries and the switch mounts were mounted on a 3D printed avionics sled made from Polyethylene terephthalate glycol (PETG). The altimeters are fastened to the threaded inserts placed inside standoffs. This keeps the altimeters elevated to prevent blocking the pressure sensors located below them. The 9V batteries are stored inside a 3D printed battery housing that fastens on to the avionics sled. The altimeter wires are managed with zip ties and printed wire runaways, included as a part of the avionics sled design. The fully wired and assembled avionics sled can be seen in Fig. 13. The functionality of the switches and altimeters were proven to reliably work from the test launch.

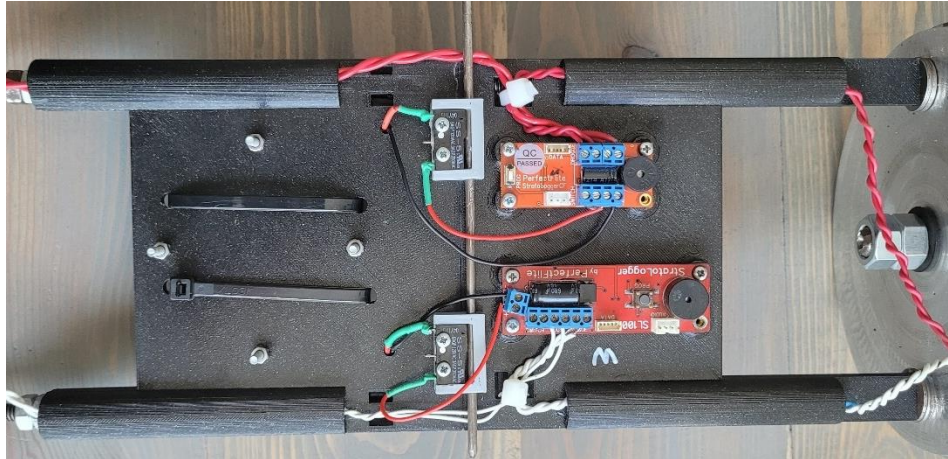


**Fig. 13 Fully wired Avionics Sled Assembly.**

The payload is located inside the forward airframe along with the main parachute. Due to the size limitations for the payload container, it was not possible to seal the quadcopter. This meant that the quadcopter would be exposed to ejection gases that are produced during an ejection event. A traditional black powder ignition method produces high temperature gases along with solid residue which would endanger the functionality of the sensitive electronics on the payload. Therefore, a cold gas ejection method was chosen over a traditional black powder method for main parachute and payload deployment event. The CO2 ejection systems commercially available were found to be very costly and outside of the team's budget. After analyzing the commercially available systems, designing and manufacturing a new system was found to be feasible. The CO2 ejection system designed releases the pressure from a CO2 cartridge into the airframe by puncturing the cartridge seal with a sharp point. The method of puncturing needed to integrate with COTS altimeters. So, ignition of a small black powder charge with an e-match was found to be the easiest method to build up pressure and accelerate a puncture piston towards the CO2 cartridge while keeping system integration easy. The components for the designed system can be seen in Fig. 14.

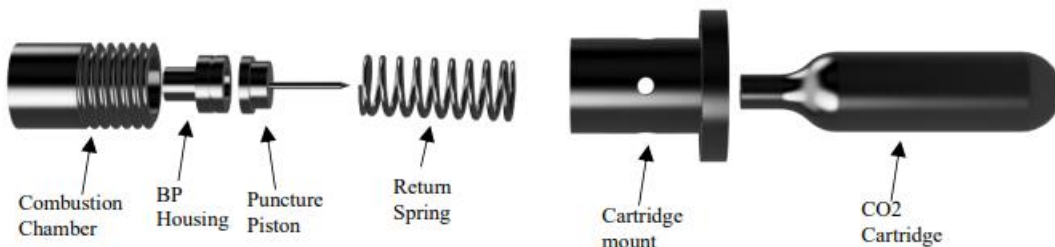


**Fig. 14 Exploded View of the CO2 Ejection System.**

The CO2 ejection system consists of a combustion chamber assembly that threads into a cartridge mount and a CO2 cartridge that threads into the cartridge mount. The combustion chamber stores the black powder housing, puncture piston, and return spring. O-rings were added around the puncture piston and black powder housing to seal the pressure. The ejection event ignites the black powder charge inside the black powder housing. This creates pressure that is sealed inside the combustion chamber between the black powder housing and puncture piston. The pressure accelerates the puncture piston to impact and break the CO2 cartridge seal. After the seal is broken, the return spring



prevents clogging by pushing the puncture piston out of the cartridge to release the CO<sub>2</sub> into the airframe through the venting holes on the cartridge mount. The system is fastened on the forward avionics bay bulkhead with mounting holes located on the cartridge mount. The components that make up the system are manufactured out of 6061 aluminum because of its low density and cost. They were manufactured using a manual lathe and milling machine. The as-built components can be seen in Fig. 15.

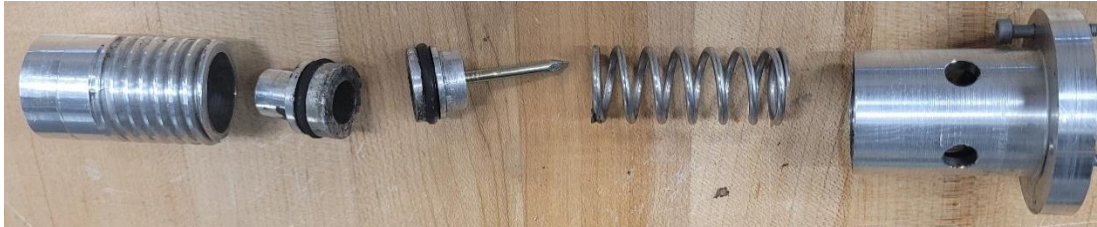


**Fig. 15 Manufactured CO<sub>2</sub> Ejection System Components.**

As well as retracting the puncture piston back after puncturing the CO<sub>2</sub> cartridge, the return spring also prevents the puncture piston and black powder housing from moving during flight. A serious concern with this system is premature puncturing of the cartridge. This can happen due to the spring compressing under the components weight with the acceleration during flight. The maximum force that acts on the spring,  $F$ , is found to be 0.525 lbf by multiplying the total mass of the components with the maximum acceleration experienced during flight. The amount the spring needs to compress for CO<sub>2</sub> cartridge to be punctured was found to be 0.105 using CAD and physical measurements of the system. The maximum amount the spring will compress,  $\Delta x$  is calculated using Eq. (4).

$$\Delta x = \frac{F}{k} \quad (4)$$

To mitigate this mode of failure, a spring with a constant,  $k$ , of 0.0536 lb/in was chosen. The maximum compression with this spring is 0.0152 in during flight which results in a safety factor of 7.0. The next system requirement that was addressed was the size of the CO<sub>2</sub> cartridges. This is determined based upon the force necessary for separation and the volume of the airframe. The separation force required is found by multiplying the force required to break a nylon shear pin with the number of shear pins. From there, the desired airframe pressure is found through relating the separation force necessary to the volume of the airframe.

The mass of CO<sub>2</sub> necessary is found using Eq. by isolating mass,  $m$ , from the equation and substituting in the desired airframe pressure,  $P$ , atmospheric temperature,  $T$ , airframe volume,  $\Psi$ , and the gas constant,  $R$ .

$$P\Psi = mRT \quad (5)$$

The mass of CO<sub>2</sub> necessary for the parachute deployment was determined to be 32 grams. The closest size that is commercially available to 32 grams was 34 grams. Thus, 34-gram CO<sub>2</sub> cartridges were chosen as the main parachute primary and backup ejection values. The quantity of black powder required to puncture the canister was determined through ground testing and was determined to be 0.05 g.

Drogue ejection is performed using traditional floating black powder charges. Black powder quantities were determined through ground ejection testing and were finalized as a primary value of 3.5 g and a backup value of 4.2 g for the test flight.

#### **D. Payload Subsystems**

The mission for the payload is to aerially deploy an autonomous quadcopter that will take images of the launch vehicles landing site. The quadcopter utilizes a SRAD 12-ply carbon fiber reinforced polymer (CFRP) frame and motor arms for sufficient strength at a minimum weight. A SRAD integrated PCB is utilized to power and wire the sensors and motors utilized throughout flight. The quadcopter achieves its flight stability through a control system that utilizes six independently tuned PID controllers. The payload design is broken up into four subsections: the quadcopter's mechanical design, electrical design, control system design, and retention system design. The quadcopter is stowed in the forward airframe of the launch vehicle and its deployment sequence is outlined in the Mission Concept of Operations Overview section.

## 1. Quadcopter Mechanical Design

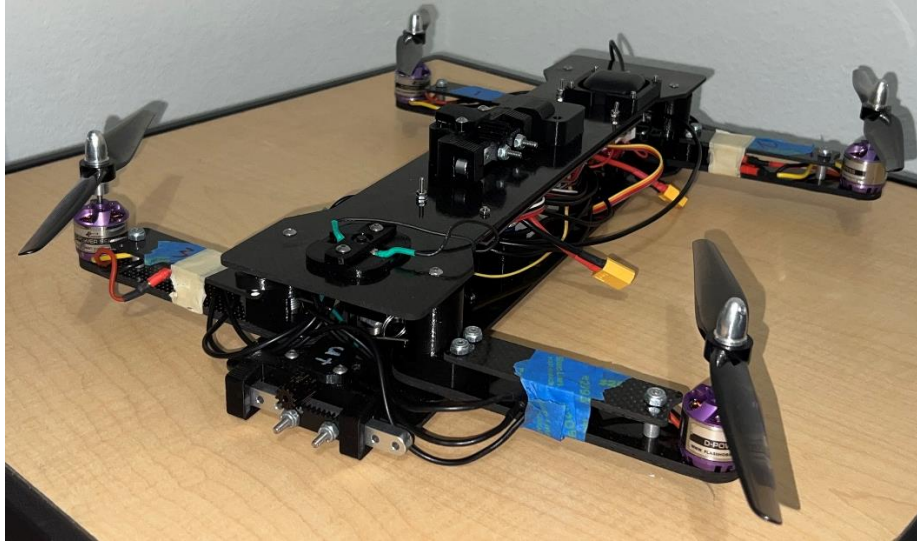


**Fig. 16 Quadcopter fully assembled in its flight configuration.**

The quadcopter has two configurations: the stowed configuration and the flight configuration (Fig. 17). The stowed configuration is when the quadcopter has its arms folded inwards, reducing its width to 4.5 in, allowing it to be retained inside of the forward airframe of the launch vehicle. The flight configuration is when the quadcopter has its arms unfolded and locked into place, allowing the quadcopter to perform flight maneuvers.



**Fig. 17 Stowed (left) and flight configuration (right) of the quadcopter.**

The quadcopter's subassemblies consist of the frame assembly, the motor arms, unfolding mechanisms, container-deployment rack and pinion assemblies, and the parachute-deployment rack and pinion assembly (Fig. 18). The frame assembly consists of a SRAD 12-ply CFRP top and bottom frame in a dog-bone shape. The frame assembly provides the main structural support for the quadcopter and houses the electronics and sensors. The top and bottom frames are fastened together via four steel threaded standoffs and eight 6-32 stainless steel fasteners. The motor arm assemblies consist of a SRAD 12-ply CFRP upper and lower motor arm, a 1300 KV brushless motor, an 8.0 in tapered propeller, a steel threaded standoff, and four 6-32 stainless steel fasteners. The motor arm assemblies provide the structural support for the brushless motors that control the quadcopters' flight. The 8.0 in tapered propellers were chosen with the 1300 KV motors to provide a maximum thrust of approximately 1.8 lb<sub>f</sub>. This provides the 3.8 lb quadcopter with a thrust to weight ratio of 1.89 utilizing the four motors and propellers. The unfolding mechanisms are the interface between the motor arms and the frame assembly. They consist of a PETG pivot housing, PETG pivot stop, 180-degree torsion spring, pin plunger locking mechanism, one 6-32 heat-set threaded insert, and two nylon thrust bearings. The

unfolding mechanisms provide the means to fold the motor arms inward while the quadcopter is stowed inside of the forward airframe during launch, unfold at deployment, and lock into the flight configuration when deployed. The two container-deployment rack and pinion assemblies consist of a 12V DC motor with a 281:1 planetary gearhead, an aluminum beam, a steel pinion, an acetal rack, a PETG motor housing, 6-32 heat-set threaded inserts, and two 6-32 stainless steel fasteners and locknuts. The container-deployment rack and pinion assemblies are located on both ends of the bottom frame, and their purpose is to retain the quadcopter inside of the retention system until deployment. The parachute-deployment rack and pinion assembly are the same as the container-deployment assembly, however it has a stronger motor housing and a PETG parachute stop that the aluminum beam mates to. The purpose of the parachute-deployment rack and pinion is to keep the quadcopter's parachute attached to the top frame until the quadcopter is ready to begin its flight operations.

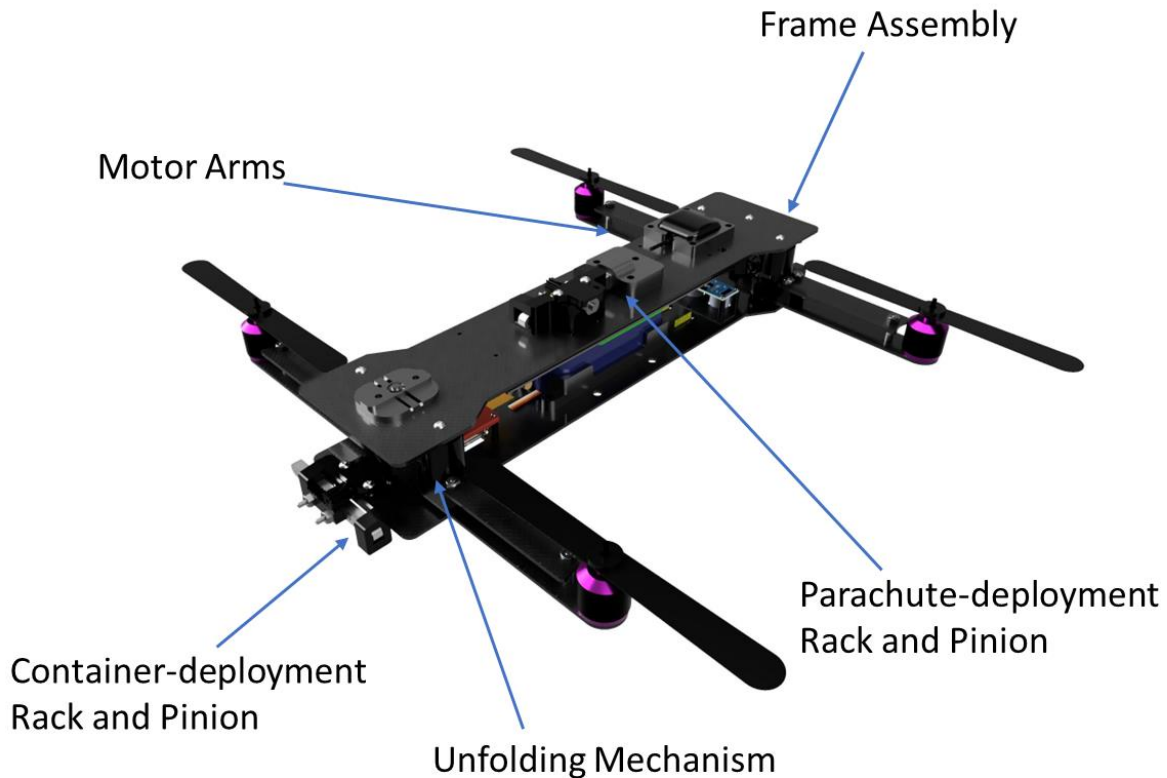


**Fig. 18 Quadcopter subassemblies in the flight configuration.**

The top frame, bottom frame, and motor arms of the quadcopter are SRAD 12-ply CFRP cut on a waterjet. CFRP was chosen as the material of choice for the core structural components of the quadcopter as it is lightweight with enough strength to withstand launch and flight loads. To minimize weight and increase room for the folding of the motor arms, a dog-bone structure was utilized for the top and bottom frames. The dog-bone shape results in minor decreases in lateral strength while maintaining stiffness (Ref. [2]). The bottom frame of the quadcopter features the largest cutouts for electronics, thus the highest stress concentrations when compared to the top frame. A stress analysis using Solidworks FEA was conducted on the bottom frame, with a desired safety factor of 2.0 or greater (Table 7). A safety factor of 2.0 was chosen to account for potential inconsistencies in the SRAD 12-ply CFRP as the curing process occurs under 1 atmosphere of pressure as opposed to autoclave that can reach pressures of 7 atmospheres. The lower curing pressure can lead to more voids and deformities throughout the final material.

A design requirement for the motor arms was to minimize the deflection at the ends of the arms to provide better control authority for the control system. The motor arms are attached to the quadcopter frames as cantilever beams. To achieve this, the motor arms went through a series of iterations, with the final design deriving from the concept of an I-beam. The motors at the end of the motor arms produce an upward thrust for the quadcopter, which results in a bending moment on the motor arms. The tip deflection of a cantilever beam is found using the following where  $\delta$  is



the tip deflection,  $F$  is the thrust load from the motor,  $l$  is the length of the motor arm,  $E$  is the modulus of elasticity, and  $I$  is the moment of inertia,

$$\delta = \frac{Fl^3}{3EI} \quad (6)$$

To decrease the tip deflection of the motor arms, the moment of inertia was increased. This was done by adding an “upper” motor arm to the design as seen in Fig. 16. The upper and lower motor arms serve as flanges of an I-beam and the fastener joining the two serves as the web of an I-beam (Fig. 19). The material properties of the SRAD 12-ply CFRP were determined by the team last year through extensive material testing. Using Eq. (6), the tip deflection of the motor arms was found to be 0.079 in for the maximum motor thrust of 1.8 lb<sub>f</sub>. A stress analysis of the lower motor arm was also conducted using SolidWorks finite element analysis (FEA) with a desired safety factor of 2.0 or greater (Table 7). Again, a desired safety factor of 2.0 was chosen to compensate for potential deformities in the SRAD 12-ply CFRP layup.

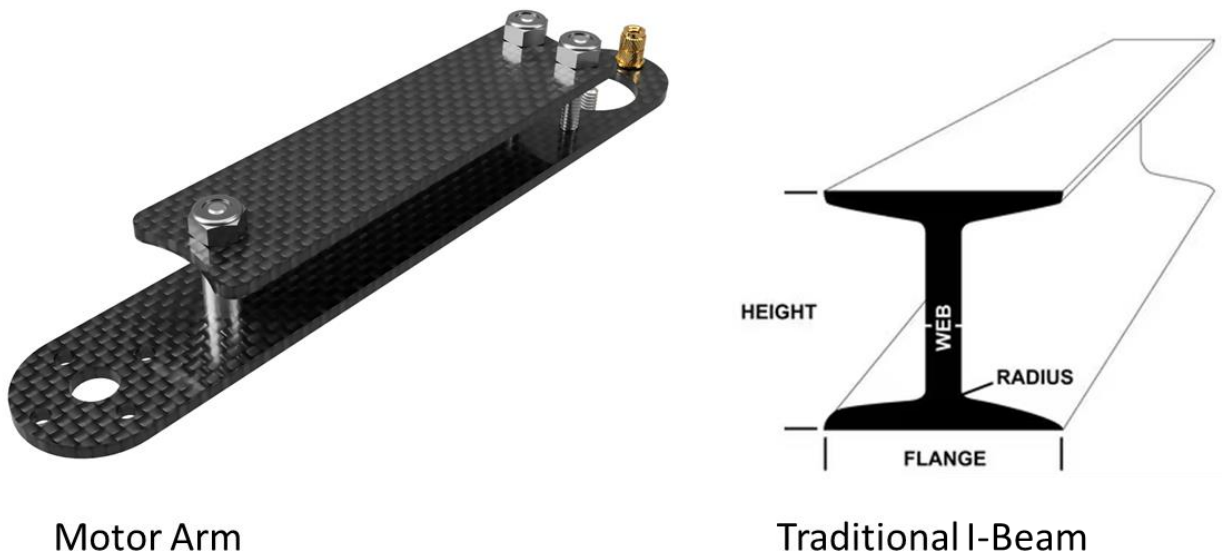


**Fig. 19 Motor arm design inspired by a traditional I-beam design.**

The pivot housing and pivot stop are both 3D printed PETG components printed at 100% infill that facilitate the folding and unfolding motion of the unfolding mechanism. The pivot housing has an attachment piece that allows two fasteners to join the upper motor arm to the housing, and a threaded insert to join the lower motor arm to the housing (Fig. 20). Through the center of the pivot housing there is a threaded standoff, two nylon thrust bearings, and a 180-degree torsion spring. The bearings on the ends of the pivot housing allow smooth rotation of the housing about the threaded standoff, and the 180-degree torsion spring allows the arms to be folded in, and passively unfolded when released from the retention system. On the top end of the pivot housing, a threaded pin plunger is fastened to a hole in the housing. This pin plunger follows a track on the pivot stop, which has a conical hole at the end of the track. When the motor arms unfold, the pin reaches the end of the track on the pivot stop and the pin fully extends into the conical hole. The spring remains in compression and the pin remains in the hole, keeping the motor arm locked in place.

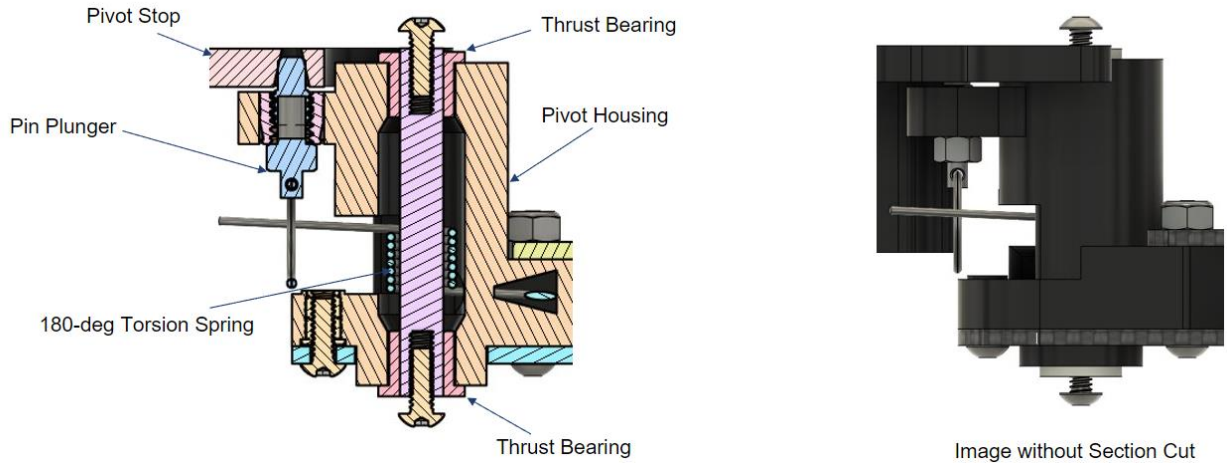


**Fig. 20 Section view and CAD model of the unfolding mechanism.**

The pivot housing transfers the loads from the motor arms to the frame assembly, thus a stress analysis was conducted (Fig. 21). The motor arm assembly was modeled as a cantilever beam, with its fixed end being the unfolding mechanism, thus the loads from the motor arm assembly are directly applied to the unfolding mechanism. Since the pivot housing is 3D printed from PETG, the yield strength and material properties were taken from the Prusament data sheet, which are for an infill of 100% (Ref. [3]). These parameters were used when setting up the Solidworks FEA, with a desired factor of safety of 2.0 or greater (Table 7). A safety factor of 2.0 was chosen to increase the possibility of the pivot housing surviving an impact load from landing or deployment. A larger than expected force was simulated to account for wind gusts during flight. The loading on the pivot housing was applied to the attachment piece, where the motor arms attach to. The highest stress was concentrated at the location joining the attachment piece and the center of the pivot housing. This is expected, as joints between two surfaces are a common stress concentration. The resulting factor of safety for the pivot housing was found to be 3.33, using the yield strength from Prusament for the z-axis orientation.

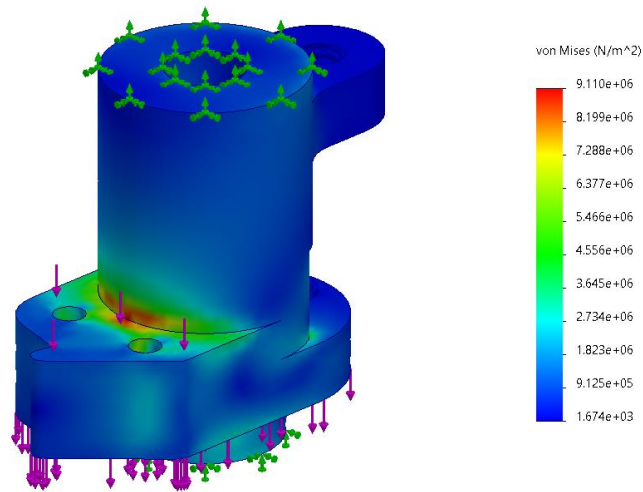


**Fig. 21 FEA of the pivot housing, with the top and bottom of the housing fixed from the thrust bearings, and the load applied on the attachment piece where the motor arms attach to.**

Both the container-deployment and parachute-deployment rack and pinion assemblies were tested on the ground using weights tethered to the aluminum beam. The expected container-deployment rack and pinion load is  $2 \text{ lb}_f$ , since each aluminum beam is carrying half of the weight of the quadcopter. The system was tested at different weights until

the motor stalled at a load of 8.0 lb<sub>f</sub>. This provides a factor of safety of 4.0 for the container-deployment rack and pinion system. The parachute-deployment rack and pinion system has an expected load of 5.0 lb<sub>f</sub>, carrying the quadcopter and the ballast mass on the parachute. The parachute-deployment rack and pinion stalled at the same load of 8.0 lb<sub>f</sub>, providing a factor of safety of 1.6 (Table 7). The safety factor for the parachute-deployment rack and pinion being under 2.0 is sufficient, as this is a physically tested and verified safety factor, whereas the other components were analyzed using FEA.

**Table 7: Quadcopter Component Stress Ratings**

Component	Load	Factor of Safety
Frame	100 lb <sub>f</sub>	5.45
Motor Arm	2.0 lb <sub>f</sub>	12.32
Pivot Housing	80 lb <sub>f</sub>	3.33
Container-deployment Rack and Pinion	2.0 lb <sub>f</sub>	4.0
Parachute-deployment Rack and Pinion	5.0 lb <sub>f</sub>	1.6

### 2. Retention System Design

The payload retention system is comprised of the 80/20 rail assembly, a 16 GA steel sheet metal container, 3D printed PETG retention mounts, a parachute shield, a steel recovery harness mount, and six 80/20 linear slides (Fig. 22). The 80/20 rail assembly consists of a 3D printed PETG concentric airframe mount with aluminum supports, two 1-foot long 80/20 T-slotted extrusions, four 90 deg corner brackets, and ¼-20 fasteners. The 80/20 rail assembly is fastened to the inside of the forward airframe through four ¼-20 fasteners that attach to the threaded aluminum supports on the concentric airframe mount. The 80/20 rail assembly provides the structure for the container to slide onto and remain inside of the forward airframe. The container is a 16 GA steel sheet metal structure that houses the quadcopter in its stowed configuration during launch. Inside of the container are two 3D printed PETG retention mounts, upon which the quadcopter's container-deployment rack and pinion aluminum beams attach to. The parachute shield is 3D printed PETG attached to one end of the container and prevents the parachute from deploying prematurely from the container. The steel recovery harness mount is fastened to the container through two 10-24 shoulder bolts and locknuts, as well as welded to the container. The recovery harness mount allows the container to be tethered to the main recovery harness. The six 80/20 linear slides are made of ultra-high molecular weight polyethylene (UHMW) and connect to the bottom of the container via M2.5 and ¼-20 fasteners. The linear slides provide a low friction interface between the container and the T-slotted extrusions, allowing the container to slide on and off the rails easily during ejection.

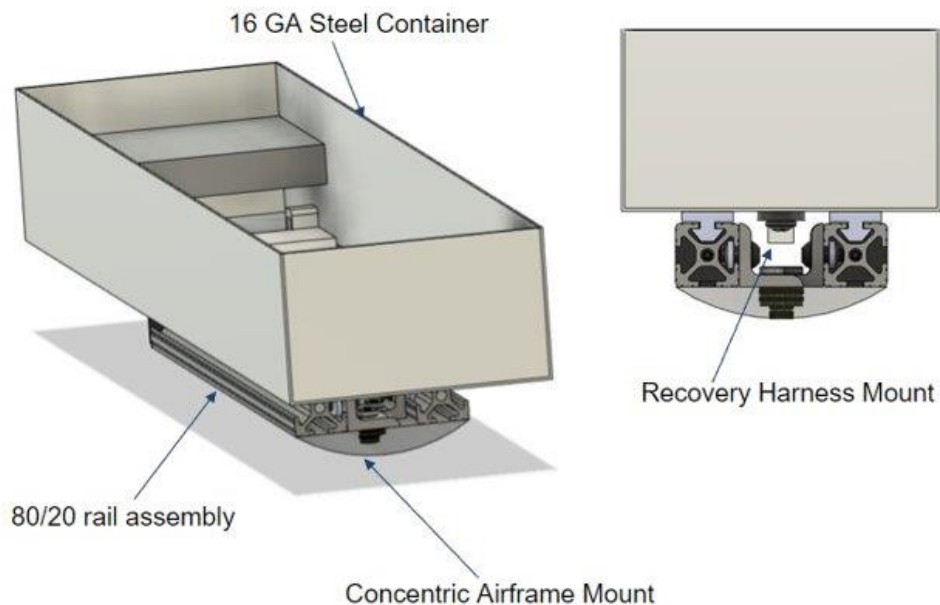


**Fig. 22 Payload retention system CAD model.**

During launch, the quadcopter is inside of the container in its stowed configuration, with the container on the 80/20 rail assembly. The recovery harness mount is attached to a four-foot section of recovery harness that is connected to the main recovery harness via a D-link. This connection helps pull the container out of the forward airframe during the main parachute ejection. The container and the quadcopter are ejected from the forward airframe with the main parachute at 800 ft. The container and the quadcopter will then be outside of the forward airframe, tethered to the main recovery harness under the main parachute. At 600 ft, the container-deployment rack and pinion systems will be actuated, and the quadcopter will release from the retention mounts and the container. Once released, the quadcopter will fall out and the arms will unfold due to the 180 deg torsion spring. Once the quadcopter is outside of the container, the 36 in parachute that is inside of the container under the parachute shield will come out and open. The quadcopter will then descend under the 36 in parachute, and the software will perform system checks to verify the sensors are functional, within their nominal operating bounds, and will check to ensure the quadcopter is descending at the expected descent rate. If the system passes all the checks, then at or below an altitude of 400 ft, the parachute-deployment rack and pinion system will be actuated, and the quadcopter will be released from the parachute. The quadcopter will then initiate its stabilization control program and begin its autonomous flight control. The parachute will descend with its GPS and ballast mass to ensure it does not drift far away. If the system does not pass the software checks, then the quadcopter will not release from its parachute and will continue descending under its parachute until it lands. The deployment sequence is illustrated and outlined in more detail in the Mission Concept of Operations Overview.

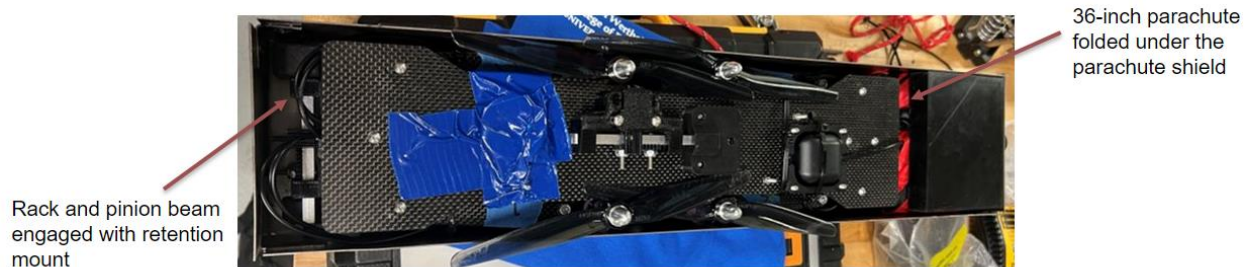


**Fig. 23 Assembled quadcopter in its stowed configuration inside of the container ready to be placed inside of the forward airframe.**

The retention system components were analyzed to ensure all components could withstand the launch loading conditions, specifically the maximum load of 225 lb<sub>f</sub> during the main parachute ejection, found using Eq. (3). Initially, the 80/20 rail assembly was going to be mounted to the 3D printed PETG concentric airframe mount without the aluminum supports. However, stress analysis showed that PETG had a potential to fail during launch and main parachute ejection, which led the team to adding the aluminum supports. The aluminum supports in the concentric airframe mount fasten the 80/20 rail assembly to the forward airframe through four ¼-20 fasteners. The weight of the entire retention system rests above the aluminum supports, with failure in the aluminum supports leading to retention system failure. Solidworks FEA was conducted on the aluminum supports with a desired factor of safety of 2.0 (Fig. 24). A desired factor of safety of 2.0 was chosen, as failure in the aluminum supports would lead to catastrophic failure of the retention system (Table 8).

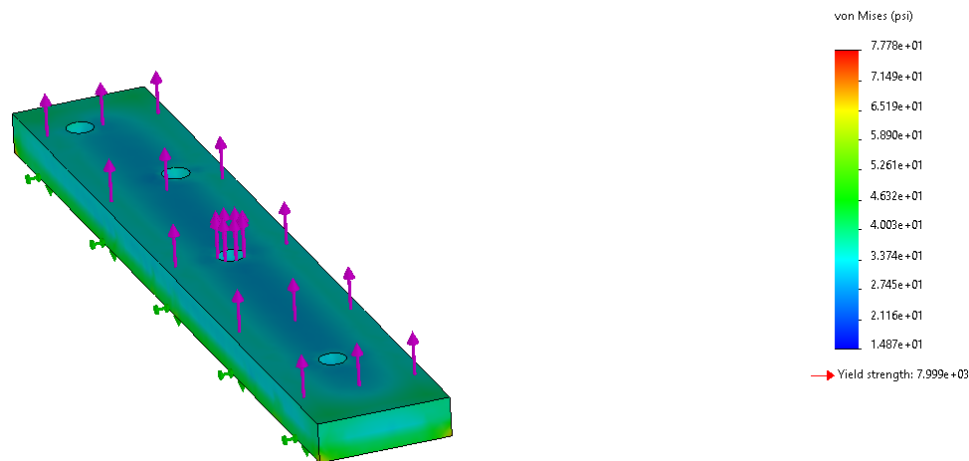


**Fig. 24 Aluminum bar support FEA with the bottom face of the bar restrained, and the load applied to the top face.**

The recovery harness mount keeps the sheet metal container tethered to the main recovery harness after main parachute ejection. The recovery harness mount is mounted to the container through two shoulder bolts, as well as welded. Since failure in the recovery harness mount could lead to a dangerous deployment of the payload, the redundancy in the fastening method to the container was chosen, ensuring the recovery harness mount will remain attached to the container throughout descent and landing. SolidWorks FEA was done on the recovery harness mount with a desired factor of safety of 2.0 (Fig. 25). A desired factor of safety of 2.0 was chosen because failure in the recovery harness mount may lead to catastrophic failure in the deployment of the payload (Table 8). A fastener analysis was also conducted for the two 10-24 shoulder bolts that connect the recovery harness mount to the container (Ref. [4]). The two joining members were steel, simplifying the analysis. The results showed that for a tensile per-bolt load of 112.5 lb<sub>f</sub>, the factor of safety is 1.3. A load of 1450 lb<sub>f</sub> is required to cause failure in the 10-24 shoulder bolts, which is 12.8 times higher than the expected loading.

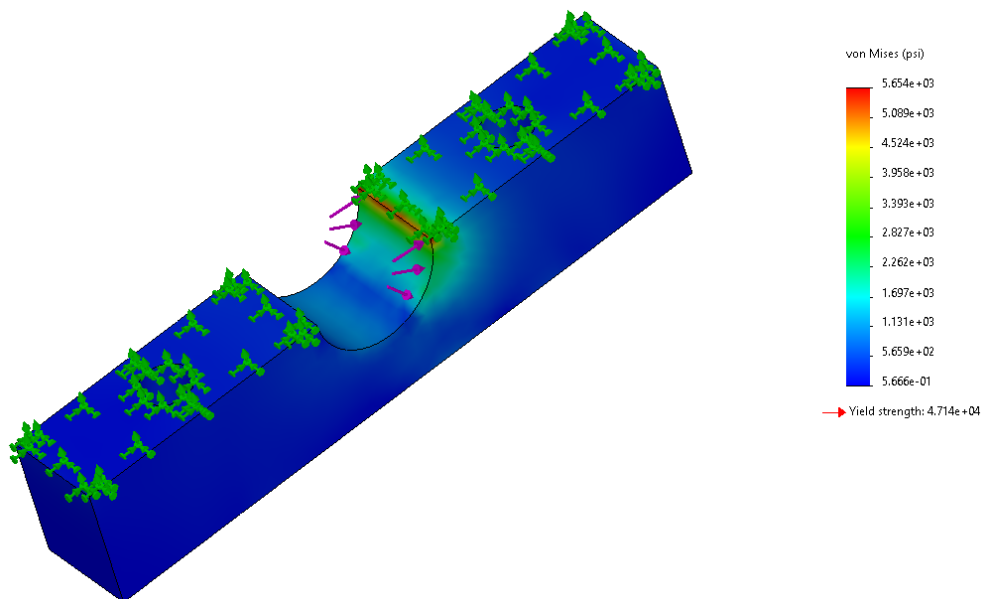


**Fig. 25 Recovery harness mount FEA with the top face restrained and the load applied to the inner half of the circular cutout, simulating the area that the recovery harness will tug on the mount.**

A fastener analysis on the fasteners used to attach the 80/20 linear slides to the container was also conducted. The fasteners utilized are eight M2.5 and two ¼-20 fasteners. The fasteners connect UHMW components to steel sheet

metal, with locknuts utilized to prevent them from coming undone during launch. Locknuts were chosen as they help dampen the effects of vibration on undoing fasteners. Since the joining members were not of the same material, and one is ductile while the other is brittle, the member stiffness is a complex combination of the two materials (Ref. [4]). The fastener analysis results show that for a per-bolt load of 28.125 lb<sub>f</sub>, the factor of safety is 1.28, with a per-bolt load of 250 lb<sub>f</sub> required to cause fastener failure. A factor of safety of 1.25 was desired, as failure in the 80/20 linear slides would occur prior to the fasteners failing. As seen in Table 8, the factor of safety for the aluminum supports, recovery harness mount, and recovery harness are much higher than the desired factor of safety. This is the case for the aluminum supports because of their thickness being more than is required to carry the expected loading. However, since the holes in the aluminum supports are threaded, the thickness of 0.4 in. was needed to ensure a minimum of 5 threads of engagement. For the recovery harness mount, the initial design was to be manufactured from aluminum, which yielded a factor of safety of 5.2. However, steel was chosen to enable the use of MIG welding between the recovery harness mount and the steel sheet metal container. The Kevlar shock cord was chosen, as the team did not have a thinner recovery harness material on-hand. The increased factor of safety is allowable for the recovery harness as its weight does not harm the payload and its high factor of safety ensures it will be reliable during launch.

**Table 8: Retention System Component Stress Ratings**

<b>Component</b>	<b>Load</b>	<b>Factor of Safety</b>
Aluminum Supports	225 lb <sub>f</sub>	102.8
Recovery Harness Mount	225 lb <sub>f</sub>	8.33
Aluminum Parachute Swivel	225 lb <sub>f</sub>	4.44
1/8" Kevlar Shock cord	225 lb <sub>f</sub>	13.33

### 3. Quadcopter Electrical Design

In terms of the quadcopter electrical subsystems, all the sensors and actuators on the quadcopter are connected through a printed circuit board (PCB), to ensure wire management and so that no wires would become loose during the flight (Fig. 26). The PCB is mounted on the top frame, inside the body of the quadcopter. Connected to the PCB is an HC-SR04 Ultra sonic Distance sensor with a range of 0.8 in to 157.4 in, which functions to detect landing and was chosen because of its low cost, accuracy of 0.3 in, and non-contact detection capabilities. It is mounted externally on the bottom frame of the quadcopter to ensure line of sight with the ground. The microprocessor that was chosen was the Raspberry Pi Zero 2 W due to its small form factor and fast processing rate of 1 GHz. An Arducam IMX219 Raspberry Pi Camera Module is connected directly to the Pi, which functions to take pictures of the launch vehicle's landing site and is also mounted externally on the bottom frame to establish line of sight with the ground. The MTi-7 GNSS/INS IMU was chosen because of its high accuracy and sensor fusion performance. It is connected to both the Adafruit BMP388 - Precision Barometric Pressure Altimeter and the uBLOX MAX-M8Q GPS, and it sends heading, position, velocity, acceleration, and barometer data back to the Pi. All of these sensors are mounted on the PCB. An Xbee Pro S3B RF module is wired externally to the PCB which allows for communication and data transmission with the ground station. The Xbee Pro S3B was selected because it had been previously used successfully by the team.



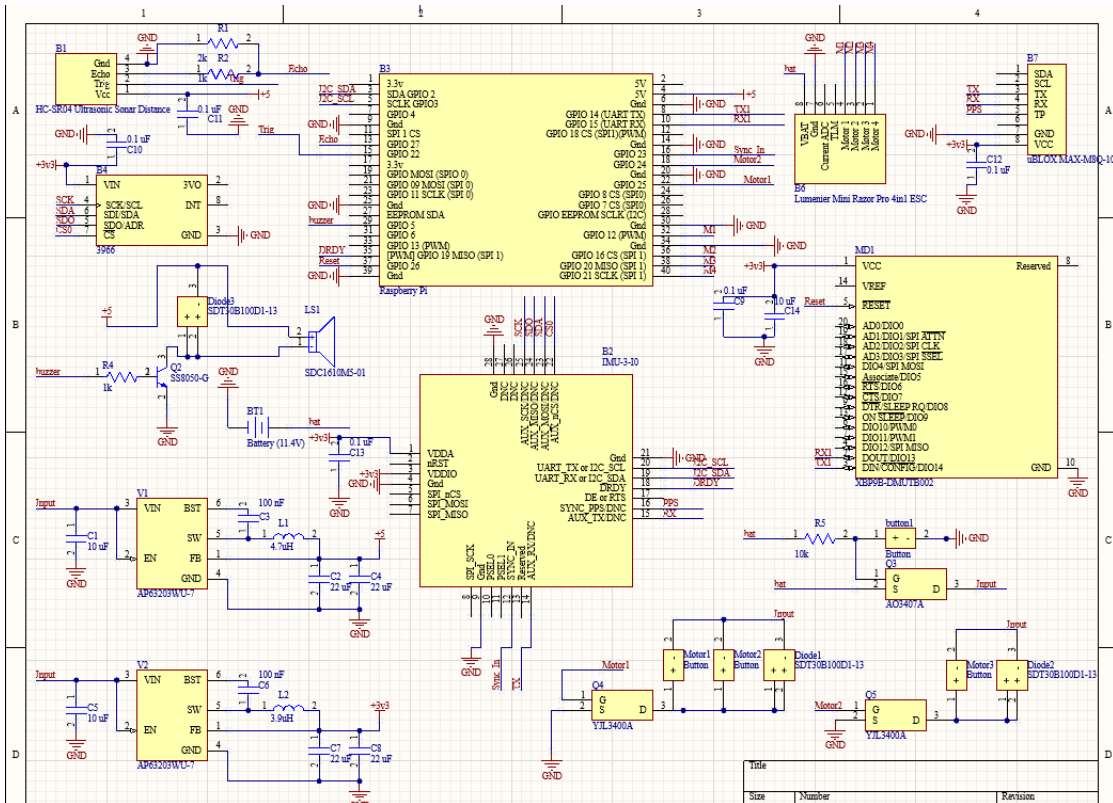


**Fig. 26 Altium Schematic showing electrical connections between all the components.**

A 5V active buzzer is also used to confirm proper operation of all of the electronics and as a method for tracking the quadcopter after landing. A Lumenier Mini Razor Pro 4-in-1 electronic speed controller was picked due to its compact size and its ability to support faster input signals with a faster update rate and a lower latency, such as with the Dshot protocol. The electronic speed controller was used to control 4 brushless FLASH HOBBY D2830 1300 KV motors, which were chosen to provide a 2:1 thrust to weight ratio to keep the drone stable during flight. Three DC motors used in the drone’s release mechanism from its container are also wired to the PCB. A pushbutton that would be accessed through a hole in the airframe is used to arm all of the electronics connected to the PCB, which would be powered using a Turnigy High Capacity 4000mAh LiPo Battery. The battery was chosen to provide the quadcopter with 5 to 10 minutes of flight time. Testing confirmed that the chosen battery would be able to power the quadcopter for 5 minutes minimum at 75% full throttle.

#### 4. Quadcopter Software Design

The quadcopter software undergoes a series of stages throughout the launch vehicle’s flight (Fig. 27). When the payload is armed on the launch pad, all sensors will be initialized, and data collection begins. The payload will remain idle on the launch pad until the IMU detects the acceleration of launch. Once launch is detected, the payload is idle until main ejection is detected. This is done through a combination of the barometer data and the expected time of ejection from the OpenRocket simulation. Once outside the airframe, the barometer and GPS will be able to collect data on the quadcopter’s altitude. Using the altitude data, the quadcopter will wait until 600 ft to deploy from the container. This will allow for time for the main parachute to deploy before the payload releases from the container. After the container release, the quadcopter checks all sensors to ensure that the data is within expected limits. Furthermore, the quadcopter waits for a signal from the ground station before deploying from its parachute at a maximum of 400 ft. This is to guarantee that the quadcopter can safely release even if it cannot maintain control after deployment. After deployment, the quadcopter avoids the descending parachute and begins its autonomous navigation. Using the launch vehicle’s GPS coordinates sent by the ground station, the quadcopter navigates to the launch vehicle and takes images of the landed vehicle. Once it completes taking images, the quadcopter will descend and land. If during the flight the quadcopter begins to pose a danger to spectators, the ground station can take manual control to shut it down, emergency land, or complete simple maneuvers.

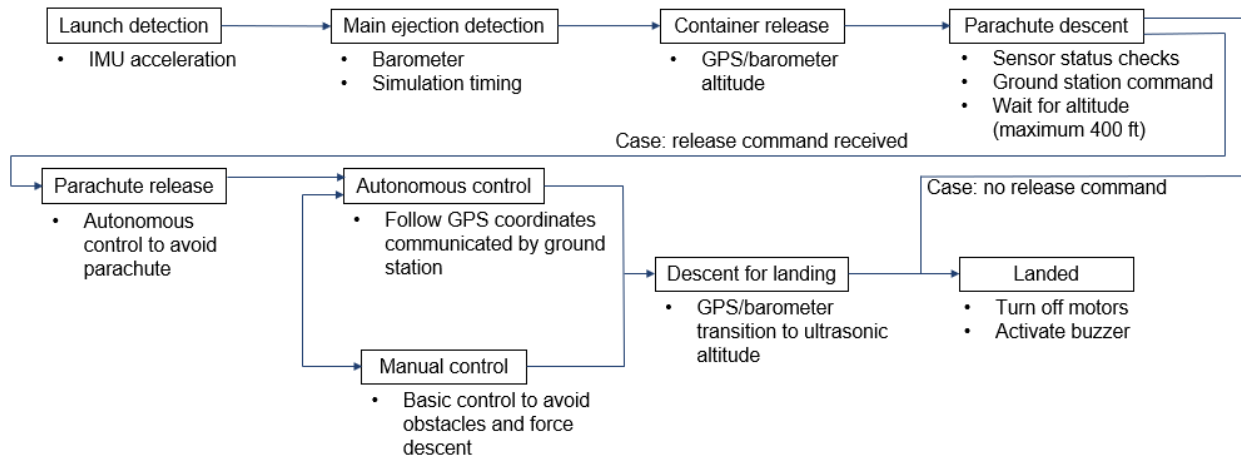


**Fig. 27 Payload software flow chart.**

The quadcopter is controlled by six PID loops: roll, pitch, yaw, thrust, and two world-conversion loops (Ref. [5]). Using the distance from the desired coordinates and yaw orientation, the world-conversion loops, one for roll and one for pitch, find the roll and pitch angles the quadcopter should rotate to reach the coordinates. These loops have maximum bounds to ensure the drone does not flip when targeting far away coordinates. The roll and pitch loops take the roll and pitch targets output by the world-conversion loops as inputs to determine the throttle commands for the roll,  $R_{throttle}$ , and pitch,  $P_{throttle}$ . The thrust controller takes the altitude determined by the barometer, GPS, and, at low altitudes, the ultrasonic sensor to determine the throttle command,  $T_{throttle}$ , for lifting the quadcopter. The yaw controller takes the yaw orientation of the quadcopter and determines the yaw throttle,  $Y_{throttle}$ , to rotate the quadcopter to the desired yaw target. These throttles are mixed using Eqs. (7)-(10) to determine the throttle of each motor where  $M_1$ ,  $M_2$ ,  $M_3$ , and  $M_4$  are the motor commands for motors 1, 2, 3, and 4, respectively (Fig. 28).

$$M_1 = T_{throttle} + R_{throttle} + P_{throttle} + Y_{throttle} \quad (7)$$

$$M_2 = T_{throttle} - R_{throttle} + P_{throttle} - Y_{throttle} \quad (8)$$

$$M_3 = T_{throttle} + R_{throttle} - P_{throttle} - Y_{throttle} \quad (9)$$

$$M_4 = T_{throttle} - R_{throttle} - P_{throttle} + Y_{throttle} \quad (10)$$

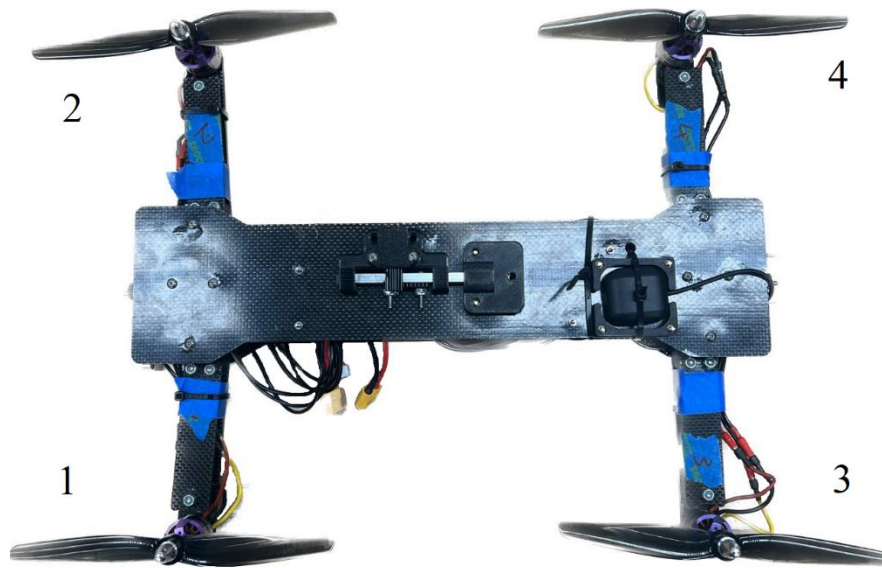


**Fig. 28 Quadcopter motor configuration.**



The motor commands are sent to the ESC using the Dshot communication protocol. Dshot was chosen over pulse width modulation (PWM) because it was found during early testing that PWM had up to a 40 ms delay in motor response time while Dshot has less than a 1 s delay. The Dshot protocol consists of 16-bit frames which include the motor command, a telemetry request bit, and a checksum (Fig. 29). The first 11 bits consist of the motor command with 2048 possible values. 48 values are reserved which results in 2000 possible throttle values for each motor. Telemetry data is not collected from the ESC, so the telemetry request is always set at zero. The checksum allows the ESC to check for interference in the Dshot command and ignore any scrambled commands. Each individual bit is determined by a short or long high time in the signal. A long high time corresponds to one and a short high time corresponds to zero.

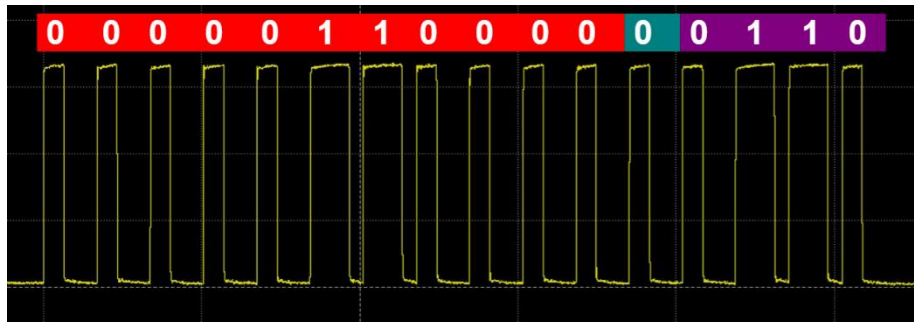


**Fig. 29** Labeled Dshot command probed by oscilloscope. The red section is the motor command, the turquoise section is the telemetry request bit, and the purple section is the checksum.

#### IV. Mission Concept of Operations Overview

The complete mission of the launch vehicle is shown in Fig. 30 from launch to end of mission for both launch vehicle and payload. The payload is left in a dormant state inside of the forward airframe, with a button that can be armed on the launch pad. The avionics bay has an arming pin that remains attached and is removed on the launch pad to arm the flight computer and altimeters. The mission concept of operations begins once the launch vehicle has been prepared by the RSO and is ready to be placed on the launch rail.

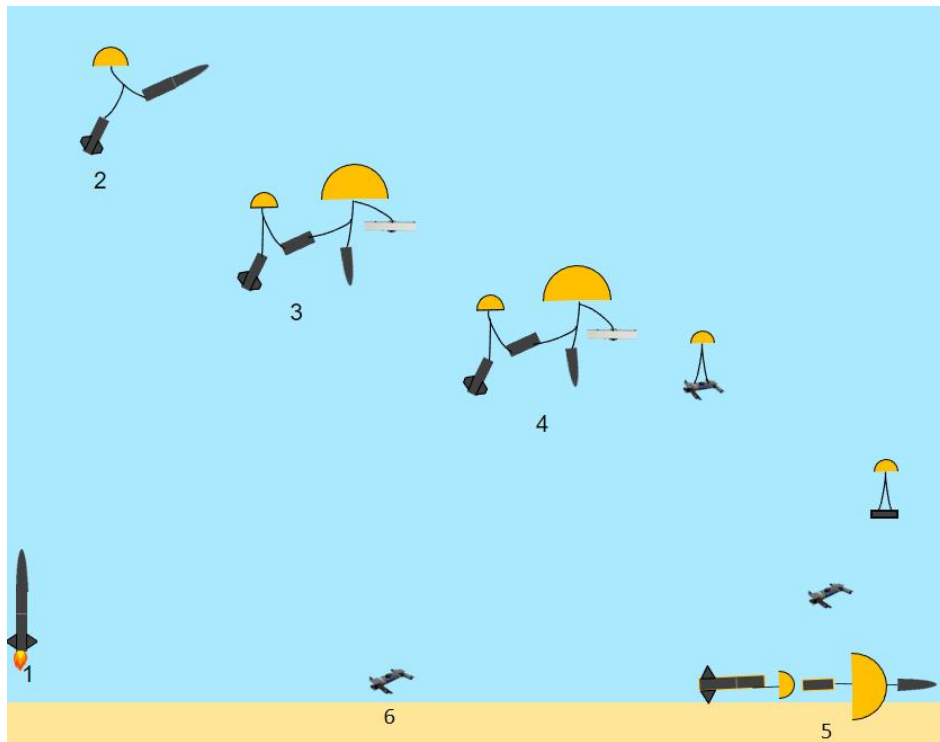


**Fig. 30** Concept of operation schematic from launch to end of mission.

0. **Preparation:** This phase begins when the team receives approval to prepare the launch vehicle from the RSO. The team will bring the launch vehicle out to the launch pad and load it on the 1515 launch rail provided by ESRA by sliding on the two rail buttons located on the aft section of the launch vehicle. When the launch vehicle is properly canted, the altimeters and the payload will then be armed via the pin on the avionics bay and the button on the quadcopter. After altimeters finish their start up beeping sequence, continuity will be confirmed by the repeating three beeps of the primary and backup flight computers. Once altimeter continuity is confirmed, dual igniters will be installed and connected to the launch control system using the provided alligator clips. This phase is concluded with the payload, altimeters, and motor armed on the launch pad.
1. **Liftoff:** This phase begins with motor ignition initiated by the RSO using the ESRA launch control system. The motor accelerates the launch vehicle off the 1515 launch rail, which helps keep the launch vehicle vertical throughout the initial stages of motor ignition. The launch vehicle ascends for 24 s, with a maximum acceleration of  $325 \text{ ft/s}^2$ . The thrust plate carries the load of the motors thrust and transfers it to the airframe and aft. The fins carry the aerodynamic loads during flight and correct the launch vehicles flight path into a stable trajectory. During ascent, the quadcopters IMU records the acceleration data and detects the large, sustained acceleration, changing the quadcopters software state to “launch”. The quadcopter then begins analyzing the barometer data to notice the main parachute deployment and tracks the time since launch to cross-reference with the OpenRocket simulation. This phase is concluded with the launch vehicle reaching its apogee.
2. **Apogee:** This phase begins with the launch vehicle reaching its apogee, beginning its downward descent. The altimeters in the avionics bay detect apogee via pressure changes through the pressure port on the avionics bay coupler. The flight computer sends current to the drogue ejection charge located in the aft of the launch vehicle. The black powder ejection charge ignites, causing a sudden, large increase in pressure between the aft and the avionics bay of the launch vehicle. This increase in pressure separates the launch vehicle, deploying the 36 in drogue parachute. The drogue parachute opens and slows the descent rate of the launch vehicle to 79 ft/s. After a 2 second delay, the backup black power ejection charge is fired as a redundancy. The quadcopter remains in the forward section of the launch vehicle, still in its “launch” state. This phase ends with the launch vehicle descending to an altitude of 800 ft, where the main parachute deployment occurs.
3. **Main Parachute Deployment:** This phase begins when the launch vehicle is descending under the drogue parachute and reaches an altitude of 800 ft. The altimeters detect the altitude and send current to black powder charges located inside the CO2 ejection system to break the CO2 cartridge seal. The CO2 released from the cartridge pressurizes the forward airframe very quickly causing the nosecone to separate and the main parachute to eject. As the main parachute is ejected and deployed, the container with the quadcopter inside is ejected from the forward airframe. The container and quadcopter remain tethered to the recovery harness that connects the main parachute to the forward and descend under the main parachute with the launch vehicle. The barometer on the quadcopter detects the sudden pressure change in the forward, checks the time of flight to verify it is approximately the OpenRocket simulation time for main ejection, and switches the state to “ejection”. The quadcopter is now outside of the carbon fiber airframe, and thus the GPS and barometer can receive data. In addition, the Xbee Pro S3B should now have a connection to the ground station. The main parachute slows the descent rate of the launch vehicle to 19 ft/s. This phase ends with the launch vehicle and quadcopter inside of the container descending under the main parachute to an altitude of 600 ft, at which the quadcopter will release from the container.
4. **Quadcopter Container Deployment:** This phase begins when the launch vehicle and quadcopter inside of the container descend under the main parachute to an altitude of 600 ft, switching the state of the quadcopter to “container release”. The barometer and GPS on the quadcopter detect the altitude, and the microprocessor sends current to the DC motors on the container-deployment rack and pinion assemblies for 1.5 s. The aluminum beams on the rack and pinion assemblies disengage from the retention mounts on the container, allowing the quadcopter to fall from the container due to its weight. The quadcopter releases from the container along with its 36 in parachute, the motor arms unfold, and the quadcopter begins descending under its parachute at 21 ft/s. While the quadcopter is descending under its parachute, it confirms that the IMU, GPS, and barometer measurements are within expected limits. This phase ends with the quadcopter

descending under its parachute to an altitude of 400 ft, at which the quadcopter awaits the command from the ground station to release from the parachute.

5. **Quadcopter Parachute Release and Flight Operations:** This phase begins with the quadcopter descending under its parachute to an altitude of 400 ft. The barometer and GPS on the quadcopter detect the altitude and are ready to release from the parachute if the software system checks were all passed. To release from the parachute, the quadcopter must receive a command from the ground station, which is given if the quadcopter is in a safe area to release away from people or hazardous terrain. If provided the release command, the quadcopter switches to the “parachute release” state and the microprocessor sends current to the DC motor on the parachute-deployment rack and pinion assembly for 1.5 s. The aluminum beam on the rack and pinion assembly disengages from the parachute stop, releasing the connection between the parachute and the quadcopter. The quadcopter releases from its parachute and switches to the “flight” state, in which it immediately stabilizes itself and performs a parachute avoidance maneuver. The quadcopter enters a hover state at a set coordinate, waiting for the launch vehicle to land and for the ground station to provide the GPS coordinates of the launch vehicle landing site. Once the coordinates have been provided, the quadcopter autonomously navigates over to the launch vehicle landing site and captures an image of the landing site. During this time, the quadcopter's parachute is descending to the ground. The parachute has a ballast mass of 0.5 lb and a GPS for recovery. This phase ends with the launch vehicle having landed, the quadcopter's parachute having landed, and the quadcopter hovering above the landing site of the launch vehicle.
6. **Quadcopter Landing:** This phase begins with the quadcopter hovering above the launch vehicle landing site after performing its mission of capturing an image of the landing site. The quadcopter changes its state to “landing” and begins to autonomously navigate to the coordinates of the landing site, which is 25 ft from the launch vehicle landing or a given coordinate from the ground station. Once the quadcopter is at the coordinates to land, it begins a slow descent, actively checking the ultrasonic sensors data, which has a range of 0.07 ft to 13.1 ft. Once the ultrasonic sensor is reporting that the quadcopter is within 13 ft of the ground, altitude control switches over entirely to the ultrasonic sensor, which is more accurate than GPS data for small altitude changes. The quadcopter continues to descend until it reaches an altitude of 1 ft, at which the command to turn off all the motors will be given. The quadcopter will then fall to the ground, and switch to the “landed” state. The quadcopter saves the launch and flight data, the images of the launch vehicle landing site, and activates a buzzer that helps locate the quadcopter. The quadcopter has a GPS onboard that relays live data to the ground station for recovering the quadcopter. This phase ends with the launch vehicle, quadcopter, and quadcopter parachute having landed and relaying GPS data to the ground station for recovery.

## V. Conclusion

### A. Lessons Learned

#### 1. Management

Many significant lessons were learned by the management team this year due to this being the team's first year successfully attending the Spaceport America Cup competition. Firstly, the team learned that the initial plan to reserve the fall semester largely for design and the spring semester for manufacturing and testing was not an appropriate division of time, as the team's schedule became very tight in the spring semester, causing the backup launch day to have to be employed for the test flight. This put the team on a very tight schedule to complete all documentation and prepare for the start of the summer. In the future, the team will begin testing and analysis during the fall and push for a much earlier launch date for any potential test flights.

Additionally, due to the scope of the projects the Spaceport America Cup allows, the team also determined that additional leadership would have been helpful. In future years, the team intends to always ensure there are separate individuals serving as the Project Manager and Chief Engineer of the project, and the team will also be adding a Vehicle Integration Engineer and a Payload Integration Engineer who are responsible for overseeing the technical teams. Lastly, the team will be adding a Composites lead to the Manufacturing Support team to assist in further developing the teams SRAD carbon fiber processes and to allow the Structural Design lead more space to analyze, test, and manufacture features of the vehicle design. The team also hopes to obtain a student member Flyer of Record to allow easier access to test flights.

None of the work done by the team this year would have been possible without external sponsors and professor cooperation. Thus, the team has learned the value of these things and intends to pursue more corporate sponsors in the

future with a focus on material donations, as this year the team was forced to alter some of the original designs, like SRAD carbon fiber fins, due to a shortage of material and funding.

## 2. *Propulsion*

The design for the propulsion system was simple as it was based on the objectives from the competition and the design objectives from the team. The team chose a motor based on simulated performance, which will continue to be the case in the future. This was by far the strongest motor the team had ever used before and designing for its use proved more complicated than expected with the failure of the modular aft section during the test flight. Further analysis will need to be done in conjunction with the structures design in the future to ensure significant mechanical failure does not occur when utilizing motors as powerful as this one.

## 3. *Structures*

The most significant lessons learned regarding the vehicle structures resulted from the design, testing, and subsequent failure of the modular aft system. A lack of proper technical analysis, including but not limited to FEA simulation and load testing, were the primary causes of failure for the system as a whole. In the future, this will be remedied through greater scrutiny and testing of the design in the early stages of the project. Greater reinforcement of the centering rings will be necessary in future versions of the design, which can be accomplished through use of thicker plate stock, a wider outside ring, the introduction of an inner ring (adjacent to the motor casing), and the inclusion of fillets on sharp corners for stress mitigation. The project also showed the importance of accurate and well-organized models in the design stage of the project, as inconsistencies and lack of model verification led to unforeseen difficulties during manufacture and assembly of the vehicle. In regard to the actual manufacture of the vehicle components, a greater reliance upon CNC machining will significantly improve the quality of aluminum components, while reducing the time needed to machine those components. A number of smaller modifications to the modular aft design are also being discussed, with the aim of facilitating the somewhat difficult assembly process. Removal of fin slots from the airframe, which potentially compromised the structural integrity of the vehicle body, is also a consideration. The viability of this solution will need to be extensively verified by testing and FEA analysis but could mitigate some of the material failure the airframe experienced during the test launch. All of the above solutions will be facilitated in future projects by dividing the work of the current Structural Design lead amongst two roles: the Structural Design lead and the Composites lead. This will reduce the workload of designing and manufacturing the vehicle and will allow for a greater emphasis on testing and analysis.

## 4. *Avionics and Recovery*

A reliable avionics and recovery system is crucial to the success of the launch vehicle since it is the only thing preventing the whole mission from failure. So, attention to detail during every phase of the project is required. During the design phase, things like puncture piston O-rings should be researched not just based on size, but their specific application case, since the O-ring material and shape affects the system's behavior as much as its size. Additionally, testing the designed system is the only way of absolutely proving its functionality, however, ensuring that the system is reliable requires the testing to be done numerous times and maybe under undesirable conditions to see how the performance changes. Finally, the CO<sub>2</sub> ejection system was designed around an ejection charge because it needed to integrate into a COTS altimeter. In the future this system can be expanded by developing SRAD flight computers to be able to employ a more robust method of releasing the pressurized gas such as use of valves or servo actuated motors.

## 5. *Payload*

The team learned multiple lessons from the design, development, and testing of the quadcopter and its retention system. From an assembly and testing point of view, it was realized how important a prototype of the quadcopter would be for the team. This was realized in the middle of October, and the team designed and assembled a prototype of the quadcopter. This prototype enabled many tests to be conducted, with the most important being the tuning of the PID flight controllers. Using the prototype and an 80/20 test stand, the roll and pitch PID controllers were fully tuned, proving the design could be properly tuned. This also provided insight into how the team could improve the tuning procedures for the final quadcopter, which has proved useful as the team is currently tuning the PID flight controllers of the quadcopter.

Similarly, manufacturing the retention system early on in the spring semester allowed for adjustments to be made that led to a successful test flight. It was realized quickly that the 80/20 linear slides impose lots of friction on the 80/20 rail assembly, risking a smooth deployment of the container and quadcopter. This was tested and improved upon

over a series of ground tests using silicon lubricant, and different fastening methods for the linear slides. The final assembly for the retention system was easily deployed from the 80/20 rail assembly.

Additionally, the layout of the PCB went through several iterations leading to the test flight. During the process of developing the PCB, a problem with the Raspberry Pi's voltage step-down converter was encountered, which would occasionally cause a short circuit between 3.3 V and ground. This was believed to be caused by a downstream component connected to the Pi being shorted. As a result, the importance of a separate 3.3 V regulator was realized to prevent overpowering the Pi and avoid the risk of damaging the component. This experience highlighted the need to conduct thorough testing of the electrical subsystems and to implement proper precautions to avoid damage to critical electrical components. In the future, proper measures will be taken to prioritize redundancy and increase the reliability of electrical designs.

## **B. Future applications**

Swamp Launch Rocket Team is an undergraduate student organization and thus is made up of a diverse group of members at all stages in their undergraduate academic career. The leadership team is composed of dedicated members who have displayed the knowledge and talent to lead a subteam and spans a wide range of academic years, both upperclassmen and underclassmen. The transfer of knowledge on the team is accomplished primarily through subteam meetings and documentation. At subteam meetings, members are given the opportunity to participate in design, testing, and manufacturing of the project. Swamp Launch does not have any requirements for subteam membership or participation; members help as they are able, and dedicated members stand out and are given additional opportunities and projects. In the future, the team will continue to run subteam meetings this way but will increase emphasis on encouraging members to read documentation on their own time, thus giving them the background they need to be equipped to directly contribute to design considerations for the current project. Documentation is performed primarily by each subteam lead. Swamp Launch has developed a Handbook of information over the years that each individual in leadership adds to at the end of their term, describing takeaways and processes from their time in leadership. This year, the team intends to expand this Handbook even further to include more technical documentation of processes specifically for the IREC team, as a lack of good documentation caused substantial delays to processes during manufacturing and testing this year.

Finally, the Swamp Launch IREC team would like to continue to put a focus on improving the diversity of team membership and leadership. This year, the leadership team was ~33% female with only 1 female subteam lead. Swamp Launch is home to multiple competition teams and has seen the benefits of a diverse leadership team in improving team culture, morale, and success. It has also been seen that the first step in creating a more diverse member community is a diverse leadership team. Thus, next year Swamp Launch intends to strive to engage with and encourage members belonging to minority groups in order to create a safe, welcoming, and diverse culture well-equipped for success.

## Appendix I: System Weights, Measures, and Performance Data

**Table 9: Launch Vehicle Information**

Number of Stages	1
Vehicle Length	131 in.
Airframe Diameter	6.0 in. (inner), 6.14 in. (outer)
Number of Fins	4
Fin Semi-Span	6.5 in.
Fin Root Chord	15.0 in.
Fin Tip Chord	5.5 in.
Fin Thickness	0.192 in.
Vehicle Weight (no motors, no payload)	38.8 lb.
Payload Weight	9.2 lb.
Propellant Weight	12.0 lb.
Liftoff Weight	60.0 lb.
Center of Pressure	105 in.
Center of gravity	83.9 in.

**Table 10: Propulsion Information**

Type	COTS
Manufacturer	Aerotech
Designation	M2500
Motor Total Impulse	10240 Ns
Motor Average Thrust	2500 N
Motor Peak Thrust	2891 N
Burn Time	3.9 s

**Table 11: Predicted Flight Data and Profile**

Launch Rail Length	17 ft
Launch Vehicle Thrust-Weight Ratio	9.39
Target Apogee	10,000 ft
Predicted Apogee	9996 ft
Rail Departure Velocity	104 ft/s
Minimum Static Margin	1.875
Maximum Velocity	1010 ft/s
Fin Flutter Velocity	1366 ft/s
Maximum Acceleration	10.1 G
Time to Apogee	24 s
Flight Time	164 s

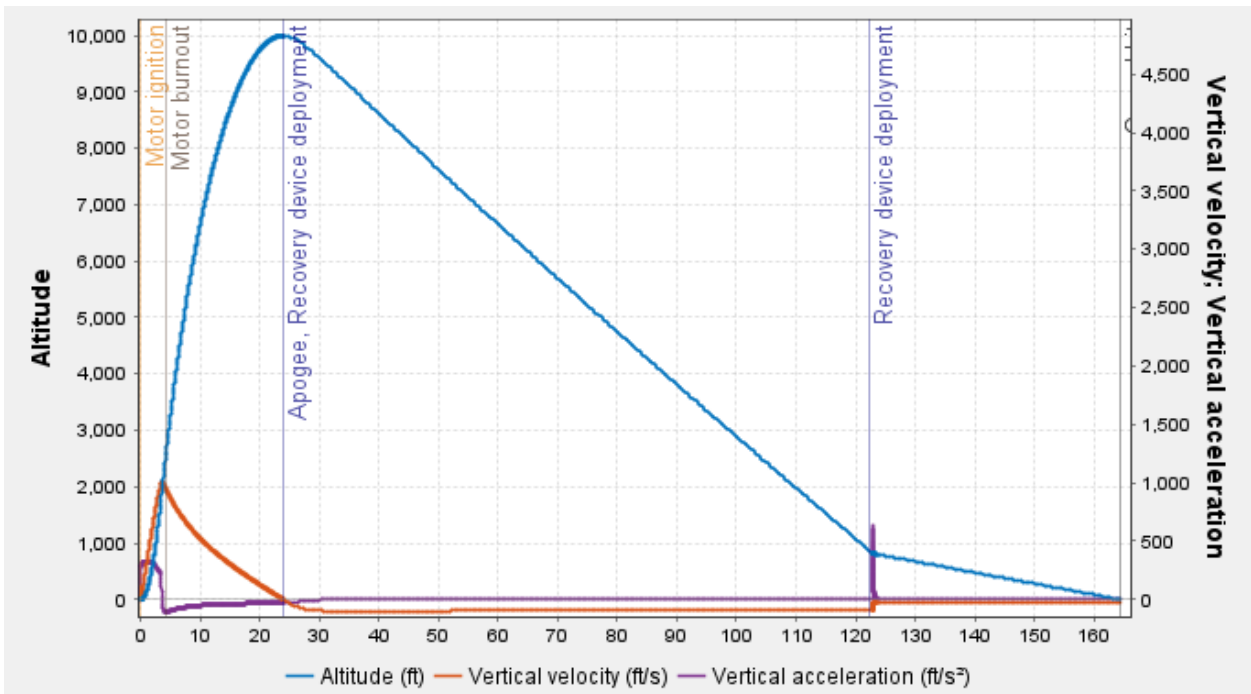


**Fig. 31 The simulated altitude, vertical velocity, and acceleration of the rocket over time.**

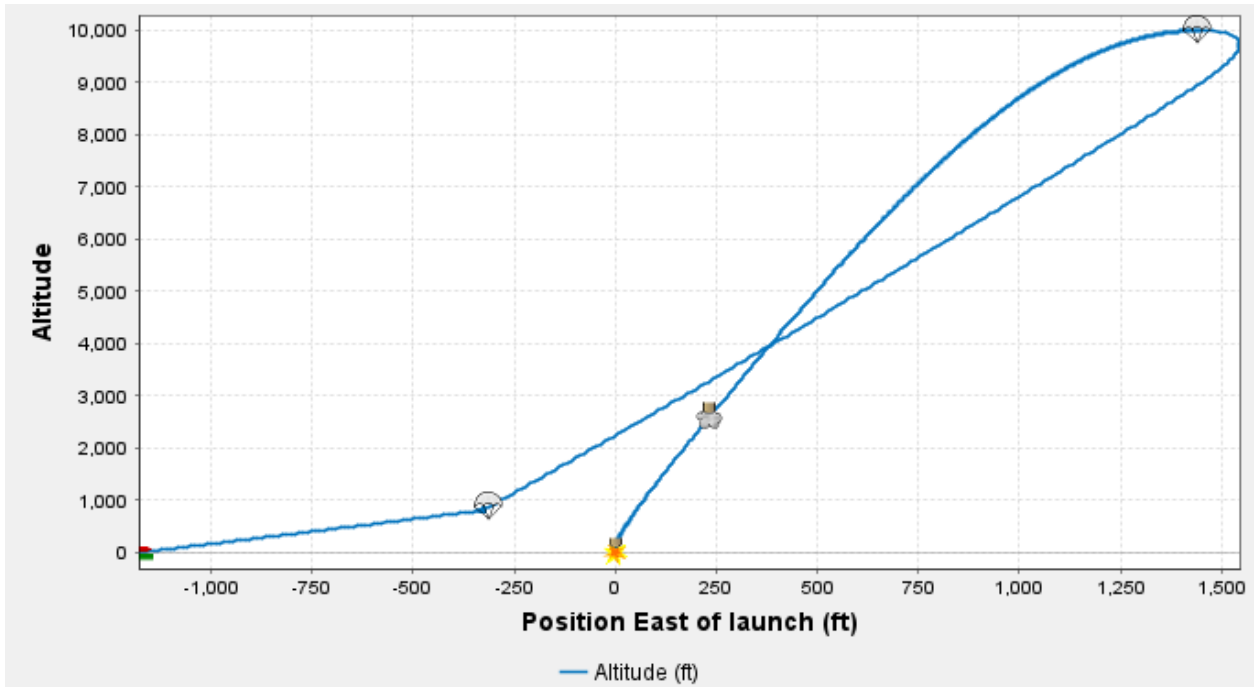


**Fig. 32 The simulated flight profile of the rocket.**

**Table 12: Recovery Information**

Primary Altimeter	StratoLogger SL100
Secondary Altimeter	StratoLogger CF
Drogue Parachute	36 in Standard Rocketman Parachute
Drogue Parachute Swivel	Steel Swivel
Drogue Parachute Deployment Charge (Primary)	3.5 g of Black Powder
Drogue Parachute Deployment Charge (Redundant)	4.2 g of Black Powder
Drogue Parachute Deployment Altitude	Apogee
Drogue Parachute Descent Rate	80 ft/sec
Aft Recovery Harness	½ in Kevlar shock cord (40 ft long)
Main Parachute	96 in Iris ultra-Standard Parachute
Main Parachute Swivel	Steel Swivel
Main Parachute Deployment Charge (Primary)	34 g of CO2 (0.05 g of Black Powder)
Main Parachute Deployment Charge (Redundant)	34 g of CO2 (0.065 g of Black Powder)
Main Parachute Deployment Altitude	800 ft
Main Parachute Descent Rate	19 ft/sec



Total Drift Radius	0.4 mi
Forward Recovery Harness	½ in Kevlar shock cord (40 ft long)
Eyebolts	3/8" Steel Eyebolts
D-Links	5/16" D-links

## Appendix II: Project Test Reports

### A. Recovery System Testing

#### 1. Drogue Parachute Deployment Test

Independent Variable: Black powder charge size

Dependent Variable: Drogue parachute deployment with aft separation

Materials:

- Nosecone
- Forward recovery harness layout
- Payload
- Payload rail system
- Avionics bay
- Avionics bay rivets
- Aft recovery harness layout
- Aft airframe
- Aft shear pins
- Drogue deployment charge (3.5 g)
- 9V battery
- Camera
- Test stand

Procedure:

- The forward recovery harness layout was assembled and placed inside the forward airframe along with the payload and payload retention system assembly. The nosecone and avionics bay were connected to the forward airframe with rivets and shear pins. Then the aft recovery harness layout was assembled and placed inside the aft airframe along with the 3.5 g of black powder as the drogue deployment charge.
- The aft airframe was secured on the avionics bay with 4 shear pins. The fully assembled launch vehicle was laid out on an elevated test stand,
- The drogue ejection charge was ignited using a 9 V from a safe distance to observe the separation of the aft airframe from the avionics bay along with drogue parachute ejection. The test was recorded with a camera for further visual analysis.
  - Note: Ejection testing utilizing flight computers performed during test flight.

Results:

The aft airframe was separated from the avionics bay and ejected the drogue parachute successfully. Thus, the test was deemed successful.



**Fig. 33 Instance of separation.**

## 2. CO<sub>2</sub> Ejection System Puncture Test

Independent Variable: black powder charge inside the CO<sub>2</sub> ejection system size

Dependent Variable: puncturing of CO<sub>2</sub> cartridges

Materials:

- CO<sub>2</sub> ejection system assembly
- 34 g CO<sub>2</sub> cartridges
- Vice
- Black powder charge (0.05 and 0.075 g)
- 9V battery
- Camera

Procedure:

- The CO<sub>2</sub> ejection system was assembled with a 0.05 g black powder charge and a 34 g CO<sub>2</sub> cartridge.
- The assembly was held by a vice to prevent it from moving.
- The black powder charge was ignited using the battery from a safe distance to observe the CO<sub>2</sub> ejection system puncturing the cartridge. The test was recorded with a camera for further visual inspection.
- The test was repeated with 0.075 g black powder charge to observe difference in puncturing.
- Tests were recorded with a camera for further visual analysis.

Results:

For 0.05 g of black powder, the CO<sub>2</sub> cartridge was punctured, and the return spring successfully retracted the puncture piston back. This resulted in all the gas being released in less than one second. When the same test was repeated with a 0.075 g charge, the CO<sub>2</sub> cartridge was also punctured. However, the release of the gas took considerably longer compared to the previous test.



**Fig. 34 The CO<sub>2</sub> ejection system is being held by the vise (yellow). The expanding CO<sub>2</sub> gas from the punctured cartridge can be seen as white gas. This happened in less than one second. The visual was captured from a slowed down recording of the test.**

Discussion:

After further inspection of the system, the longer gas release time was found to be due to the return spring failing to retract the puncture piston. Due to the bigger black powder charge, puncture piston was

pushed past the combustion chamber cylinder. This resulted in the puncture piston getting stuck outside of the cylinder and clogging the punctured hole. It was concluded that the black powder charge needed to be weighted carefully to 0.05 g.

### 3. Main Parachute Deployment Test

Independent Variables: CO2 cannister size

Dependent Variables: Main parachute deployment

Materials:

- Forward airframe
- Nosecone
- Forward recovery harness layout
- Payload and retention system
- Avionics bay
- CO2 ejection system with 34 g CO2 cartridges
- Shear pins (4, 5)
- 9V battery
- Test stand

Procedures:

- The forward recovery harness layout was assembled and placed inside the forward airframe along with the payload and payload retention system assembly. The nosecone was connected to the forward airframe with 4 shear pins and the avionics bay was connected to the forward airframe with 4 rivets.
- The CO2 ejection system was fired using the 9V battery to observe the nosecone separation and main parachute ejection.
  - Note: Ejection testing utilizing flight computers performed during test flight.
- The test was repeated with 5 shear pins instead of 4 shear pins.
- Tests were recorded with a camera for further visual analysis.

Results:

The main parachute deployment test with 4 shear pins resulted in the nosecone separating and main parachute ejecting successfully. However, the separation force was not big enough to eject the payload outside of the airframe. The same test was repeated with 5 shear pins connecting nosecone to the forward airframe. This resulted in a much stronger ejection and successfully ejected the main parachute and the majority of the payload outside of the airframe, which can be seen in Fig. 35.



**Fig. 35** This image was taken shortly after the deployment test. The nosecone was ejected outside of the camera's angle. The black parachute protector and the parachute can be seen on the ground after ejection. The payload container (steel box sticking outside of the forward airframe) came out almost completely. The rest of the container being stuck in the airframe was thought to be due to the airframe resting on the chair.

Discussion:

The CO2 takes a certain amount of time to fully release from the cartridge into the airframe. So, when configured with 4 shear pins, the airframe reached the pressure to break the shear pins before all the CO2 was fully expanded. This resulted in a weaker ejection force than expected. When the test was repeated with 5 shear pins, the airframe had more time to build up pressure inside before the shear pins broke. This resulted in a stronger ejection force.

#### 4. *Altimeter Functionality Ground Test*

Independent Variables: Stratologger SL100/Stratologger CF

Dependent Variables: LED light turning on

Materials:

- Stratologger SL100
- Stratologger CF
- Stratologger data transfer cable
- LED lights
- Laptop
- PerfectFlite software

Procedure:

- The Stratologger SL100 was connected to a laptop using the data transfer cable. LED lights are connected to drogue and main charge terminals.
- Using the PerfectFlite software, current readings for the sensors were recorded.
- Using the PerfectFlite software, self-tests for the altimeters were run on the altimeters.
- Drogue and main charge were fired using the software to observe the LED light.
- The same procedure was repeated with StratoLogger CF.

Results:

Both altimeters output sensor data that was within the manufacturer uncertainty. The self-tests that were run by the PerfectFlite software were successful. When the drogue and main ejection charges were triggered, both LED lights lit up. The tests were successful, so the altimeters were deemed functional.

## 5. Test Flight

Independent Variables: Black powder and CO2 ejection system

Dependent Variables: Drogue and main parachute ejection

Materials:

- Fully assembled launch vehicle
- Fully assembled payload
- Fully assembled avionics bay

Procedures:

- The avionics bay was fully assembled along with the CO2 system.
- Two 34 g CO2 cartridges were used in the CO2 system, with the primary cartridge having a 0.05 g black powder charge and the backup having a 0.065 g black powder charge.
- The avionics bay was assembled into the launch vehicle, and the altimeters were armed on the launch pad.



**Fig. 36 The recovery site shows the launch vehicle with both sections fully separated. The main parachute was caught in a power line, however the launch vehicle and payload were fully recovered.**

Results: The launch vehicle separated at apogee as expected, however both the forward and aft section of the vehicle separated. This caused the launch vehicle and the payload to drift 2.2 mi, due to the drogue and main parachute deploying at apogee. The quadcopter also deployed from the container at a higher-than-expected altitude due to a time-sync error in the software, which partially occurred due to the main ejection happening at apogee.

Discussion: Upon further analysis, the altimeter data showed that the drogue ejection charges were fired at apogee and the CO2 system ejection charges were fired at 800 ft as planned. It is hypothesized by the team that the force of drogue ejection caused the payload container to hit the nosecone shoulder, shearing the shear pins and deploying the main parachute at apogee. It was also found that the CO2 cartridges were not punctured by the puncture pistons, leaving the cartridges still full. The black powder charges were analyzed, and it was found that they had properly fired, eliminating any errors in the altimeters. It was determined that there was a mechanical failure in the puncture piston, which led to a failure in breaking the CO2 cartridge seal.

## 6. Recovery System Dual-Redundancy

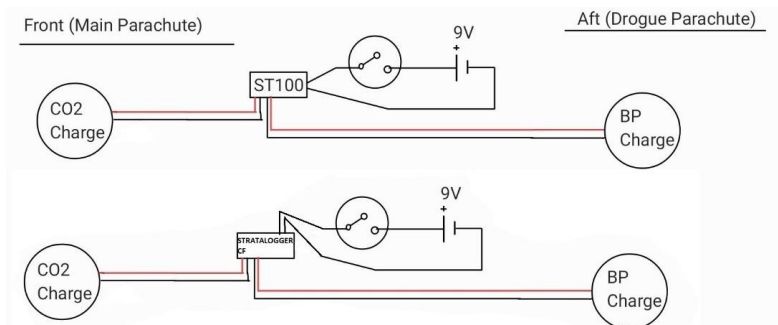


**Fig. 37 The wiring diagram for the Primary (top) and Redundant (bottom) Altimeters.**

Two independent flight computers that are powered by independent batteries were implemented into the avionics bay design to ensure redundancy in the system and to meet competition requirements. Reliability and cost were the prominent factors that affected the recovery design choices. So, the flight computers were chosen based on team inventory and testing with various models' reliability. A COTS StratoLogger SL100 has been used as the primary altimeter by the team for more than five flights and has reliably collected flight data and fired ejection charges for all the flights. Since it has been reliable in the past and was available in the team's inventory, it was chosen as the primary flight computer for this design. The redundant altimeter is chosen based upon similar criteria. However, the redundant altimeter cannot be identical to the primary altimeter to account for similar failure points. So, a different altimeter was sought after. An additional altimeter that the team has flown on numerous occasions with reliable performance is a StratoLogger CF. Since reliability and the team's familiarity with the device were the main considerations, the StratoLogger CF was chosen as the redundant flight computer. Both the primary and redundant altimeter are powered by individual 9 V batteries. They are disarmed before flight and armed at the launch pad using two SS-5 micro switches. These switches are mounted on a 3D printed switch mount to create a pin plunger arming mechanism. The system is open (disarmed) when the pin is inserted into the mount and closed (armed) when the pin is removed. The switch mounts are accessible from the outside of the avionics bay since they are aligned with the pressure port holes on the switch band.



**B. SRAD Propulsion system testing**

THIS PAGE INTENTIONALLY LEFT BLANK.

**C. SRAD Pressure Vessel Testing**

THIS PAGE INTENTIONALLY LEFT BLANK.

## **D. SRAD GPS Testing**

### *1. GPS Cold Start Test*

Independent Variables: time uBLOX MAX-M8Q GPS is left unpowered.

Dependent Variables: time to a satellite fix.

Materials:

- uBLOX MAX-M8Q GPS
- Raspberry Pi Zero 2 W

Procedure:

- The uBLOX MAX-M8Q GPS was left unpowered for 4 hours.
- The uBLOX MAX-M8Q GPS was connected to the Raspberry Pi Zero 2 W but left unpowered.
- The uBLOX MAX-M8Q GPS was provided power.
- A timer measured the time until a satellite fix was received.

Results:

The GPS took approximately 30 s to receive a satellite fix under a cold start. This matched the GPS specifications. If this occurred during flight at a descent rate of 21 ft/s, the quadcopter would descend 630 ft. This is undesirable and, thus, a hot start will be required for the flight.

## 2. *GPS Hot Start Test*

Independent Variables: time uBLOX MAX-M8Q GPS is left unpowered.

Dependent Variables: time to a satellite fix.

Materials:

- uBLOX MAX-M8Q GPS
- Raspberry Pi Zero 2 W
- Aluminum foil

Procedure:

- The uBLOX MAX-M8Q GPS was left unpowered for 4 hours.
- The uBLOX MAX-M8Q GPS was connected to the Raspberry Pi Zero 2 W but left unpowered.
- The uBLOX MAX-M8Q GPS was provided power and given time to receive a satellite fix.
- The uBLOX MAX-M8Q GPS was wrapped in aluminum foil to interrupt satellite fix.
- The uBLOX MAX-M8Q GPS was unwrapped.
- A timer measured the time until a satellite fix was received.

Results:

The GPS took less than 1 s to receive a satellite fix under a hot start. This matched the GPS specifications. This is ideal for the flight on the launch vehicle. Therefore, the GPS should be given time to receive a satellite fix at the launch site before being loaded into the launch vehicle.

### 3. *GPS Communication Interference Test*

Independent Variables: XBee Pro S3B and uBLOX MAX-M8Q GPS shielding.

Dependent Variables: reliability of communication with ground station and satellites.

Materials:

- uBLOX MAX-M8Q GPS
- Raspberry Pi Zero 2 W
- Two XBee Pro S3B
- Laptop
- Quadcopter
- Launch vehicle
- Container

Procedures:

- The XBee Pro S3B and uBLOX MAX-M8Q GPS was connected to the Raspberry Pi Zero 2 W and assembled on the quadcopter.
- The quadcopter was placed into the container.
- The XBee Pro S3B and uBLOX MAX-M8Q GPS communication reliability was measured.
- The quadcopter was placed inside the forward airframe and launch vehicle is assembled.
- The XBee Pro S3B and uBLOX MAX-M8Q GPS communication reliability was measured.

Results:

Both the GPS and radio had reliable communication while placed inside the container alone. However, when placed inside the forward airframe the radio communication was intermittent when the ground station receiver was aligned with the launch vehicle's centerline and completely lost when the receiver was not aligned with the centerline. The GPS also had intermittent satellite fixes while placed inside the airframe. This result was not unexpected as the carbon fiber airframe and steel container block the radio communication. This gives practice with what to expect when communicating with the payload on the launch field.

#### 4. *GPS Range Test*

Independent Variables: distance between XBee Pro S3B modules.

Dependent Variables: communication reliability.

Materials:

- Two XBee Pro S3B
- Raspberry Pi Zero 2 W
- Laptop

Procedures:

- The XBee radio communication was started while both radios were next to each other.
- One XBee radio was moved further from the other while communication reliability was observed.
- When communication became unreliable and was completely lost the distance between the XBee radios was marked.

Results:

The radios maintained reliable communication up to about 1,000 ft and had unreliable communication for another 300 ft. This is a lower range than expected, as a result, a 5 dBi gain antenna was purchased for the ground station radio to provide more reliable communication between the radios.

## E. Payload Recovery System Testing

### 1. Container Ejection Test

Independent Variables: CO2 ejection system

Dependent Variables: Container deployment

Materials:

- Forward airframe
- Sheet metal container
- Quadcopter
- 80/20 rail assembly
- CO2 ejection system
- Main parachute recovery hardware
- 9V battery
- Test stand

Procedure:

- The retention system was fully assembled inside of the forward airframe, with the quadcopter in its stowed configuration inside of the container.
- The CO2 system was fully assembled with two 34 g canisters and their associated black powder piston puncture charges.
- The main parachute recovery hardware was packed into the forward airframe, and the nosecone was attached, sealing the forward airframe.
- Ejection testing of the forward airframe was conducted using the 9 V battery, with a camera recording to visualize the ejection of the container with the quadcopter stowed inside.
  - Note: Flight computers utilized during test flight.

Results:

As seen in Fig. 38, the main parachute was fully deployed and the container with the quadcopter can be seen coming out of the forward airframe. As the forward airframe was resting on a chair, the container was not able to fully come out of the airframe and fell back inside. This was deemed successful, as the container with the quadcopter would be able to fully eject from the forward airframe during flight.



**Fig. 38 Ejection testing of the forward airframe with the payload retention system and quadcopter fully assembled. The nose cone successfully sheared off, with the main parachute and its recovery hardware fully deployed. The container with the quadcopter inside (silver box sticking out of the forward airframe) was fully deployed off the 80/20 rail assembly.**

Discussion:

Initial concerns for the deployment of the container was that the ejection would not be powerful enough to overcome the static friction between the 80/20 linear slides and the T-slotted extrusions on the 80/20 rail assembly. However, it was shown during multiple ejection tests that the CO2 system and the force of the main parachute recovery harness pulling on the container was enough to reliably eject the container with the quadcopter inside.

## 2. Rack and Pinion Actuation Test

Independent Variables: Static load applied to the aluminum beam.

Dependent Variables: DC motor actuation of the rack and pinion.

Materials:

- Container-deployment and parachute-deployment rack and pinion assembly
- Kevlar recovery harness
- Standardized COTS weights
- Scale
- 12V Power supply with a power and ground wire
- Parachute stop

Procedures:

- The rack and pinion assembly was fully assembled, with the aluminum beam in the engaged position.
- The Kevlar recovery harness was tied to one of the aluminum beams, at the end where the loading would be experienced.
- A standardized weight was weighed and added to the other end of the Kevlar recovery harness.
- The 12V power supply was turned on, and the positive wire was connected to the positive terminal on the Dc motor and the negative wire was connected to the negative terminal on the DC motor.
- The wires were connected long enough to allow the DC motor to drive the rack and pinion, moving the aluminum beam to the disengaged position.
- The weight was increased by 0.5 lb until the DC motor stalled.

Results:

**Table 13: Rack and Pinion Stall Test Results**

<b>System</b>	<b>Stall Load</b>	<b>Expected Load</b>
<b>Container-Deployment System</b>	8.0 lb <sub>f</sub>	2.0 lb <sub>f</sub>
<b>Parachute-Deployment System</b>	8.0 lb <sub>f</sub>	5.0 lb <sub>f</sub>

As shown in Table 13, the stall loads for both systems were 8.0 lb<sub>f</sub>, which is greater than the expected load both systems will experience. This test proves the system performance during a static loading scenario for the actuation of the rack and pinion system. Also, this test proves the functionality of the DC motor rack and pinion system, but not the structural integrity of the components involved.

Discussion:

This testing showed the expected results, which was a similar performance between both rack and pinion assemblies. This is because the test is to stall the motor, which is the same for both assemblies. The container-deployment rack and pinion assembly was flown on the test flight. The quadcopter was successfully retained throughout flight and deployed from the container successfully. The rack and pinion system operated correctly with respect to the actuation of the aluminum beam.



### 3. Retention System Test Flight

Independent Variables: N/A

Dependent Variables: N/A

Materials:

- Launch vehicle in its final configuration.
- Payload retention system in its final configuration.
- Quadcopter in its final configuration.

Procedures:

- The quadcopter was fully assembled with all of the sensors functioning to record data and release the quadcopter from the container.
- The retention system was fully assembled in the forward airframe, and fasteners were locked down using Loctite.
- The quadcopter was armed, placed in the container, and stowed in the forward airframe.
- The quadcopter was flown on the fully assembled launch vehicle, and completed its mission up until parachute release, as the autonomous control system was not ready to be flown.

Results:



**Fig. 39 The quadcopter and its parachute after deploying from the launch vehicle and container.**

As seen in Fig. 39, the quadcopter and its parachute were recovered post-launch. The container-deployment retention system was successful at keeping the quadcopter retained until deployment. The container-deployment rack and pinion assemblies were successful at releasing the quadcopter from the container; however, it did sustain structural damage on one of the motor housings. The shroud lines of the parachute caught on one of the motor arms, causing the quadcopter to descend at a faster rate than expected.

Discussion:

The retention system and deployment of the quadcopter was largely successful, except for the quadcopter tangling in the parachute shroud lines. The root cause of this was determined post-launch, as the quadcopter released from the container in the incorrect orientation. This caused the quadcopter to flip when the parachute opened, tangling one of the motor arms in the shroud lines. This can be remedied by editing the design of the parachute shield, which will ensure the quadcopter releases from the container in the correct orientation. The motor housing of the rack and pinion was 3D printed at a higher infill to increase its strength. It could not be determined if the motor housing broke due to an impact load or during nominal loading.

### Appendix III: Hazard Analysis

A personnel hazard analysis was conducted to identify potential hazards to the health and well-being of team members, spectators, and the environment. These hazards may result from manufacturing, testing, and launching the vehicle in addition to the storage and transportation of components and chemicals. The analysis is conducted by identifying hazards, potential causes and likelihood of occurrence, a mitigation approach, and the risk of injury after mitigation. The subsections for this analysis include: Launch Hazards, Testing Hazards, Manufacturing Hazards, Storage Hazards, Transportation Hazards, Environmental Hazards, and Chemical Hazards. By adopting the mitigation approaches listed in the analysis, risk to members, spectators, and the environment can be reduced.

**Table 14: Launch Hazards**

<b>Hazard</b>	<b>Possible Causes</b>	<b>Risk of Mishap and Rationale</b>	<b>Mitigation Approach</b>	<b>Risk of Injury After Mitigation</b>
Motor ignites near person	Ignition during motor loading	Medium; experienced members responsible for motor assembly, safe distance maintained from rocket during launch. This is the first year this particular motor has been used by the team, which could cause a higher chance of mishap	Abide minimum distance code	Low
	Delayed motor ignition after failed launch attempt		Wait at least 60 seconds before approaching rocket in the case of delayed ignition	
Falling debris due to assembly error	Recovery system fails	Medium; assembly is verified for security prior to launch, consistent method used for parachute folding to prevent tangling, but little space could cause chute lines to become tangled when fitting into the vehicle	Verify correct knots and that parachutes are secure to prevent untying	Low
	Main/drogue chute does not open after deploying		Ensure shroud lines are not tangled and parachutes have been folded correctly	
			Direct rocket launch away from members and spectators	
Falling debris due to mechanical failure	Shock cord fails	Low; components such as shock cord, altimeters, and fin material are verified as appropriate for use before launch	Inspect shock cord for frayed portions to prevent tearing	Low
			Direct rocket launch away from members and spectators	
	Main/drogue parachute does not deploy		Conduct redundant altimeter testing prior to launch	
			Conduct main and drogue deployment testing prior to launch	

	Fins are damaged		Ensure fin material is strong enough to undergo expected loads	
Ballistic rocket	No separation events after apogee	Low; test flight completed before competition launch proving appropriate stability, rail velocity, and parachute deployment for avoiding ballistic event	Conduct redundant altimeter testing prior to launch	Low
			Conduct CO <sub>2</sub> cartridge puncture testing prior to launch	
			Conduct main and drogue deployment testing prior to launch	
			Verify acceptable stability prior to launch	
	Verify acceptable rail velocity prior to launch			
Vehicle significantly changes trajectory mid-flight		Direct vehicle launch away from members and spectators		
Rocket launches too slowly off rail				
Black powder ignites near person	Static electricity ignites black powder	Low; experienced members handle black powder. Charges created ahead of time rather than at launch site, decreases risk of ignition near spectators	Members handling black powder ground themselves	Low
Electrical shock/burns from component wiring	Exposed live wire	Low; experienced members responsible for wiring	Component wiring completed before attaching power supply	Low

**Table 15: Testing Hazards**

<b>Hazard</b>	<b>Possible Causes</b>	<b>Risk of Mishap and Rationale</b>	<b>Mitigation Approach</b>	<b>Risk of Injury After Mitigation</b>
Premature ejection test	Black powder ignites during loading	Low; black powder handled with care to avoid premature ejection	Members handling black powder will <u>ground themselves</u>	Low
	Altimeter issue causes premature CO2 cartridge puncture		Maintain safe distance from any open flame Redundant altimeter testing completed	
Components impact person during ejection test	Members/spectators stand in the line of ejection	Low; members stand on the sides of the vehicle when carrying it to be ejection tested so they are not in the line of ejection. Safe distance verified for members and spectators prior to testing	Ensure the line of ejection is clear before testing	Low
	Members/spectators stand too close to ejection		Maintain a safe distance from ejection	
	Warning is not given prior to test		Warn spectators and members prior to test by counting down	
Debris impact person during drop test	Members/spectators stand directly beneath drop test	Low; safe distance verified for members and spectators prior to testing	Maintain a safe distance from drop test	Low
	Failed drop test results in broken components that can impact members/spectators standing too close			
	Warning is not given prior to test		Warn spectators and members prior to test	
Impact from drone flight testing	Members/spectators stand too closely	Low; test stand utilized for quadcopter tuning, which should make test flight less erratic; net enclosure utilized for flight testing	Maintain safe distance from test enclosure	Low
	Warning is not given prior to test		Warn members and spectators to exit net enclosure prior to test	
	Flight issues during testing result in components detaching		Wear proper protective gear including safety glasses in the case of components detaching during flight test	

**Table 16: Manufacturing Hazards**

<b>Hazard</b>	<b>Possible Causes</b>	<b>Risk of Mishap and Rationale</b>	<b>Mitigation Approach</b>	<b>Risk of Injury After Mitigation</b>
Contact with bandsaw blade	Placing hands in blade path	Low; proper safety training given to members using bandsaws, sacrificial pieces available to push small workpieces against blade. Members that are new to machining are supervised.	Keep hands on opposite sides of the blade path	Low
	Small workpiece limits space between hand and blade		Use sacrificial piece to push small workpieces being cut, preventing hands from getting too close to blade	
	Wearing gloves causes fingers to be pulled toward the blade		Never wear gloves when using machinery with rotating saw blades	
Contact with rotating lathe chuck jaws	Hands/face too close to rotating jaws	Low; proper safety training given to members using lathes, lathe will not turn on if chuck shield is not engaged. Members that are new to machining are supervised.	Maintain at least 6 inches of distance from chuck	Low
	Long hair or dangling jewelry caught by rotating jaws		Tie long hair into a bun and remove dangling jewelry	
	Chuck shield is not utilized while machining		Always use chuck shield	
Chuck key ejection from rotating chuck	Key left in chuck combined with faulty chuck shield sensor	Low; danger of leaving chuck key in when machining on lathe emphasized strongly to all users. Safety signs in the machine shop also emphasize this point, so this should not occur. In the case that the chuck key is left in, the lathe will not turn on unless the chuck shield is engaged. The chuck shield cannot be pulled down far enough to engage if the chuck key is left in. For ejection to be a risk, the key would have to be left in and the chuck shield sensor would also have to fail.	Be sure all new users undergo safety training before use	Low
			Report any lathes with a faulty chuck shield sensor	
Contact with rotating drill	Hands/face too close to rotating drill	Low; proper safety training given to members using the	Maintain at least 6 inches of distance from rotating drill	Low

	Long hair or dangling jewelry caught by rotating drill	drill press or milling machines. Members that are new to machining are supervised.	Tie long hair into a bun and remove dangling jewelry	
	Gloves catch on drill and cause fingers to be pulled to it		Never wear gloves when using machinery with a rotating tool	
			Turn machine off when applying oil to workpiece so contact is avoided	
			Use safety shield to help maintain safe distance when possible	
Workpiece ejection	Workpiece not properly secured to undergo forces while machining	Low; protocols for securing workpieces are taught on each machine. Maximum material removal of 0.100" and maximum drill step-up of 0.250" set in place to prevent dangerous forces on workpiece	Follow protocols for securing workpieces before machining and use clamps when necessary	Low
			Use gentle engagement between workpiece and tools to prevent unnecessary forces on the workpiece	
			Follow maximum material removal rules to prevent unnecessary forces that could loosen the workpiece	
Fiberglass/carbon fiber debris/fumes causing skin irritation and respiratory hazard	Proper protective gear not utilized	Medium; debris can possibly be missed during cleanup if not performed thoroughly	Wear protective gear such as closed-toed shoes, long sleeves, pants, gloves, and safety glasses to prevent skin irritation	Low
	Workspace is not thoroughly cleaned		Wear appropriate facemask when cutting fiberglass/carbon fiber	
			Vacuum debris while cutting to minimize cleanup where debris can be missed	
	Fiberglass/carbon fiber utilized in		Work in well-ventilated area	
			Vacuum and wipe workspace when finished	

	improper environment			
Contact with sharp tools	Incorrect handling	Low; safety training includes proper handling of tools by wrapping sharp cutting edges with a rag when carrying, installing, and removing. Users of the machine shop are told to give a verbal warning before starting an operation that will cause a sudden and loud noise	Always wrap a rag around sharp cutting edges on a tool, never hold directly with hand	Low
	Sudden and excessively loud operation		Always give a verbal warning before starting a loud operation so others are not startled when using sharp tools	
Spray paint exposure	Painting occurs in improper environment	Low; members spray paint outside and maintain safe distance from fumes	Spray paint outside for increased ventilation	Low
			Maintain safe distance while spray painting to prevent fume inhalation	
Hearing damage	Headphones are not worn for loud manufacturing processes, such as waterjet use	Low; most processes are not loud enough to impact hearing other than waterjet use where headphones are provided. Headphones are available for use at any machine if desired.	Always wear headphones when using the waterjet. Otherwise use as desired	Low
Vision damage	Protective gear is not worn while welding	Low; members must always wear safety glasses when machining and a welding mask when welding. Welding safety training includes closing the safety curtain and giving a verbal warning to those in and out of the welding bay before beginning to weld.	Always wear a welding mask when welding	Low
	Verbal warning is not given before starting to weld		Close protective curtain to protect those outside the welding bay from the arc	
	Protective curtain is not closed before starting to weld		Give a verbal warning so those in the welding bay put on their masks and those outside know not to come into the welding bay	
	Protective gear is not worn while machining		Always wear safety glasses when machining	

Contact with hot workpiece/tool causing burns	Cutting oil not used	Medium; cutting oil use taught to members along with maximum material removal rules. Welding safety training informs members of proper protective gear. If a soldering iron or recently welded piece is left unattended, a member could accidentally get burnt	Use cutting oil when drilling or making rough cuts	Low
	Too much material removed at once		Follow maximum material removal rules for the shop	
	Proper protective gear not worn while welding		Wear welding gloves, jacket, and mask when welding	
	Contact with melted solder or hot soldering iron		Inform others of melted solder and recently welded piece and avoid leaving it unattended	
			Turn off soldering iron before leaving it unattended	



**Table 17: Storage Hazards**

<b>Hazard</b>	<b>Possible Causes</b>	<b>Risk of Mishap and Rationale</b>	<b>Mitigation Approach</b>	<b>Risk of Injury After Mitigation</b>
Black powder ignition	Black powder residue left in workspace	Medium; small amounts of residue can be hard to see	Clean any trace of black powder in the workspace with methods that do not create static	Low
	Black powder stored in location where it will be near open flame		Store black powder far from open flame in the workspace and inform members of its location	
Carbon fiber decomposition	Material stored at the incorrect temperature can result in thermal decomposition	Low; material is stored in a dry, cool environment	Store material inside in a temperature-controlled environment	Low
CO2 cartridge rupture	Cartridges exposed to direct sunlight	Low; cannisters are kept out of direct sunlight in a dry, temperature-controlled environment	Keep cannisters out of direct sunlight	Low
	Cartridges stored at higher than recommended temperature		Store cannisters at the correct temperature and keep from excessive heat	
Lacerations from sharp tools	Tools are not put away correctly	Medium; shared workspace with other student groups increases risk. During heavy manufacturing times, tools are used more constantly and may not always be put away	Be sure to always put away tools after use	Low
			Be sure not to cover sharp tools in a way that they can accidentally be grabbed, such as with a rag	
			Pick up items such as rags carefully in case the previous user did not put away a tool	
Lacerations from stock with sharp edges	Remaining stock is not deburred before placing back into storage	Medium; during heavy manufacturing times this step can be forgotten	Debur all stock and workpieces with a proper file before storing	Low
			Handle stock and workpieces with care in case they were not previously deburred	

Carbon fiber and CO2 cartridge storage hazards obtained from carbon fiber safety documentation and gas cylinder safety information (Ref. [6], Ref. [7]).

**Table 18: Transportation Hazards**

<b>Hazard</b>	<b>Possible Causes</b>	<b>Risk of Mishap and Rationale</b>	<b>Mitigation Approach</b>	<b>Risk of Injury After Mitigation</b>
Motor ignition	Motor is jostled during travel, resulting in elevated friction	Low; motor is difficult to ignite just by movement, team will obtain motor at competition to reduce travel with motor	Obtaining motor at competition reduces the distance the team must travel with the motor	Low
	Motor is dropped when loading/unloading		Pack motor in such a way that prevents movement while driving	
			Wait to fully assemble motor until after it has been transported to the launch site	
Component damage can create hazard during launch if unnoticed	Components are not packed gently	Medium; team will be travelling a long distance with vehicle components which can increase the chance of components shifting or getting damaged	Avoid dropping components while packing	Low
	Components are jostled during travel		Pack components to prevent shifting, specifically for components that are more likely to be damaged	
			Inspect components prior to assembling for launch	
			Bring tools and replacement parts in case of damage	
Black powder ignition	Black powder charges are jostled during travel, resulting in elevated friction	Low; ammo can is used to protect charges when traveling, charges handled with care	Use ammo can to protect charges	Low
	Black powder charges dropped when loading/unloading		Pack in location that prevents movement while driving	

**Table 19: Environmental Hazards**

<b>Hazard</b>	<b>Possible Causes</b>	<b>Risk of Mishap and Rationale</b>	<b>Mitigation Approach</b>	<b>Risk of Injury After Mitigation</b>
Water pollution from epoxy resin	Creation of uncured epoxy resin waste	High; incinerator is the best, least harmful method of resin disposal but the team does not have access to this. The next best option is to cure resin waste with its hardener before disposing	Minimize epoxy resin waste	Medium
	Incorrect disposal of epoxy resin waste down the drain		Cure any resin waste with its hardener before disposing	
Litter in the event of vehicle damage/detached components during flight	Forces sustained during flight damage components or cause them to fall off	Medium; test flight resulted in a single fin separating, though it was recovered and was not damaged. It is likely the fin was loosened by forces during flight, causing it to separate upon landing, which is expected to be a nonissue with the new aft that should withstand flight forces. The risk is attributed to the chance of components detaching during flight in a manner where they are not able to be found.	Ensure materials are strong enough to undergo expected flight and landing forces to prevent damage/separation of components	Medium
	Landing velocity is too high and can break components into pieces		Ensure attachment methods are strong enough to undergo expected flight and landing forces to prevent damage/separation of components	
	Vehicle and/or quadcopter lost entirely and cannot be found		GPS sensors used to locate the vehicle and quadcopter	

Environmental hazards from epoxy resin obtained from its safety sheet (Ref. [8]).

**Table 20: Chemical Hazards**

<b>Hazard</b>	<b>Possible Causes</b>	<b>Risk of Mishap and Rationale</b>	<b>Mitigation Approach</b>	<b>Risk of Injury After Mitigation</b>
Skin irritation from contact with epoxy resin	Proper protective equipment is not worn	Low; appropriate nitrile gloves are worn while working with epoxy resin	Wear proper protective gear including nitrile gloves, long sleeves, and eye protection	Low
	Proper cleanup protocol is not followed		Clean workplace of any resin to avoid accidental exposure	
Respiratory irritation from inhalation of resin fumes	Members work in close proximity with resin	Low; workspaces are well-ventilated	Always work with resin in ventilated areas	Low
			Inform members to keep resin a safe distance from face to avoid accidental inhalation	
Epoxy reaction/decomposition with other chemicals	Epoxy resin exposed to oxidizers, specifically peroxides	Low; epoxy resin is not combined with the use of oxidizers	Inform members of dangerous interactions before use	Low
Carbon fiber reaction with other chemicals	Carbon fiber exposed to strong oxidizing agents	Low; carbon fiber is not combined with the use of oxidizers	Inform members of dangerous interactions before use	Low

Chemical hazards associated with epoxy resin and carbon fiber are determined from their safety sheets (Ref. [6], Ref. [8]).

### Appendix III: Risk Assessment

**Table 21: Propulsion Risk Assessment**

<b>Hazard</b>	<b>Possible Causes</b>	<b>Risk of Mishap and Rationale</b>	<b>Mitigation Approach</b>	<b>Risk of Injury After Mitigation</b>
Incomplete propellant ignition or propellant burnout, unpredictable and unstable flight path, personnel hazard	Inconsistencies in propellant grain	Low; motor performed as expected during test flight	Store propellant in climate-regulated room	Low
	Improper grain bonding		Perform visual inspection of grain to ensure inconsistencies are not present	
	Improper propellant storage		Take proper precautions when bonding motor grain and follow correct procedures	
Damage to motor casing and motor assembly, motor is not properly retained and causes an unpredictable and unstable flight path, personnel hazard	Structural defect in motor casing causes casing to crack	Low; motor casing performed as expected during test flight	Use motor casing material durable enough to sustain expected loads	Low
	Motor casing material not durable enough to sustain propulsion forces		Perform visual inspection of casing prior to assembly to ensure no defects are present	
Damage to motor tube and motor assembly, motor is not properly retained and causes an unpredictable and unstable flight path, personnel hazard	Structural defect in motor tube causes tube to crack	Medium; motor tube has not yet been tested during a test flight, but material is expected to sustain propulsive loads from previous experience	Use motor casing material durable enough to sustain expected loads	Low
	Motor tube material not durable enough to sustain propulsion forces		Perform visual inspection of casing prior to assembly to ensure no defects are present	
	Improper epoxy application causes tube to shift		Follow correct epoxy procedure to ensure epoxy cures correctly and apply sufficient amount	
Forward and aft motor closures are damaged, motor propellant does not remain properly retained, motor damages forward rocket components, personnel hazard	Structural defect in forward and aft closures causes closures to crack	Low; forward and aft closures performed successfully during test flight	Fasten closures to the proper torque	Low
	Closures improperly fastened onto aft and does not remain properly placed		Perform visual inspection of closures prior to assembly to ensure no defects are present	
	Failure of threads causes closures to come loose and motor to shift			

Motor retainer is damaged, motor assembly does not remain properly retained, motor damages forward rocket components, personnel hazard	Structural defect in motor retainer causes retainer to crack	Low; motor retainer performed successfully during test flight	Fasten retainer to the proper torque	Low
	Motor retainer improperly fastened onto aft and does not remain properly placed		Perform visual inspection of retainer prior to assembly to ensure no defects are present	
	Failure of retainer threads causes retainer to come loose and motor to shift			

**Table 22: Vehicle Structural Hazard Analysis**

<b>Hazard</b>	<b>Possible Causes</b>	<b>Risk of Mishap and Rationale</b>	<b>Mitigation Approach</b>	<b>Risk of Injury After Mitigation</b>
Airframe and coupler become damaged, internal components improperly retained and risk falling out of vehicle, aerodynamic interferences, personnel hazard	Cracks in airframe due to pressurization	Medium; SRAD airframe and fins, limited load testing. Single test flight resulted in some failure of airframe	Visually inspect all structural components for cracks or unintended gaps	Low
	Improper transportation causes damage to structure		Follow correct procedure when creating layups and cutting features	
	Manufacturing accident causes damage to structure			
	Structural defect in material during layup			
Fin fillets weaken and cause separation of fins from vehicle, personnel hazard	Weak epoxy fillets	Medium; fin fillets undergo limited load testing	Use recommended epoxy for HPR vehicles	Low
	Improper application		Make epoxy fillets sufficiently thick to mitigate failure risk	
			Follow proper procedures for applying epoxy to fins	
Centering rings fail, disrupting flight path and risks unstable descent	Epoxy failure	Medium; during test flight, alterations to vehicle design since test flight introduce additional variables. Single test flight resulted in failure of aluminum centering rings, which have been newly designed and manufactured for competition	Inspect launch vehicle before and after each launch	Low
	Manufacturing defects		Use recommended epoxy for HPR vehicles	
			Follow proper procedures for applying epoxy to centering rings	
			Inspect components for defects immediately after manufacturing	
Bulkheads fail, vehicle does not adequately pressurize, and separation events fail, rocket becomes ballistic, internal components damages, personnel hazard	Manufacturing defects	Low; bulkheads performed as expected during test flight	Inspect components for defects immediately after manufacturing and testing	Low
	Bulkhead material not durable enough to withstand ejection forces			
Shear pins do not shear, and rocket becomes ballistic; shear pins shear too	Insufficient ejection charge size (vehicle does not separate)	Low; ejection testing was performed prior to test flight that	Perform ejection testing to verify correct energetic amounts	Low



early, causing vehicle to separate, disrupting rocket's path and risking unstable descent; rivets do not remain intact, causing vehicle to separate, disrupting rocket's path and risking unstable descent	Excessive pressure in the airframe (vehicle separates too quickly)	proved sufficient energetic amounts	Taking precautions when packing and assembling vehicle to ensure vehicle is not over-pressurized	
Fins become damaged, falling debris, causes an unpredictable and unstable flight path, personnel hazard	Fasteners securing thrust plate subassembly to airframe shear under motor load	Medium; SRAD airframe and fins, limited load testing Single test flight resulted in failure of airframe	Use high-strength steel alloy fasteners to prevent shearing	Low
	Cracks in airframe due to pressurization		Ventilate airframe to prevent airframe failure due to pressurization	
	Fin material not durable enough to withstand motor and ejection forces		Use high-strength composite (epoxyglass) for fins	
			Visually inspect all structural components for cracks or unintended gaps	
			Launch crew 200 ft from vehicle at launch, behind barrier	
Structural components fail to retain propulsion, payload, or recovery systems	Thrust plate separates from airframe due to fastener failure or weak epoxy fillets	Medium; while thrust plate subassembly remained secured during test flight, alterations to vehicle design since test flight introduce additional variables. Single test flight resulted in failure of airframe	Use high-strength alloy steel fasteners to prevent shearing	Low
	Premature separation of vehicle sections from one another due to airframe failure at point of fastening		Use recommended epoxy for HPR vehicles	
			Ventilate airframe to prevent airframe failure due to pressurization	
			Visually inspect all structural components for cracks or unintended gaps	
			Launch crew 200 ft from vehicle at launch, behind barrier	
Thrust plate separates from	Weak epoxy fillets	Medium; While thrust plate subassembly	Use recommended epoxy for HPR vehicles	Low

airframe, causing personnel hazard	Manufacturing defects	remained secured during test flight, alterations to vehicle design since test flight introduce additional variables. Single test flight resulted in failure of airframe	Make epoxy fillets sufficiently thick to mitigate failure risk	
	Fastener failure		Follow proper procedures for applying epoxy	
			Inspect components for defects immediately after manufacturing	
			Use high-strength alloy steel fasteners to prevent shearing	
			Visually inspect fasteners before assembly	
			Launch crew 200 ft from vehicle at launch, behind barrier	

**Table 23: Avionics and Recovery Hazard Analysis**

<b>Hazard</b>	<b>Possible Causes</b>	<b>Risk of Mishap and Rationale</b>	<b>Mitigation Approach</b>	<b>Risk of Injury After Mitigation</b>
Drogue parachute fails to inflate and detaches from launch vehicle, causing the launch vehicle to accelerate towards the ground, leading to the catastrophic failure of the mission and launch vehicle coming in contact with personnel	Electrical connections between the altimeter and its power supply or the drogue black powder charge loosen	Low; the altimeters successfully ignited the black powder charge at apogee and deployed the drogue parachute during test flight. However, the launch vehicle has gone through design changes which needs to be taken into consideration	Secure wires connecting the altimeters to the ejection charges using zip ties and wire runways to keep them from excessively moving during flight	Low
	Altimeter fails to detect apogee and not fire the ejection charge		Wire a redundant altimeter independently to a backup black powder charge	
	Drogue parachute and its shroud lines, parachute protector, or the recovery harness tangle		Connect parachute to the shock cord 15 feet away from the parachute protector and the parachute is folded according to the manufacturer instructions to prevent tangling	
	Drogue black powder charge fails to eject the drogue parachute		The ejection of the drogue parachute and separation of the sections with 3.5 g of black powder is tested on the ground before flight	
	Shock cord, D-links, swivel, or eyebolts suffer mechanical failure, disconnecting the launch vehicle sections from the parachute		Ensure recovery hardware can withstand the expected maximum loads with sufficient factor of safety Test altimeters for functionality using the software given by manufacturer Wire a backup (redundant) altimeter independently to a backup ejection charge	
The CO2 ejection system encounters a mechanical failure, causing the CO2 cartridge to not be	Connection between the altimeter and CO2 system black powder charge	Medium; the use of a small pyro charge to pressurize a small volume introduces	Secure wires connecting the CO2 system's black powder charge to altimeters with wire	Low

punctured leading to the failure of deploying the main parachute and high-speed crash into the ground	disconnects or short circuits	variables such as volume, the mass of black powder and packing tightness that needs to be consistent every time. The inconsistency between the variables may have caused the failure of puncturing the CO2 cartridges	run-aways and zip ties to prevent excessive movement during flight	
	Altimeter fails to detect the altitude data		Wire a redundant altimeter independently to a redundant CO2 ejection system as a backup to the primary system	
	Black powder charge is not big enough to compress the return spring and puncture the CO2 cartridge		Test different black powder amounts to determine the necessary amount to puncture cartridges reliably	
			Place O-rings around components to minimize pressure leaking after combustion  The black powder housing volume is minimized to only fit the black powder necessary and E-match to keep the volume variable consistent	
The main parachute fails to deploy, causing launch vehicle to crash into the ground or spectators at high speed	CO2 cartridge is not big enough to create necessary pressure inside the airframe to eject payload and main parachute	Medium; successful deployment of the main parachute depends on first, a successful separation and parachute ejection, second the parachute unrolling out of the parachute protector and lastly pulling out the payload while it is inflating, so failure at any of these steps may result in the failure of the system	Size CO2 cartridges based on launch vehicle volume to provide 1.5 times of the necessary deployment force	Low
	Puncture piston clogs the punctured hole on the CO2 cartridge slowing down the pressurization of the forward airframe		Seal airframe volume with the nosecone bulkhead and avionics bay bulkhead to prevent pressure leaks	
	Main parachute and its shroud lines getting tangled with itself, the payload, parachute protector or the recovery harness		Puncture piston utilizes a spring that retracts it out of the punctured hole to prevent clogging.	
	Shock cord, D-links, swivel, or eyebolts		Connect main parachute, parachute	

	suffer mechanical failure, disconnecting the launch vehicle sections		protector and payload to the recovery harness away from each other to prevent interference	
			Torque down recovery hardware to prevent them from getting unscrewed. Loctite is also used where threaded	

**Table 24: Payload Hazard Analysis**

<b>Hazard</b>	<b>Possible Causes</b>	<b>Risk of Mishap and Rationale</b>	<b>Mitigation Approach</b>	<b>Risk of Injury After Mitigation</b>
Quadcopter frame suffers structural failure, leading to catastrophic failure of the quadcopter, causing loss of flight stability and debris coming into contact with personnel	Fastener failure joining the top and bottom frame	Low; SRAD 12-ply CFRP with eight joining fasteners.	Frame has a factor of safety of 5.45	Low
	Impact load on one end of the frame, imposing a large bending moment	Did not sustain damage during the test launch.	Loctite placed on all fasteners used to join the top and bottom frame	
			Steel threaded standoffs to help carry the stress of an impact load	
Payload recovery harness mount suffers structural failure, causing the container and quadcopter to eject from the launch vehicle at main parachute ejection	Shoulder bolts and welds between the container and mount fail due to higher-than-expected loading	Low; redundancy by using both fasteners and welds to keep the recovery harness mount attached.	Locknuts on shoulder bolts will be properly torqued down prior to assembly into the launch vehicle.	Low
	Recovery harness snaps due to higher-than-expected loading	Did not sustain any damage during the test launch, and was successful at keeping the container tethered to the main recovery harness	Proper attachment of recovery harness to the recovery harness mount and D-link	
Unfolding mechanism locking/structural failure, resulting in the loss of a motor arm and motor causing the quadcopter to lose stability	Shearing of the 3D printed PETG pivot housing or pivot stop	Medium; complexity of pivot housing component and lightweight requirement led to 3D printing. 3D printed components are typically weaker than metal, with the pivot housing having a factor of safety of 3.33	Increased the infill of the pivot housing from 60% to 100%	Low
	Pin plunger does not achieve lock due to motor wire obstruction		Add wire “guides” to the pivot stop to ensure they will not hinder the unfolding of the motor arms	
	Impact load causes misalignment in the motor arm		Conical hole in the pivot stop provides a better lock for the pin in the pin plunger	
PCB becomes loose from the top frame of the quadcopter, resulting in large vibrations for the IMU and other hardware. This may lead to instability in the quadcopter flight control, leading to injury	M2.5 fasteners become undone	Low; there are four M2.5 fasteners with locknuts to prevent the fasteners from coming undone. The PCB was flown on the test flight and was properly attached	The M2.5 fasteners and locknuts will be properly torqued down prior to being placed inside of the launch vehicle	Low
	Top frame structurally fails, resulting in loosening of the PCB attachment			

		when recovered after the flight.		
<p>Container-deployment rack and pinions fail to release the quadcopter from the container. Failure to release from the container will not result in any personnel injury, as the quadcopter will remain inside of the container throughout descent. Premature release from the container will open the quadcopter parachute, preventing injury</p>	<p>Damage to the rack and pinion assembly, causing failure to drive the aluminum beam out of the retention mounts</p>	<p>Medium; the retention mounts on the container are 3D printed PETG and can experience structural failure during a high shock load. Extensive structural damage would need to occur to restrict the motion of the aluminum beams on the rack and pinion assemblies. This was flown on the test flight and sustained minor cracking, but was successful at keeping the quadcopter retained and allowing the quadcopter to release</p>	<p>The infill of the retention mounts and the motor housing on the rack and pinion assembly was increased from 40% to 80%. Support was added to the retention mounts and filleting was improved on the rack and pinion motor housing</p>	<p>Low</p>
	<p>Electrical failure from the PCB that results in the DC motors not receiving current</p>			
	<p>Damage to the retention mounts causing the aluminum beams to get stuck</p>			
<p>Quadcopter 36-inch parachute does not open once the quadcopter is deployed from the container, causing the quadcopter to free-fall</p>	<p>The parachute gets stuck in the container and breaks off</p>	<p>Medium; the quadcopters release from the container is difficult to accurately simulate/test on the ground. A shroud line tangled with one of the quadcopter arms on the test flight, causing the quadcopter to descend quicker than expected.</p>	<p>The parachute shield is being redesigned to include an extended piece that forces the quadcopter to fall out of the container in the proper orientation. This ensures the quadcopter will not flip when the parachute opens, preventing shroud lines from tangling</p>	<p>Low</p>
	<p>The parachute shroud lines tangle in the quadcopter</p>			
	<p>The parachute-deployment rack and pinion assembly has structural failure, releasing the parachute</p>			
<p>Quadcopter motor failure resulting in loss of control for the quadcopters flight</p>	<p>Electrical power failure to the motors through the ESC</p>	<p>Low; the motors are reliable quadcopter motors that have strong wired connections</p>	<p>Zip ties will be used to hold wires in place</p>	<p>Low</p>
	<p>Physical damage to the motors rotary housing</p>			
<p>Battery connection between components is temporarily or permanently lost, causing one or more electrical systems to fail</p>	<p>Poor connection or loose wiring</p>	<p>Medium; PCB used to minimize the number of wired connections needed. The PCB is exposed to ejection gases during ejection,</p>	<p>Ensure connection of all wires using “tug” test and secure all loose wires using tape and hot glue. Strain relief such as zip ties and heat shrinks applied to</p>	<p>Low</p>



		which would result in strain on the wires. The wires did not come loose, and the battery did not die during the test launch	prevent wire breakage	
One or more electric components on PCB lose functionality, preventing accurate data collection.	Impact force at landing damages electronics	Low; black powder is used as backup charge with CO2 being the primary charge. Impact forces upon landing at test launch did not damage any electrical components	Make sure the PCB is properly secured to the top frame of the drone	Low
	Black powder charges interact with electronic components and fry them			
Battery overheats or catches on fire	Overheating of payload inside airframe due to high external temperatures	Low; the payload exterior painted white to minimize heat absorption. The LiPo battery bought is enclosed in a protective case. An extensive ignition would need to occur elsewhere in the rocket to compromise the integrity of the payload battery	The quadcopter would be run at levels that are acceptable not to overexert the battery. Battery voltage would be verified before connecting to electronics	Low
	Low battery voltage or faulty battery			
	Ignition within rocket compromises security of payload			

## Appendix IV: Assembly, Pre-flight, Launch, and Recovery Checklists

### A. Assembly

#### Avionics Bay:

1. Securely fasten the altimeters and the battery housing on the avionics sled using M3 screws.
2. Secure the drogue and main parachute charge wires connected to the altimeters terminals by using zip ties and running them through the designated wire tunnels on the avionics sled.
3. Mount the CO2 ejection system on the forward avionics bay bulkhead using M3 screws and nuts. Screw sealed CO2 cartridges on to the CO2 cartridge mount as the mount won't be accessible after assembling the avionics bay.
4. Connect the male connectors on the forward bulkhead to the female connectors at the end of the charge wires to carry the current through the bulkhead.
5. Align the bulkheads with the avionics bay coupler using the markings to ensure accessibility to the arming switches from outside.
6. Fasten the avionics bay bulkheads on two sides of the avionics bay coupler by placing nuts on the threaded rods connecting the assembly.
7. Place the arming pin from outside of the coupler through the switches to disarm the system before preparing the ejection charges.

#### Ejection preparation:

1. Prepare the primary drogue ejection charge by loading the 3.5 g of black powder inside the cardboard tube and pack the rest of the volume with cellulose insulation to ensure instantaneous burning. Close the top of the cardboard tube with tape to prevent it from spilling during flight.
2. Repeat the same process as the primary drogue charge, however, pack the redundant charge with 4.2 g of black powder instead to ensure successful deployment.
3. Prepare the CO2 ejection system by placing the e-match inside of the black powder housing and running its wire through the hole behind it.
4. Pack the bottom of the black powder housing with cellulose insulation enough to where only the e-match is exposed.
5. Place the premeasured 0.05 g of black powder on top of the insulation inside the black powder housing and pack the rest of the volume with more insulation. Tape the opening on top of the black powder housing to prevent the contents from spilling.
6. Place the black powder housing inside the CO2 ejection combustion chamber wire side down. Follow that up by placing the puncture piston and the return spring. Push everything down where black powder housing is resting on the combustion chamber shoulder at the end.
7. Screw the combustion chamber into the CO2 cartridge mount to finalize CO2 ejection preparation.
8. Repeat the same steps to arm the redundant CO2 ejection system. However, this time pack it with 0.075 g of black powder instead.
9. Connect both primary and redundant drogue charges to the charge wires coming from the altimeters.
10. Connect both primary and redundant CO2 ejection charges to the main charge wires coming from the altimeters.
11. Seal around the wire holes using clay to prevent pressure leaks.

#### Parachute and Recovery harness preparation:

1. Place D-links on both ends of the Recovery harness for aft and forward sections.
2. Prepare the forward recovery harness by first attaching the payload recovery harness 14 ft away from the forward avionics bay eyebolt. Tie the main parachute protector to the forward recovery harness 2 ft after the payload recovery harness. Follow that up by attaching the main parachute and the swivel to the recovery harness 11 ft after the parachute protector using another D-Link.
3. Prepare the Aft recovery harness by attaching the drogue parachute and its swivel 16 ft away from the aft avionics bay eyebolt using a D-Link. Tie the drogue parachute protector 16 ft away from the drogue parachute along the Aft recovery harness.
4. Fold the parachutes seam to seam until all the seams are folded while making sure the shroud lines aren't tangled. Fold the shroud lines on top of the parachute and z-fold the parachute until it is packable inside the parachute protector.

5. Place the folded parachute on the parachute protector. Fold the parachute protector around the parachute to keep it from getting undone during flight and protect it from hot ejection gases.
6. Connect the forward recovery harness to the Avionics Bay eyebolt using the D-Link at its end. Connect the other end of the recovery harness to the nosecone eyebolt.
7. Connect the aft recovery harness to the aft Avionics Bay eyebolt using the D-Link at the end. Connect the other end of the recovery harness to the motor mount eyebolt to complete the Recovery layout.

**Mounting the GPS:**

1. Mount the GPS and its LiPo battery on the GPS mount that is inside the Nosecone shoulder.

**Motor:**

1. Wearing gloves, Flyer of Record follows manufacturer instructions for cleaning motor liner and bonding the motor grains with their spacing O-rings using manufacturer specified glue.
2. Flyer of Record unpacks motor components in a safe, clear environment.
3. Wearing gloves, Flyer of Record follows manufacturer instructions for cleaning motor liner and bonding the motor grains with their spacing O-rings using manufacturer specified glue.
4. Per manufacturer instructions, bonded grains are allowed to sit at least 12 hours before launch.

**Payloads:**

1. Tie the recovery harness of the parachute to the rack and pinion on top of the quadcopter.
2. Remove the rack and pinion motor covers for the two container release motors and set aside, leave the motors in their mounts.
3. Lift the two motors away from the rack and position the rack into the “released” position. Be sure not to drive the motors while this is completed. Push the motors back into their mounts to ensure they are not lost and engage the rack and pinion gears.
4. Plug battery into PCB using XT60 connectors.
5. Attach the Big Red Bee GPS to the parachute ballast using a 3D printed mount that is attached to the quadcopter’s parachute recovery harness.
6. Fold the parachutes seam to seam until all the seams are folded while making sure the shroud lines aren’t tangled.
7. Fold the shroud lines on top of the parachute and z-fold the parachute until it is packable inside the parachute shield.
8. Fold in the arms by pulling back each pin plunger. The trailing edge propeller is folded on top of the frame first, then the leading-edge propeller.
9. Gently lower the quadcopter into the container making sure that the propeller motor wires are not sitting beneath the quadcopter. Make sure to hold the arms in during this process so they do not unfold.
10. Lift the two-container release rack and pinion motors away from the rack and push the racks into the container retention mounts. Push the motors back into the motor mounts, ensure the rack and pinion gears engage, and reattach the motor covers.
11. Rest the parachute ballast in the gap between the parachute shield and quadcopter.

**Final Assembly:**

1. Inspect forward and aft airframe, fins, and nose cone for any cracking or visible damage.
2. Attach D-link to nose cone eyebolt and torque down.
3. Align the container slides with the 80/20 rails inside the forward airframe. Slowly lower the container into the forward airframe ensuring that the slides align with the 80/20 rails. Furthermore, the main parachute recovery harness must run past the side of the container and not catch on the container or propellers.
4. Insert main recovery assembly and nosecone shoulder into forward airframe. Secure via four nylon shear pins, inserted through the airframe.
5. Attach D-link to forward avionics bay eyebolt and torque down.
6. Insert avionics bay into forward airframe. Secure via four plastic rivets, inserted through the airframe.
7. Attach D-link to motor casing eyebolt and torque down
8. Attach D-link to aft avionics bay eyebolt and torque down
9. Insert drogue recovery assembly and avionics bay into the aft airframe. Secure via four nylon shear pins.

## **B. Pre-Flight**

### **Payload:**

1. While the quadcopter is inside of the launch vehicle, ground station connection will be monitored. The quadcopter will be inactive until it is armed on the launch pad.

### **GPS:**

1. Connect GPS to battery just before going out to pad.

### **Motor:**

1. While wearing gloves, Flyer of Record follows manufacturer instructions for greasing casing threads, closure threads, and O-rings for final motor assembly.
2. Following manufacturer's instructions, Flyer of Record inserts liner with bonded grains into casing and assembles the appropriate O-rings with the nozzle and forward seal disk.
3. Following manufacturer's instructions, Flyer of Record threads on the aft and plugged forward closure.
4. When vehicle is fully launch ready, Flyer of Record slides casing assembly into motor tube on the aft section and the threads the motor retainer securely around.

### **Final Simulation:**

1. Fully constructed rocket is weighed.
2. Location of CP is marked from simulation.
3. True CG is measured using a rope and is marked.
4. True stability margin is measured.
5. Simulation is updated with launch day conditions.

## C. Launch

### Altimeters:

1. Arm the altimeters by removing the arming pin before flight.
2. Listen to the altimeter start-up beeping sequence.
  - a. The first number reported through the number of beeps is the currently selected program preset. There should be 2 beeps corresponding to the second Program preset.
  - b. After a two second pause, the main parachute deployment altitude within the program preset is reported. There should be 8 beeps followed with 10 beeps and another 10 beeps which corresponds to main parachute deployment at 800 ft.
  - c. After a two second pause a 5-second-long beep indicates the apogee delay programmed. This should only happen with the redundant altimeters beeping sequence.
  - d. After a two second pause, a 3-to-6-digit number corresponding to the last recorded flights altitude is listened to from the number of beeps.
  - e. After a two second pause, the number of voltages from the altimeter's battery is reported with a 2- or 3-digit number. The number of beeps should indicate 9 volts from the battery.
  - f. After a two second pause, the continuity between the altimeter and the ejection charges is reported. These beeps repeat every 0.8 seconds. 1 repeating beep indicates continuity with drogue charges is okay, 2 beeps indicate continuity with main charges are okay, and 3 beeps indicate both drogue and main charge continuity is okay. The beeps heard from the altimeters should be 3 beeps repeating every 0.8 seconds to indicate both main and drogue charges are ready for flight.
3. If the number of beeps indicating the program preset, main parachute deployment altitude, battery voltage or the continuity between the charges are not correct, the launch vehicle is disarmed by inserting the arming pin back in and taken off the launch pad. Based on the reported problem the altimeters are either reprogrammed to the right settings, batteries are replaced, or charge wiring is fixed.
4. After the altimeters finish their start-up beeping sequence, if all the reported information is correct, the launch vehicle's recovery system is ready for flight.

### Payloads:

1. Once on the launch pad, arm the quadcopter by inserting a long, thin rod into a hole in the forward airframe and press the button on top of the drone.
2. The buzzer on the drone will turn on and remain on until the software begins. If the buzzer does not turn off after one minute, press the button again, wait five seconds, and press it again. Repeat this process until the software begins properly.

### Motor:

1. Install dual igniters and connect to launch control system through provided alligator clips.

## **D. Recovery**

### **GPS Tracking:**

1. Connect the Tele Dongle antenna to the laptop and start the manufacturer tracking application.
2. Ensure the same frequency is selected for Tele Dongle and the GPS. Wait for the antenna to find enough satellites to connect to the GPS.
3. Check the coordinates transmitted and the battery voltage of the GPS to ensure data transmitted is correct.

### **Payload GPS tracking:**

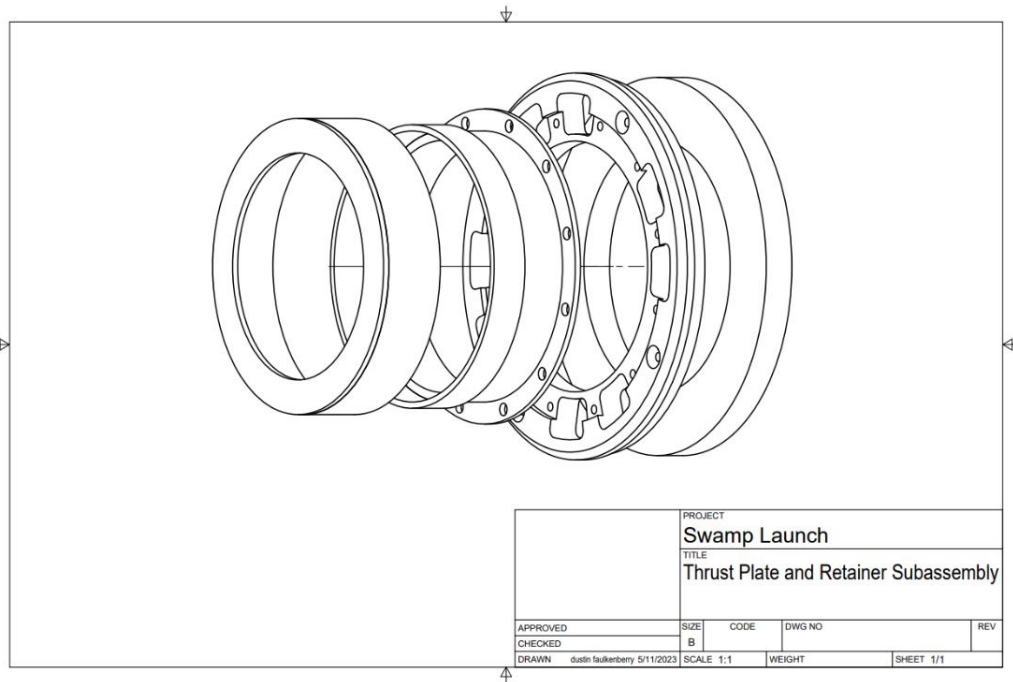
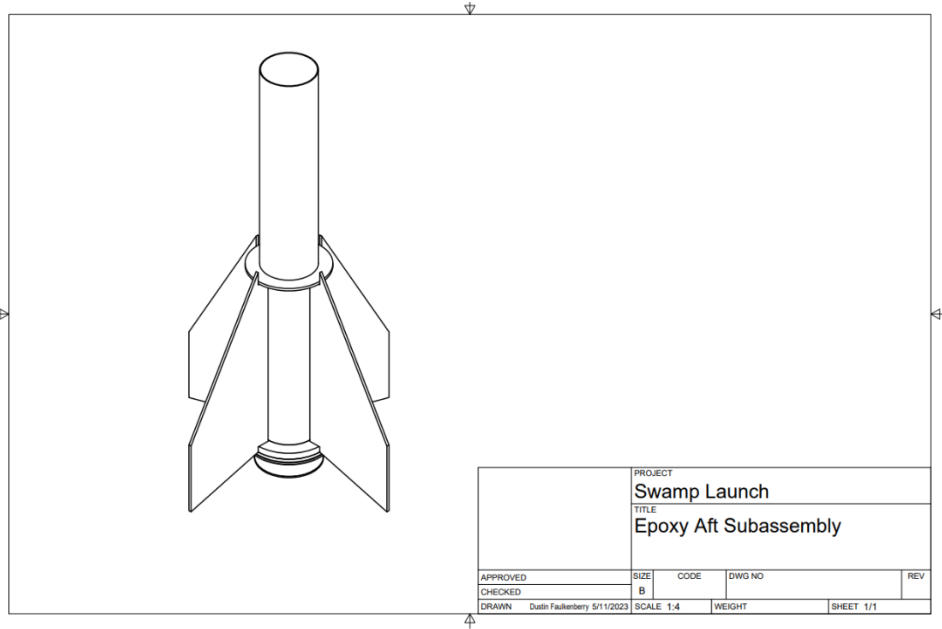
1. Read GPS coordinates from Big Red Bee and retrieve the quadcopters parachute.
2. Read the quadcopter's coordinates from the ground station and retrieve the quadcopter. The quadcopter buzzer will be beeping.

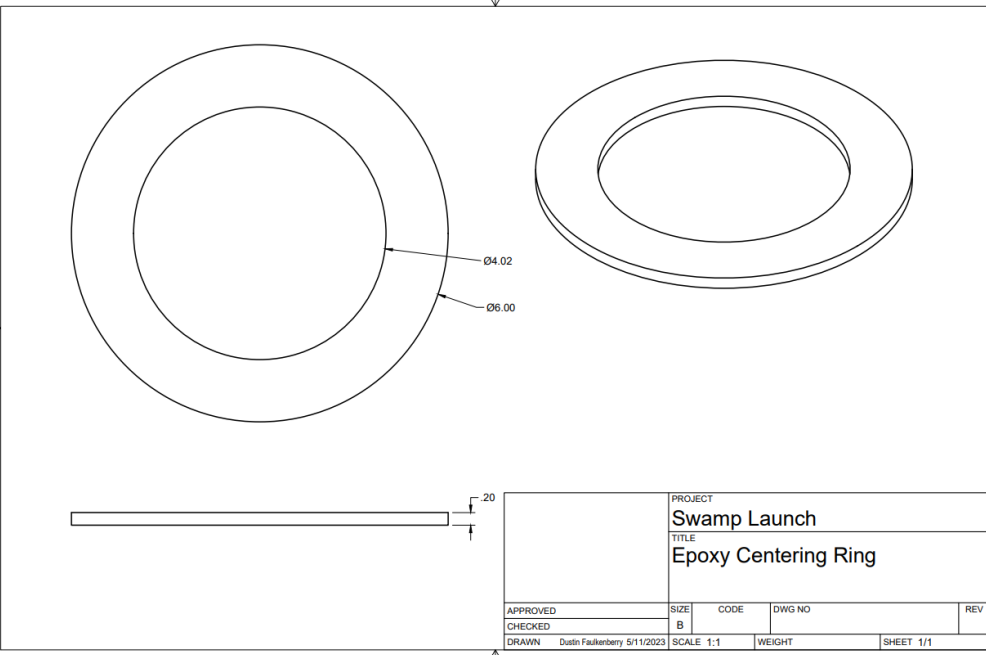
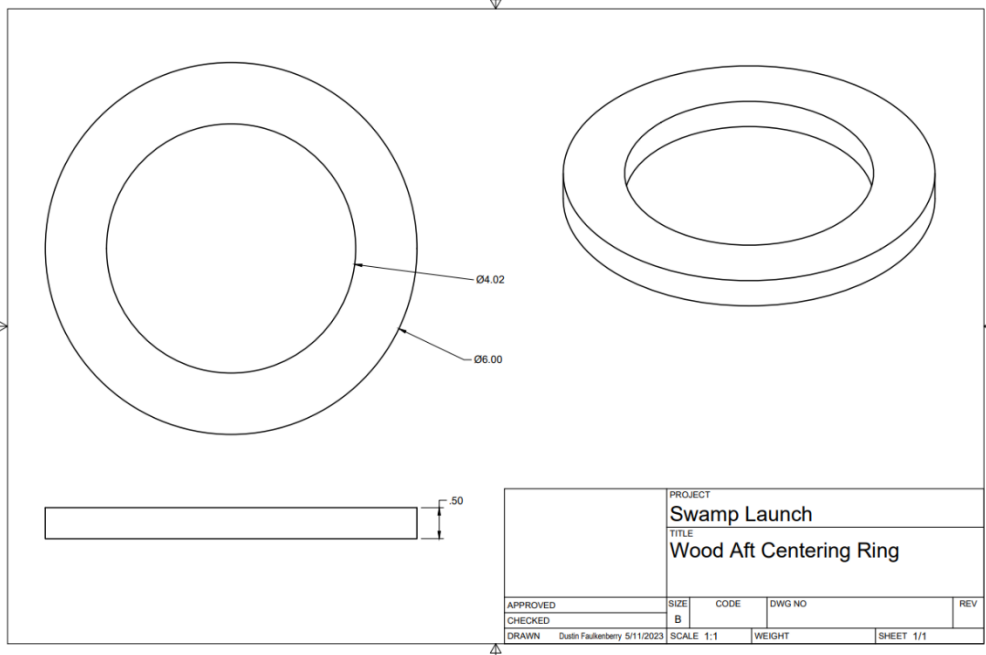
### **Vehicle Recovery:**

1. Upon arriving at the recovery site, immediately assess if any unfired charges remain.
2. Disarm altimeters.

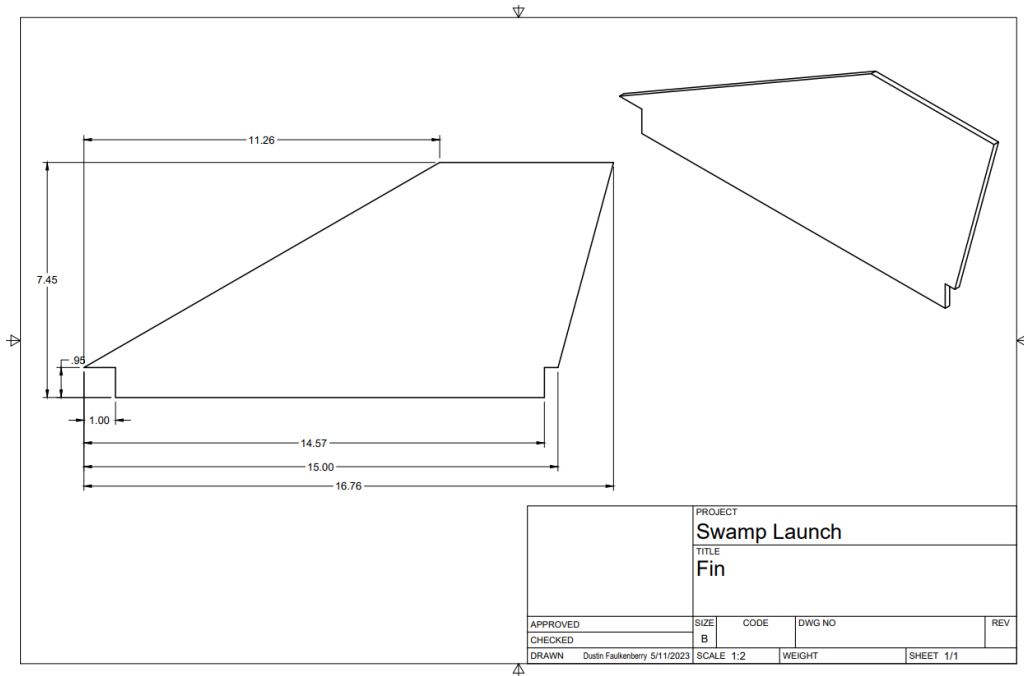
# Appendix VI: Engineering Drawings

## A. Structures

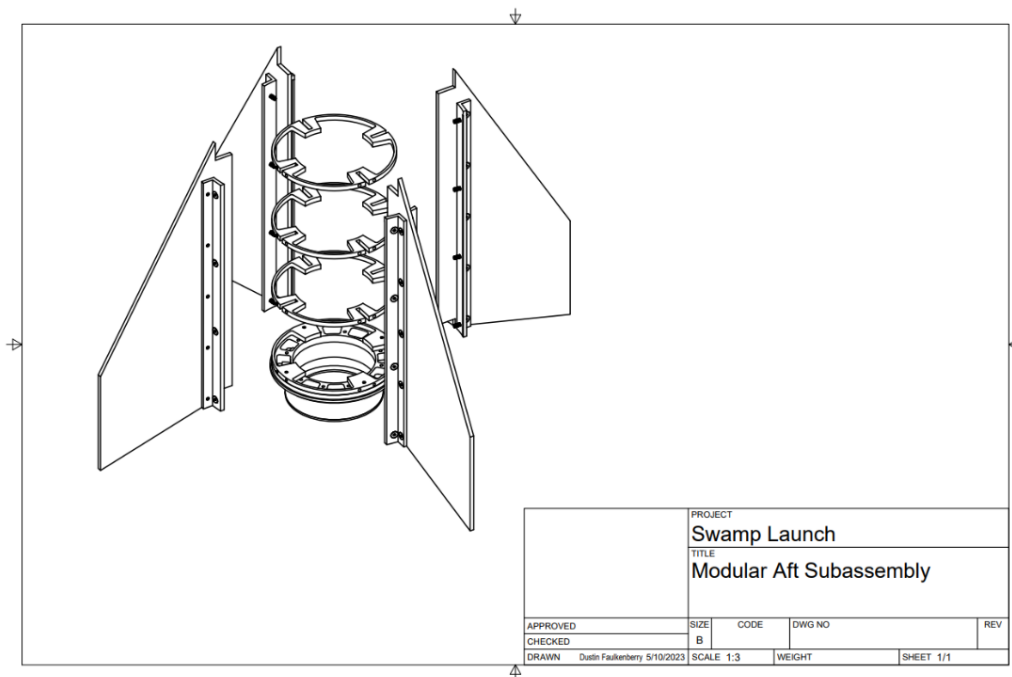


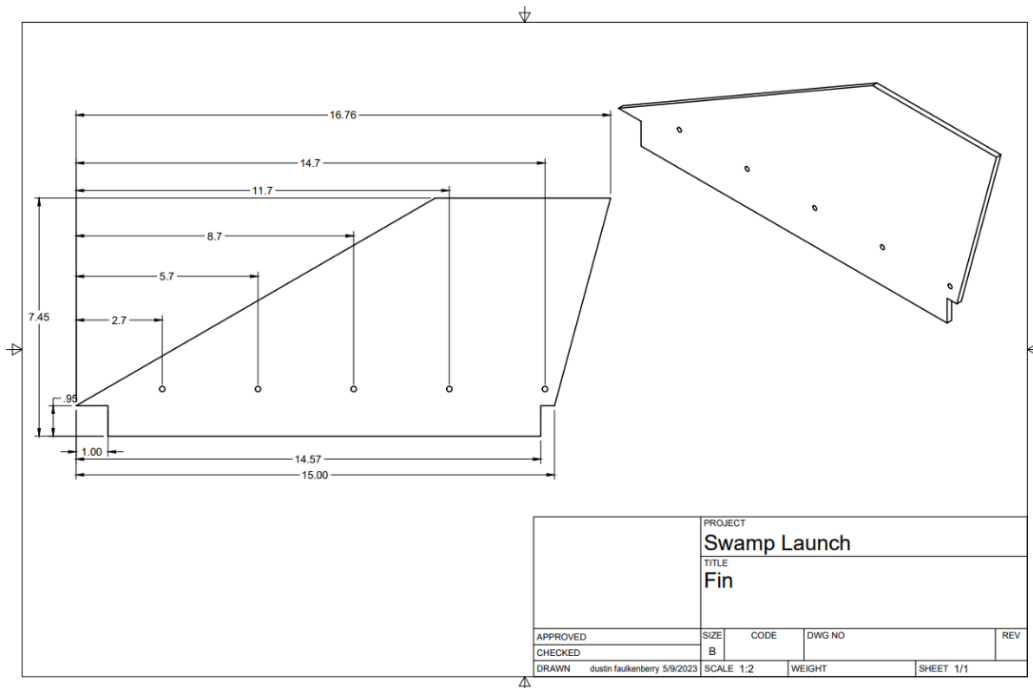
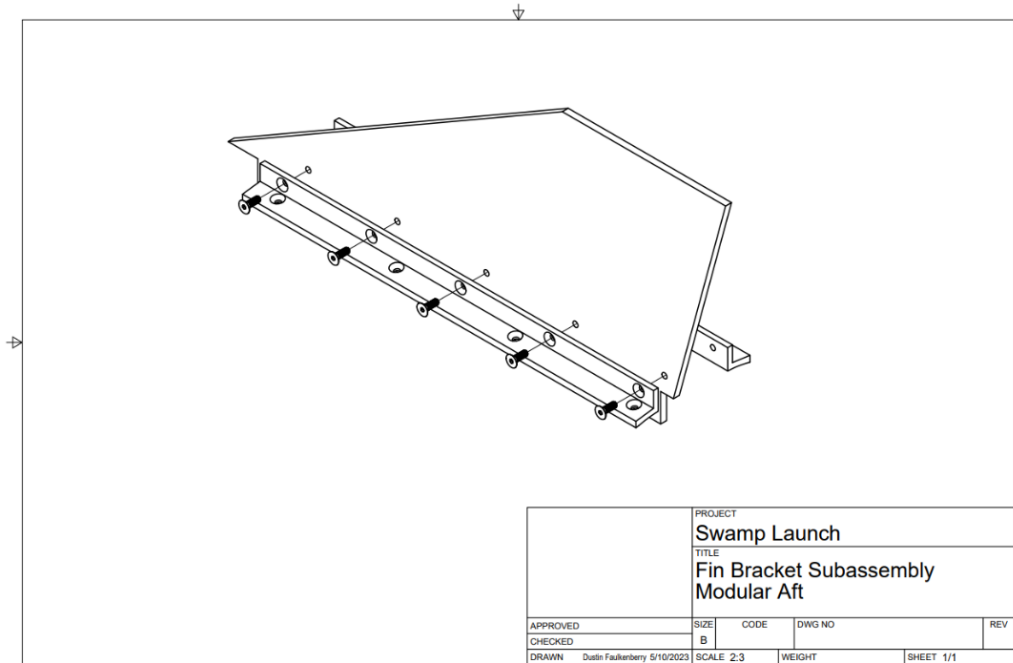


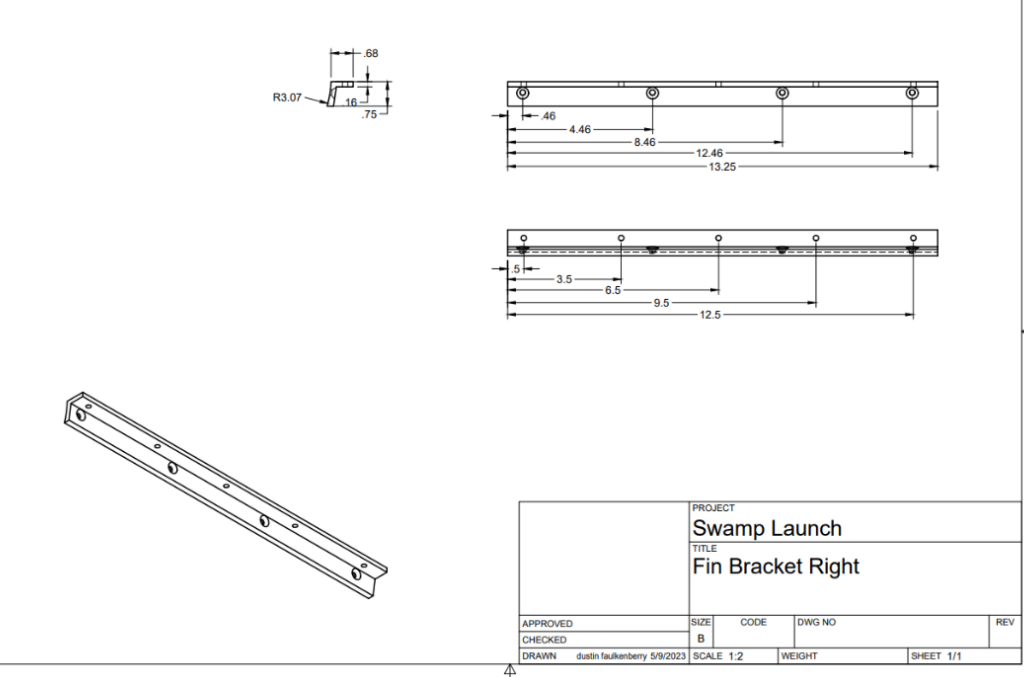
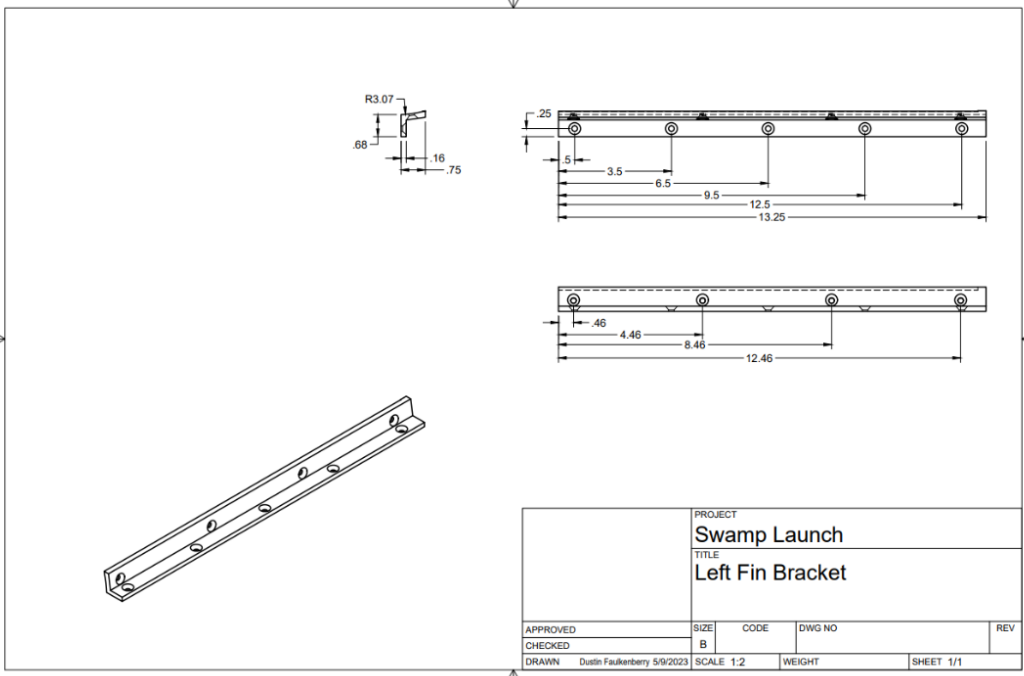


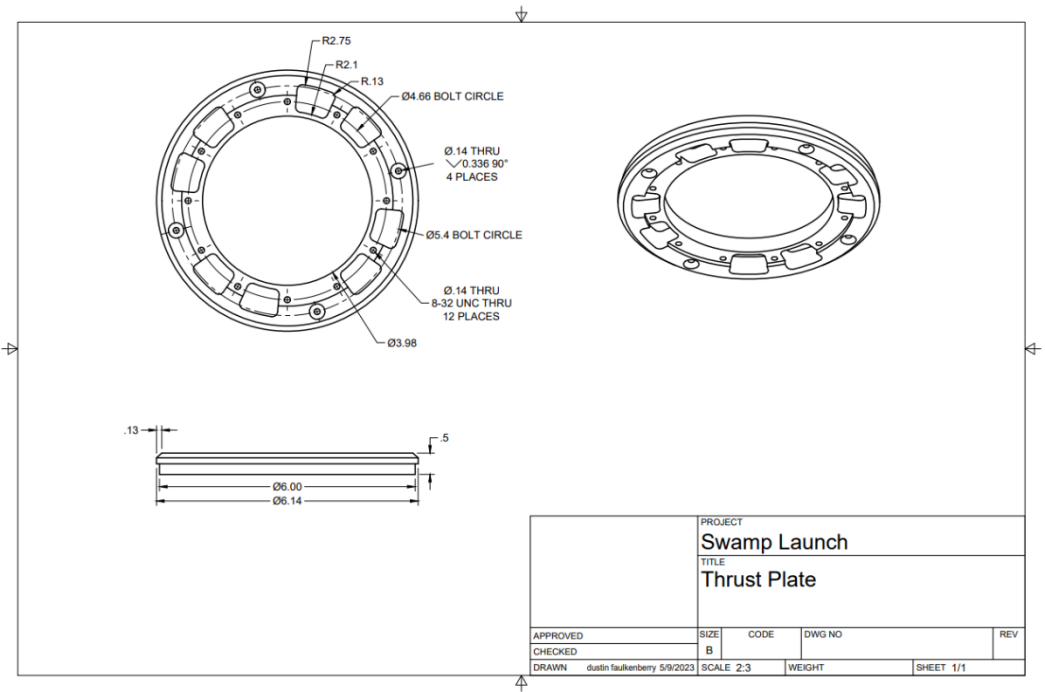
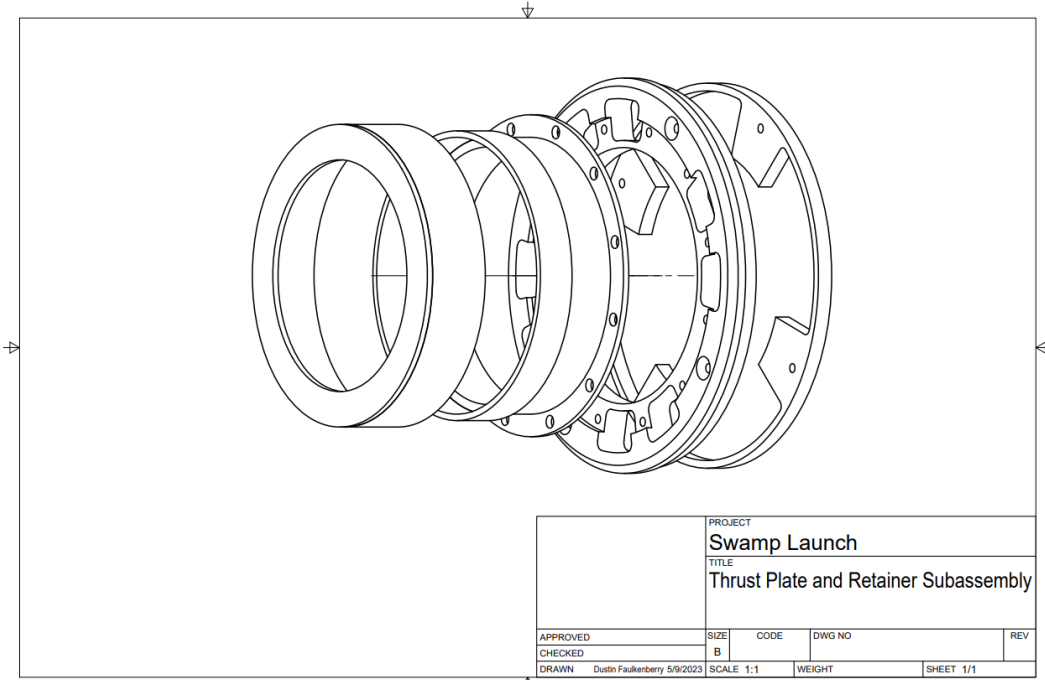


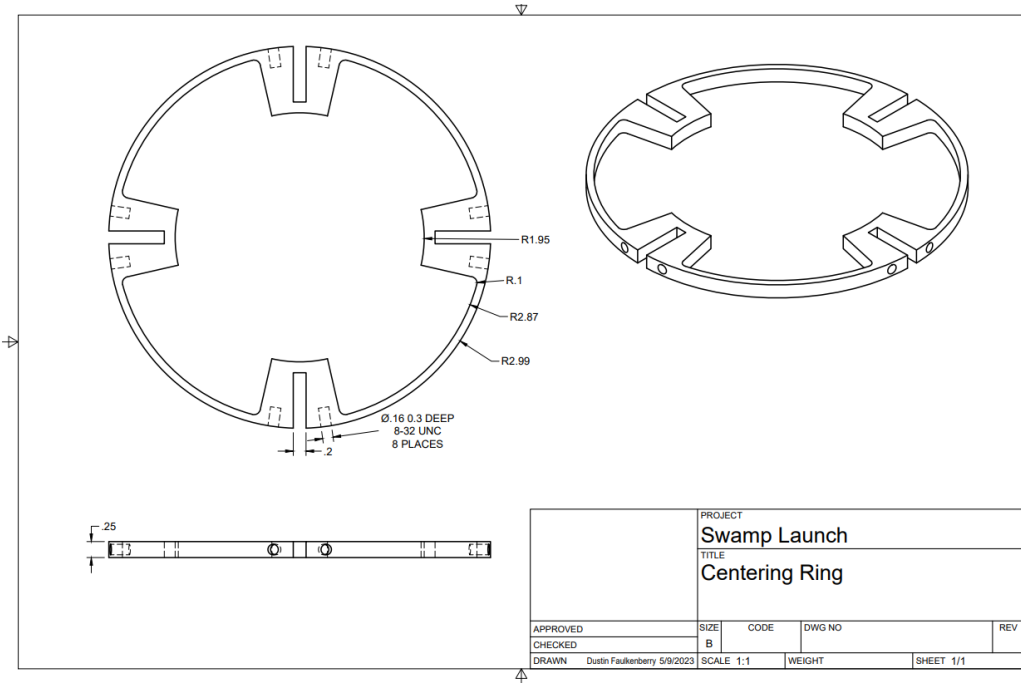
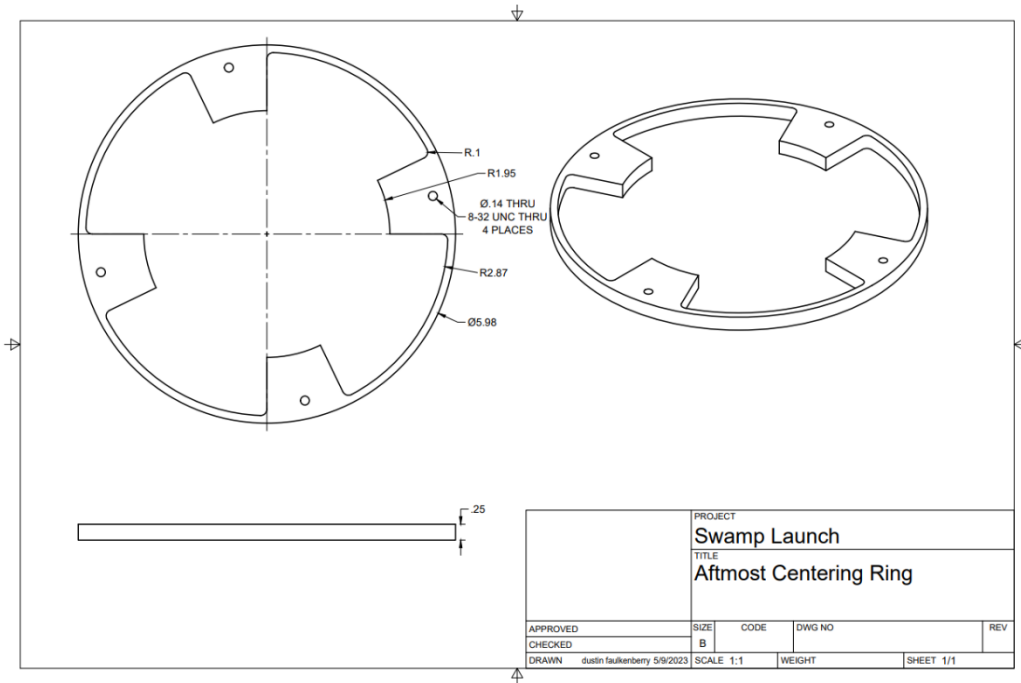
*Modular Aft Drawings*



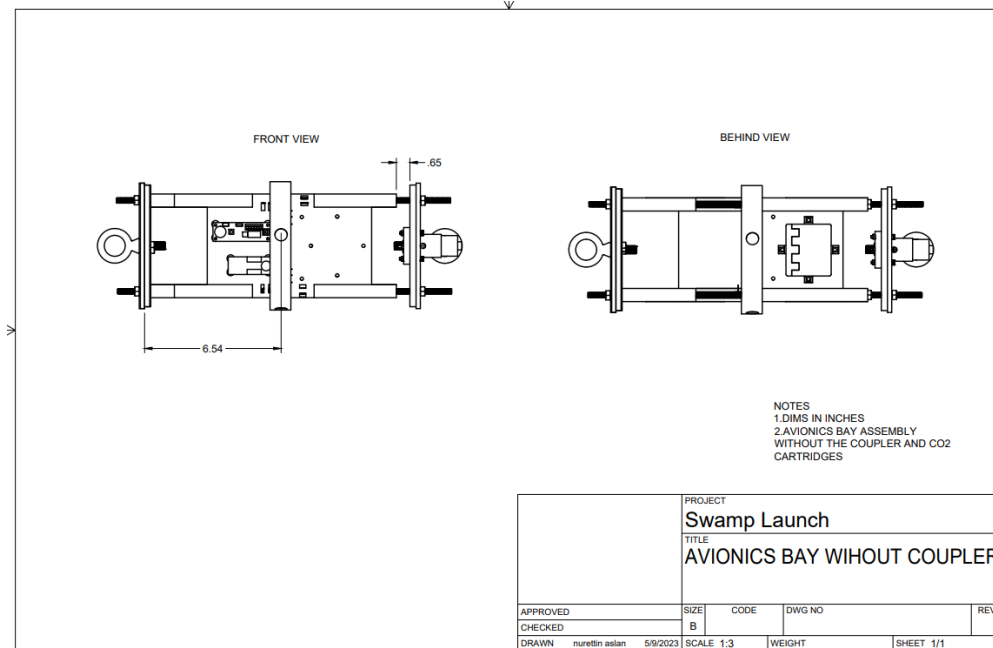
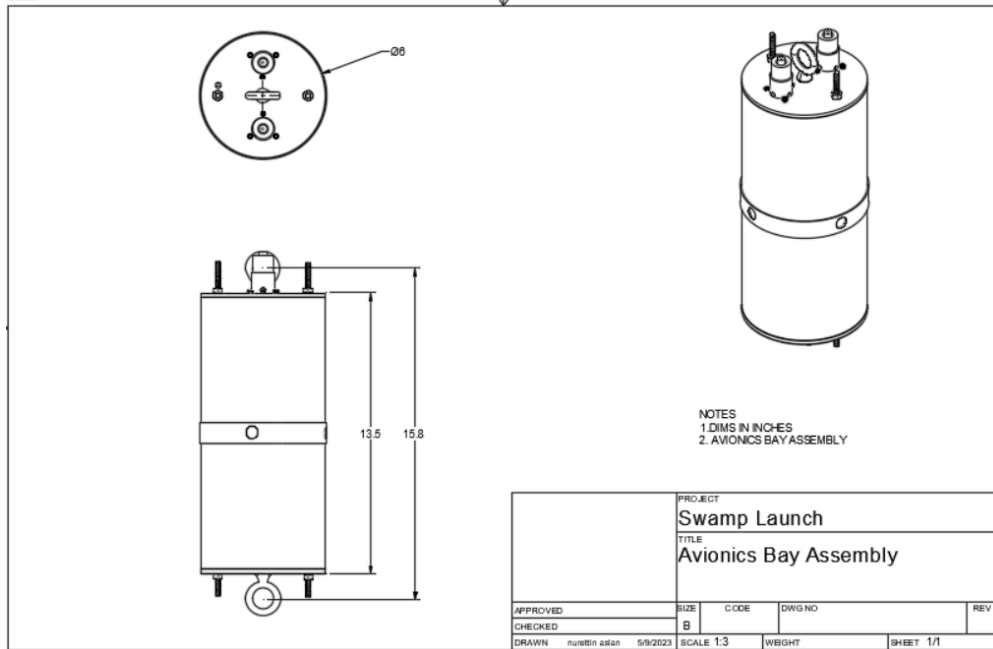


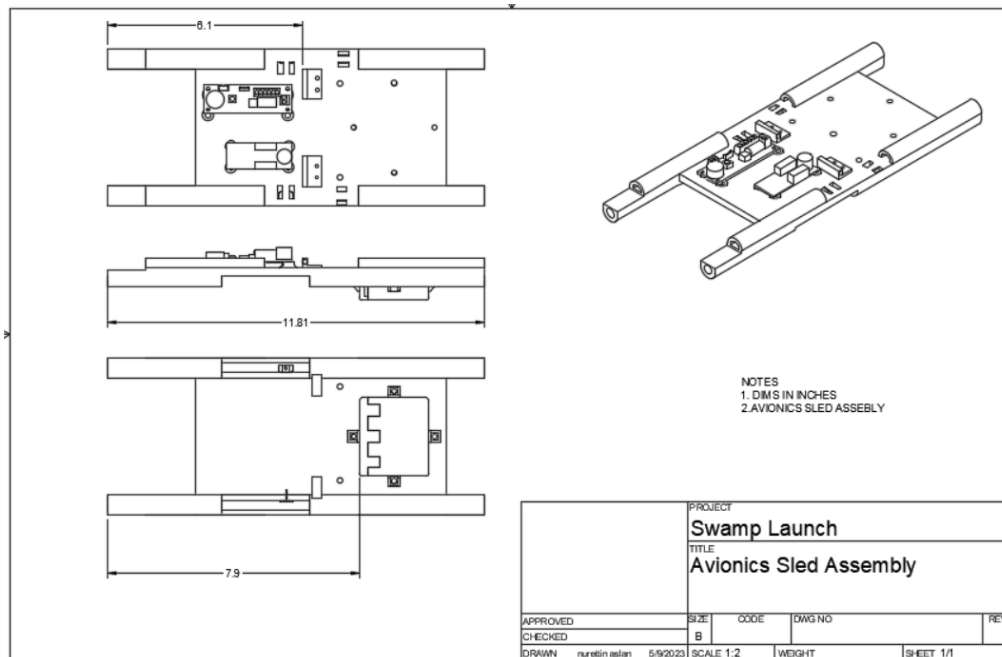
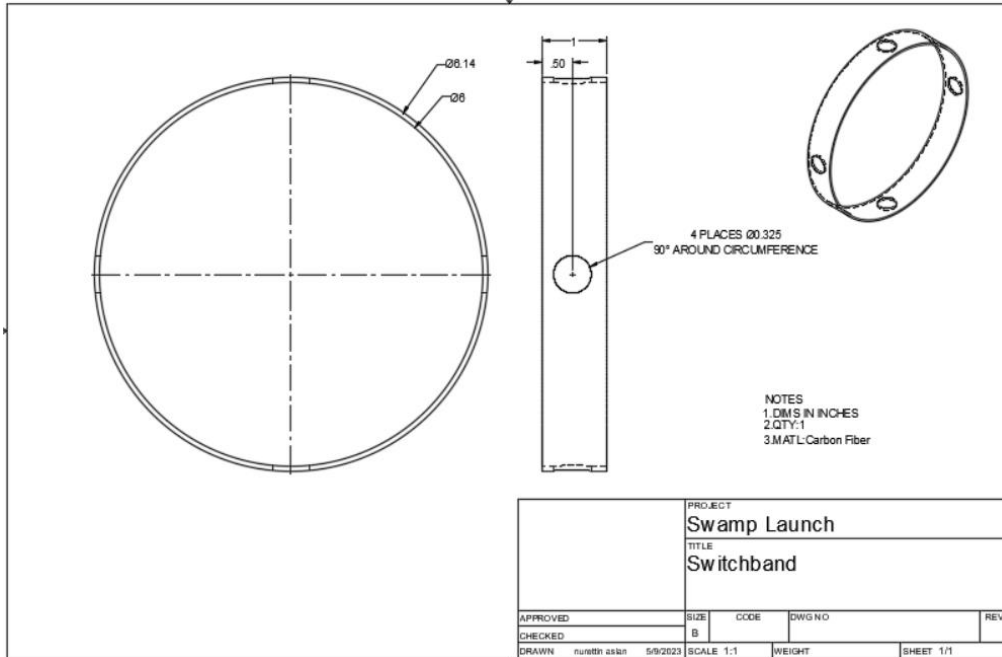


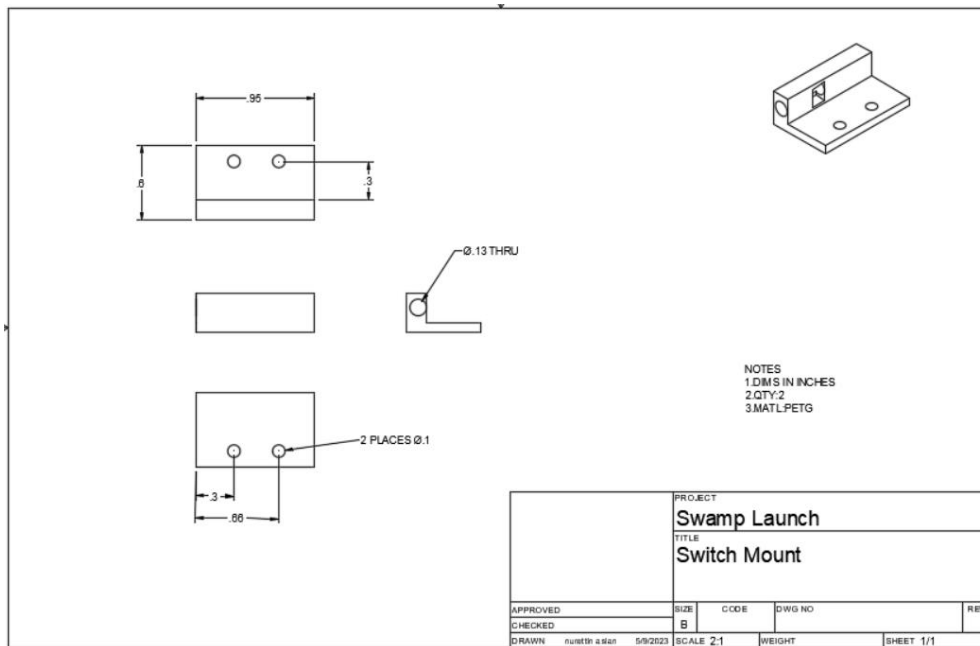
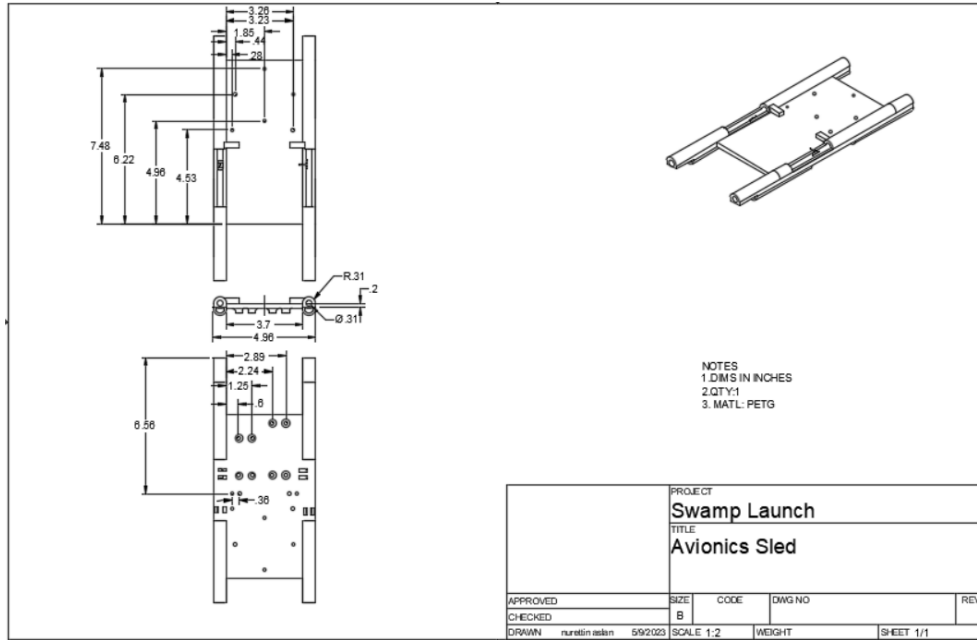




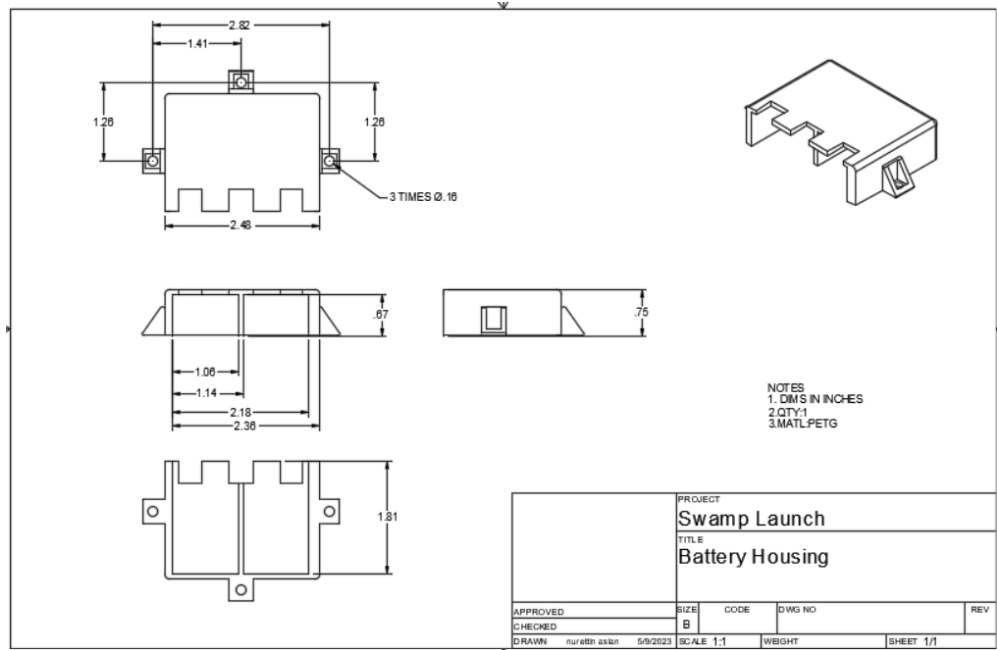
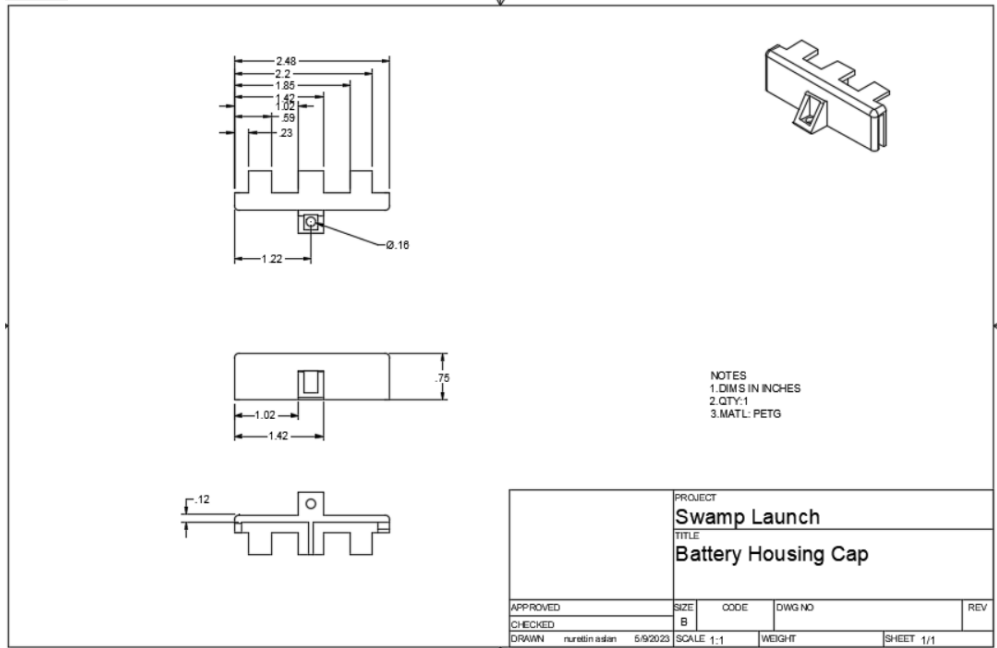
**B. Recovery**

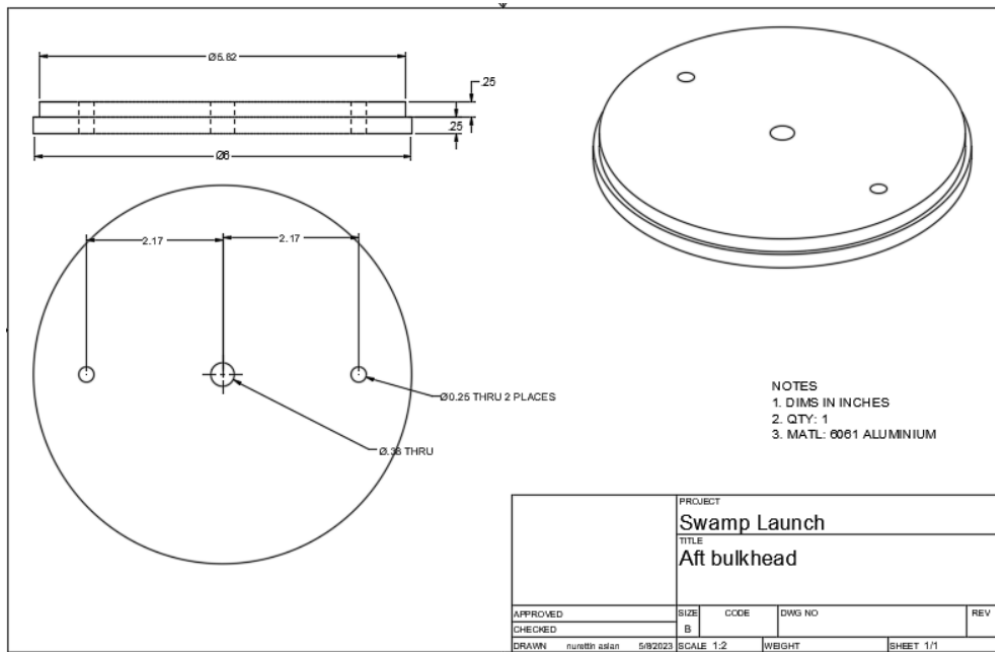
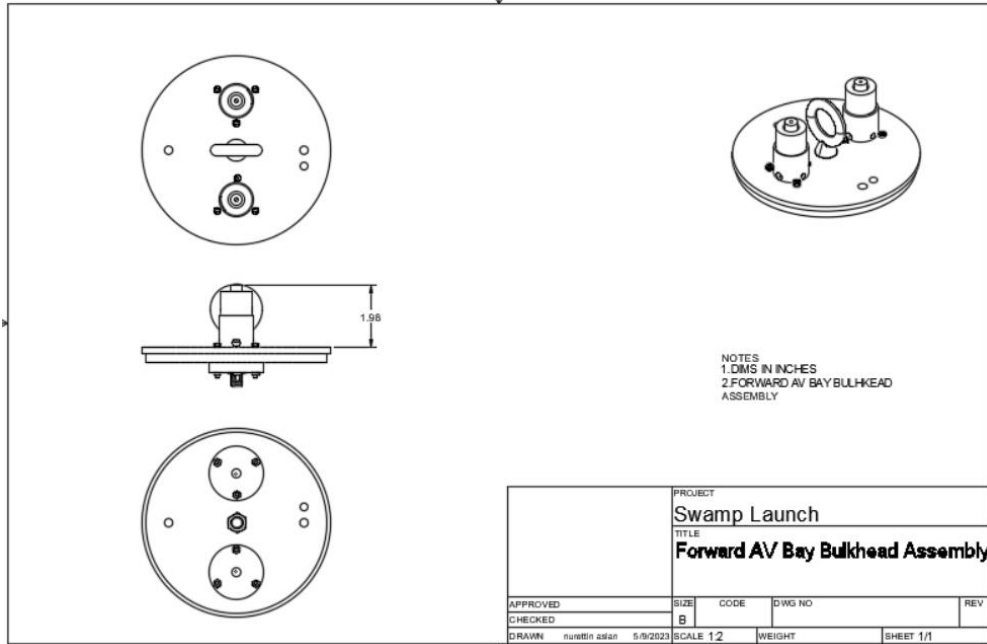


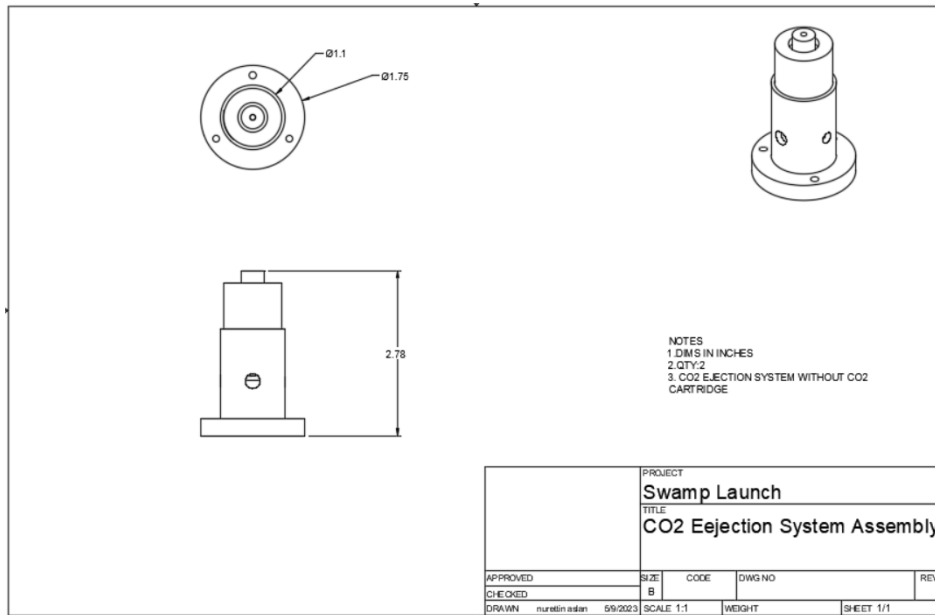
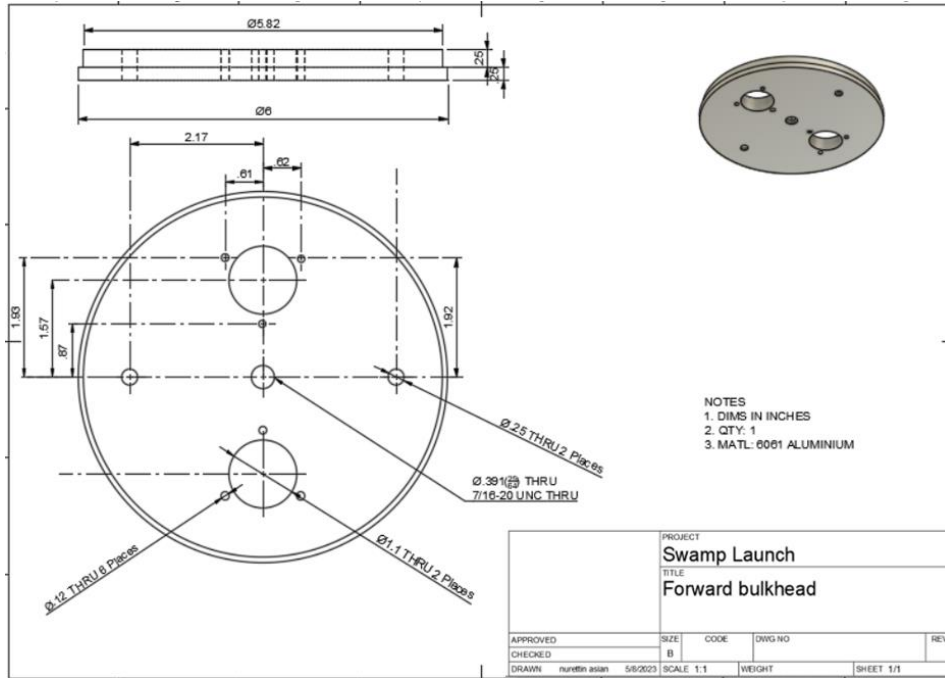


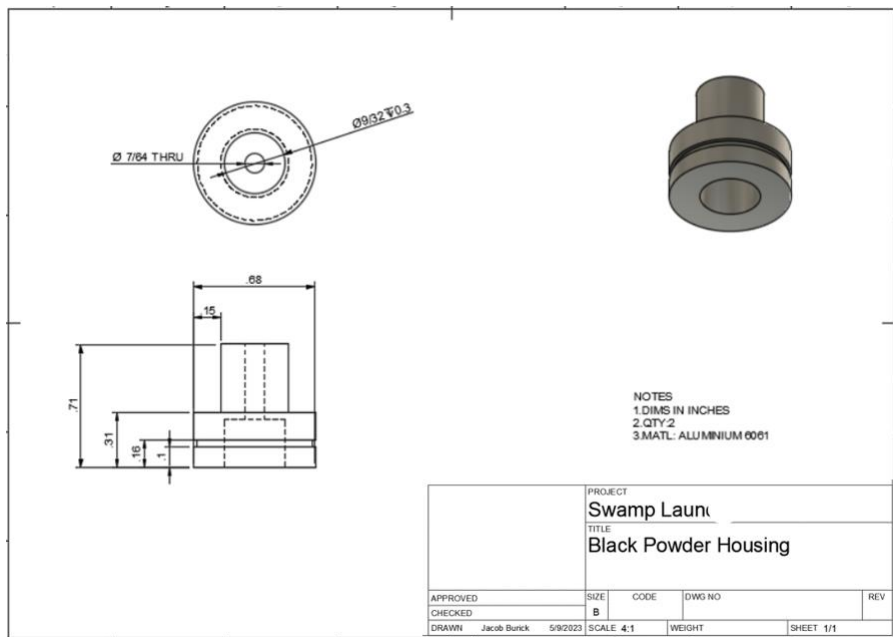
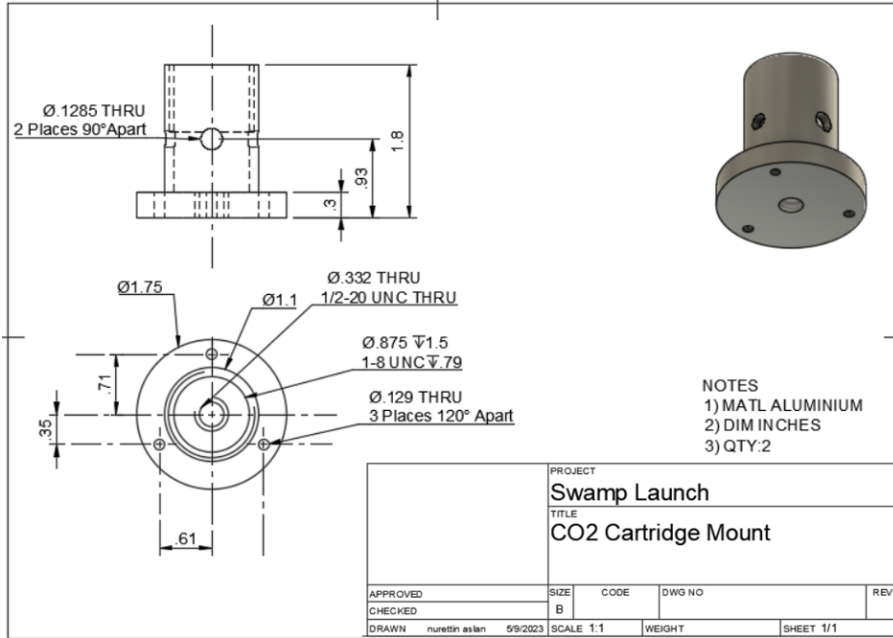


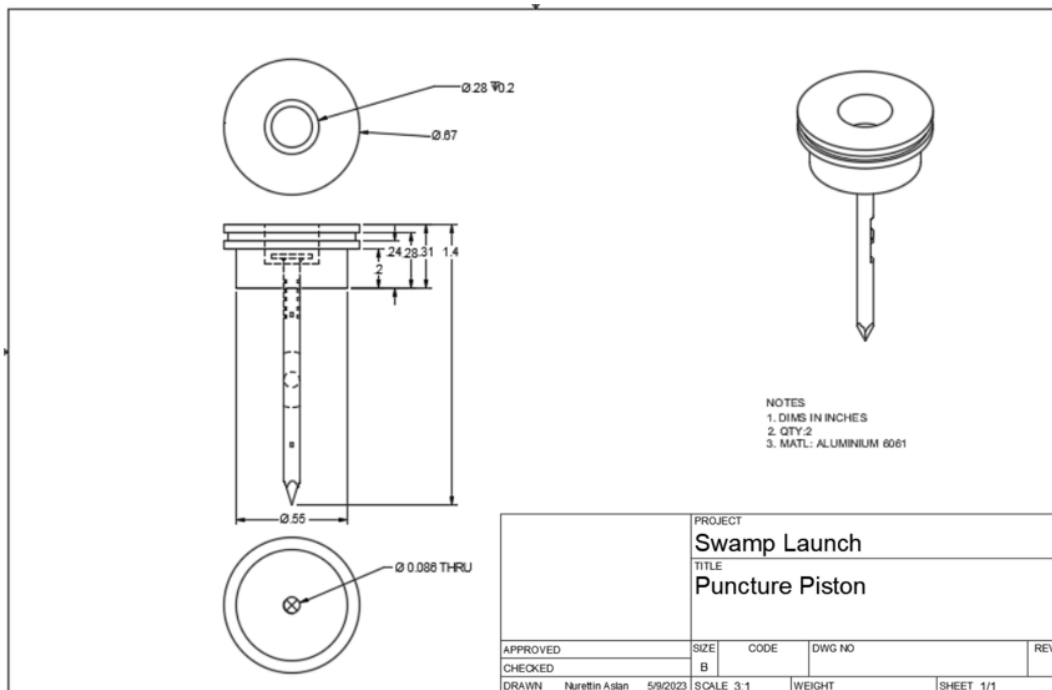
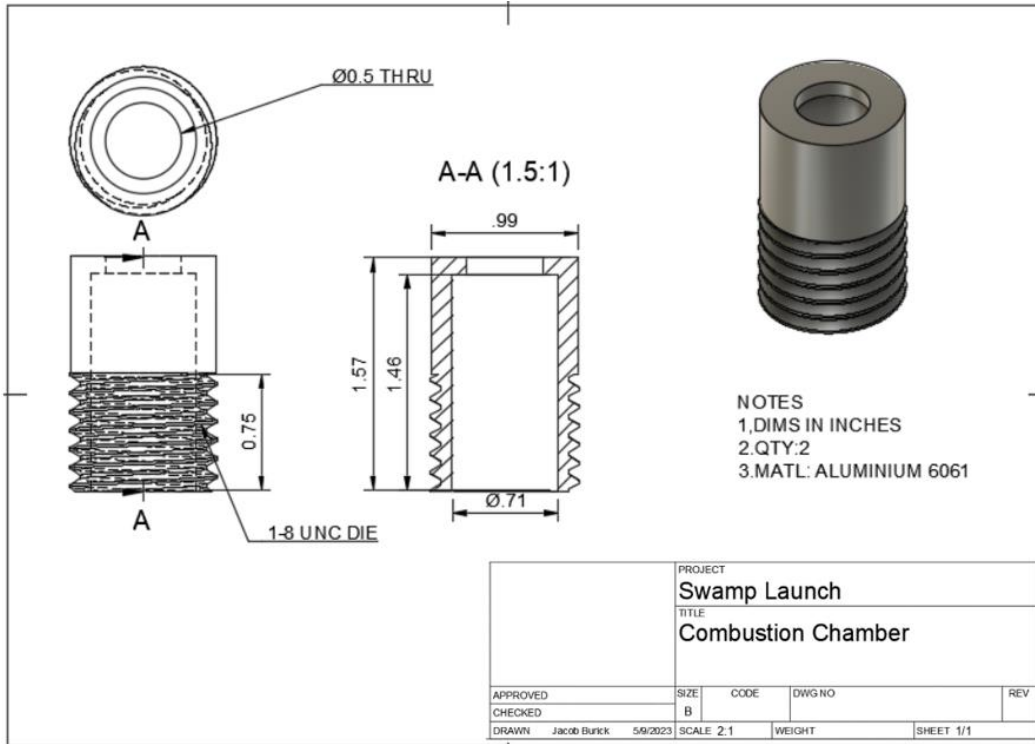




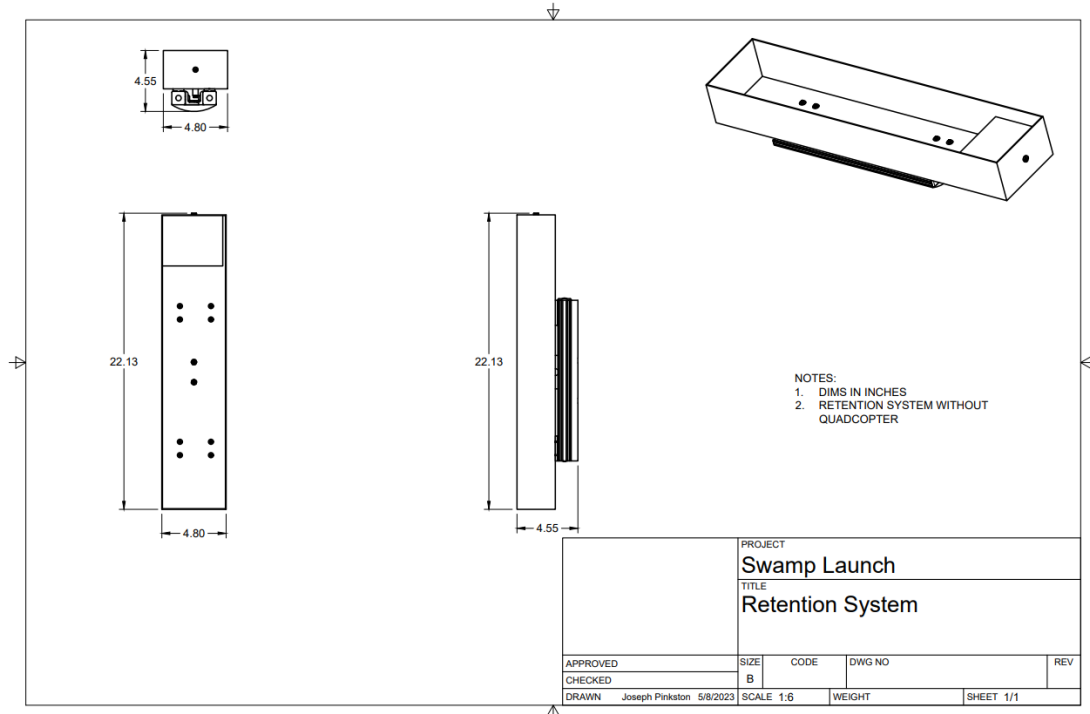
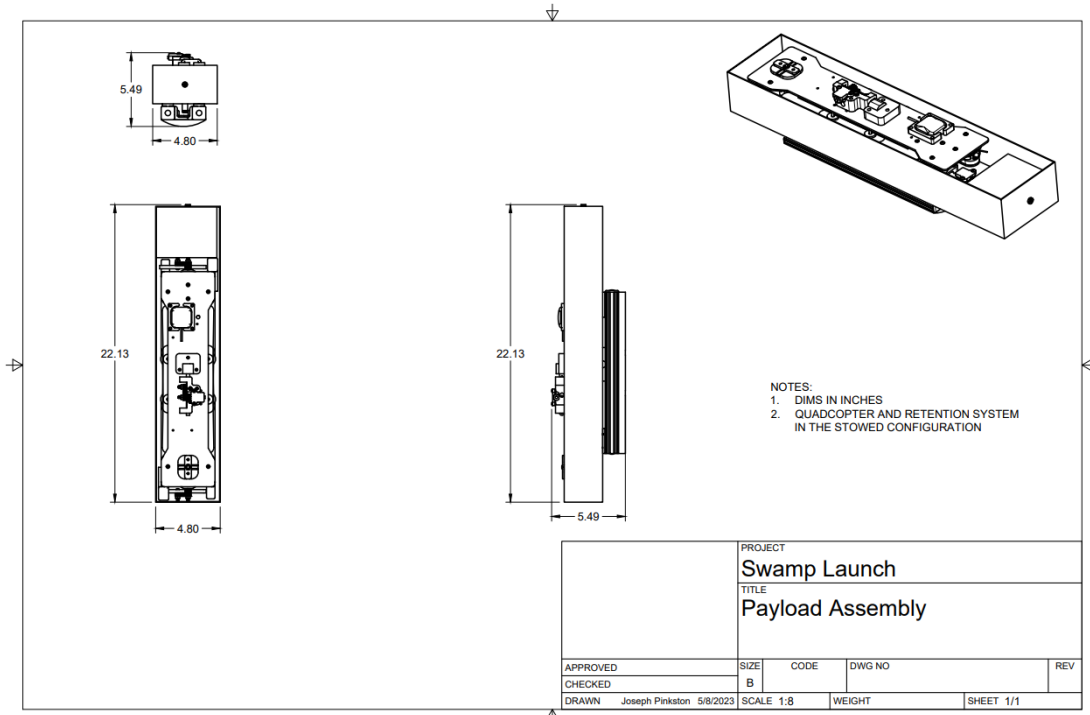


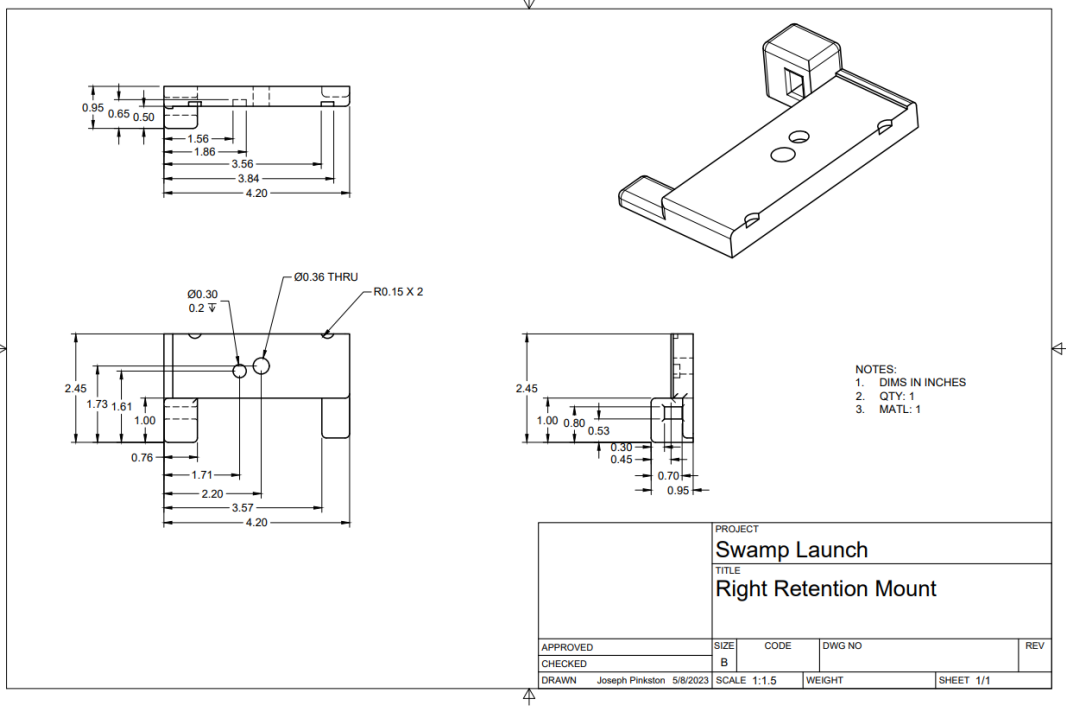
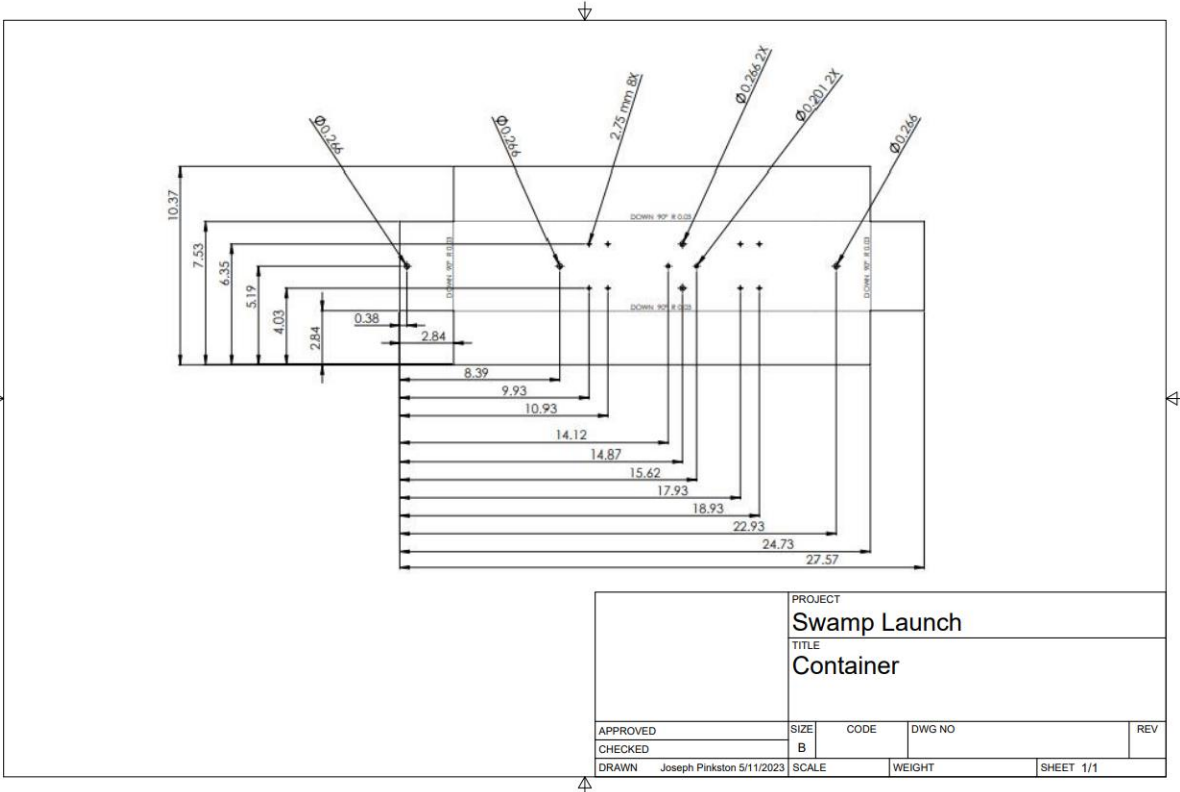


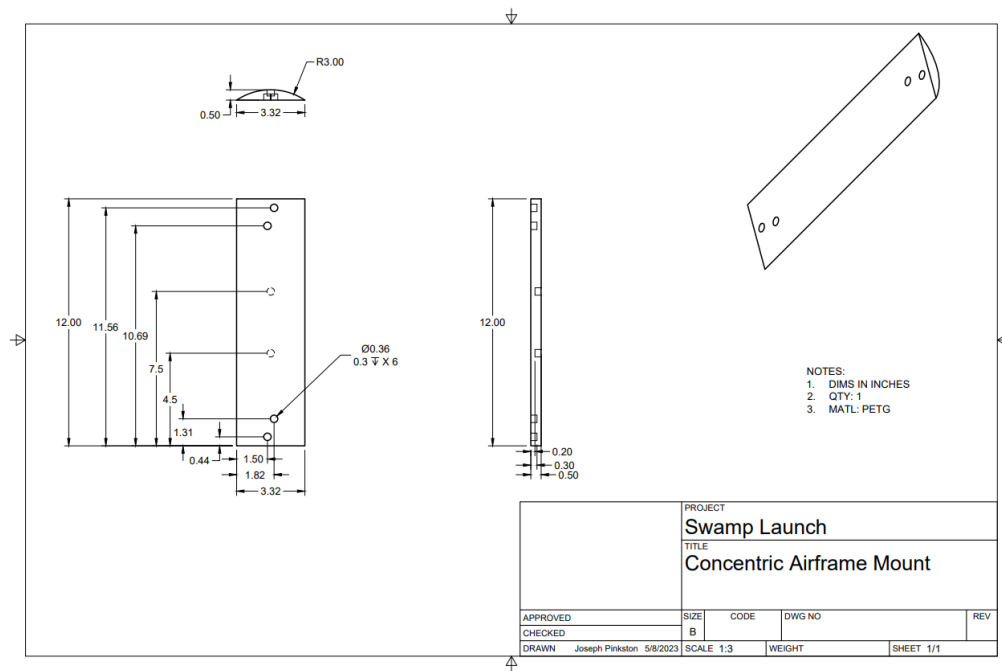
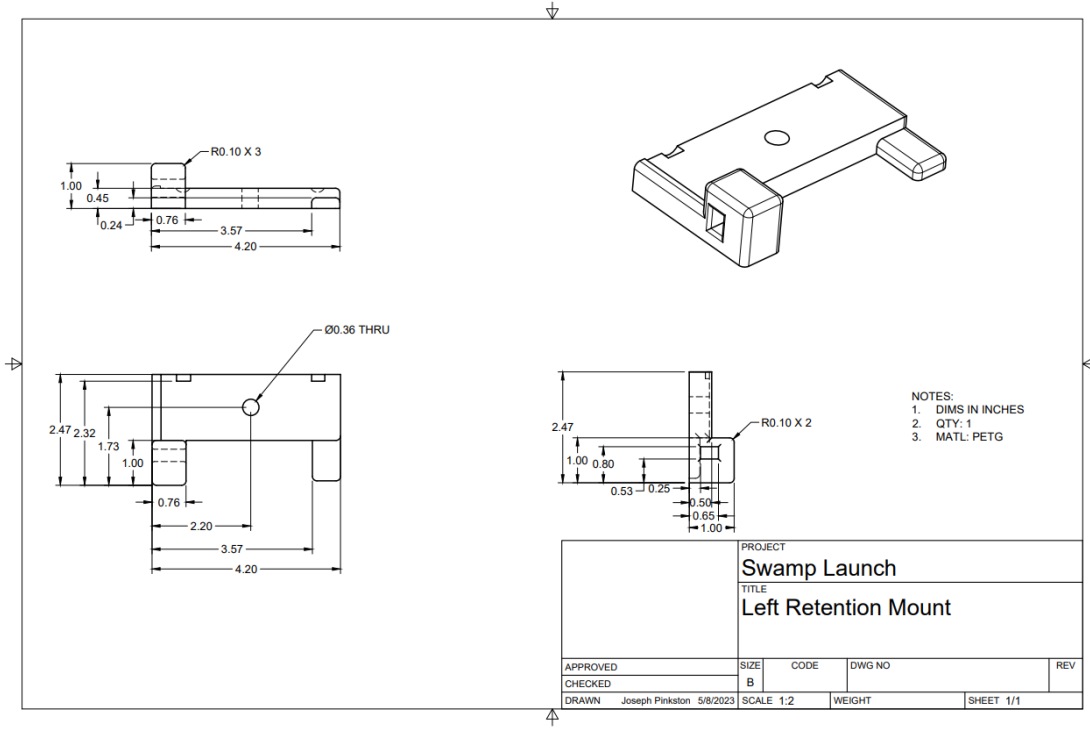




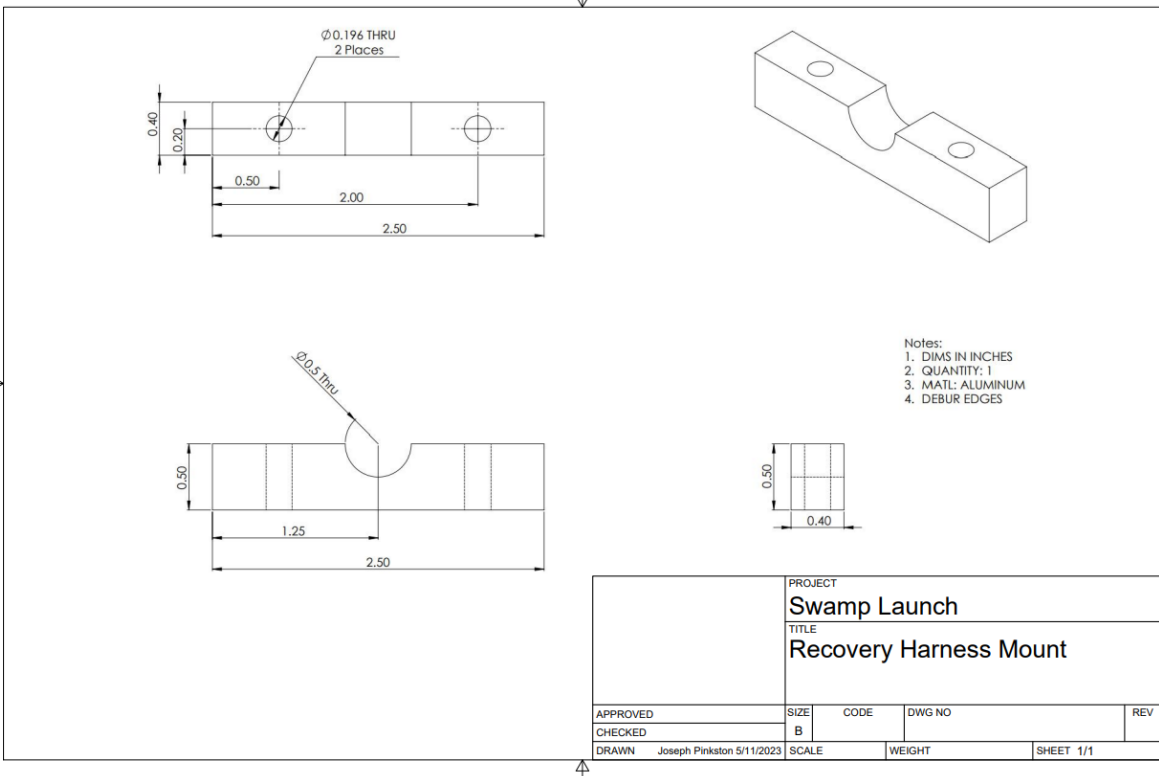
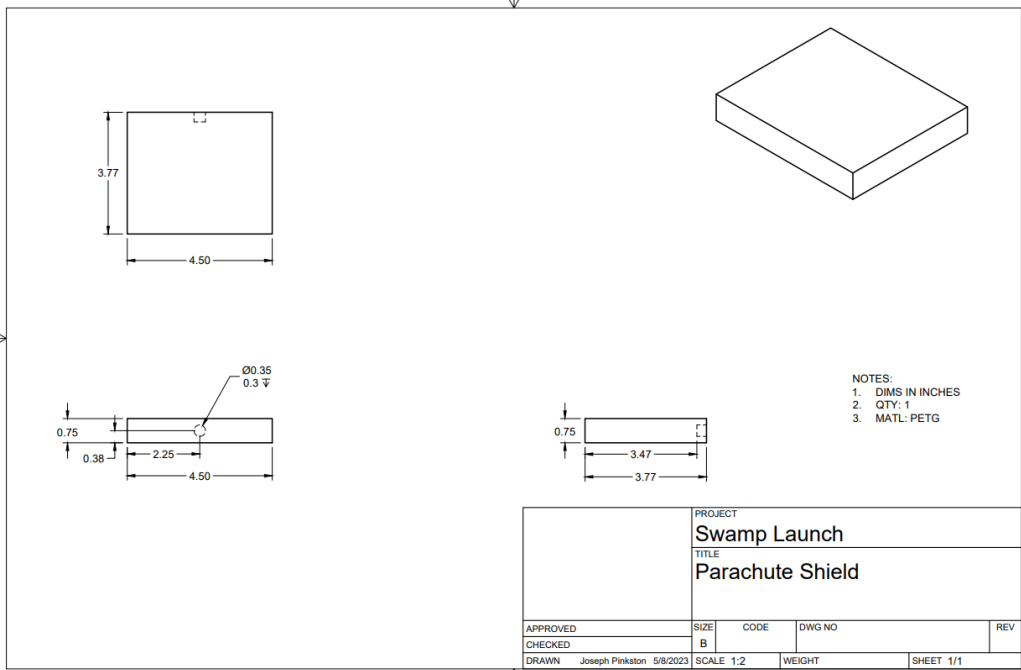
### C. Payloads

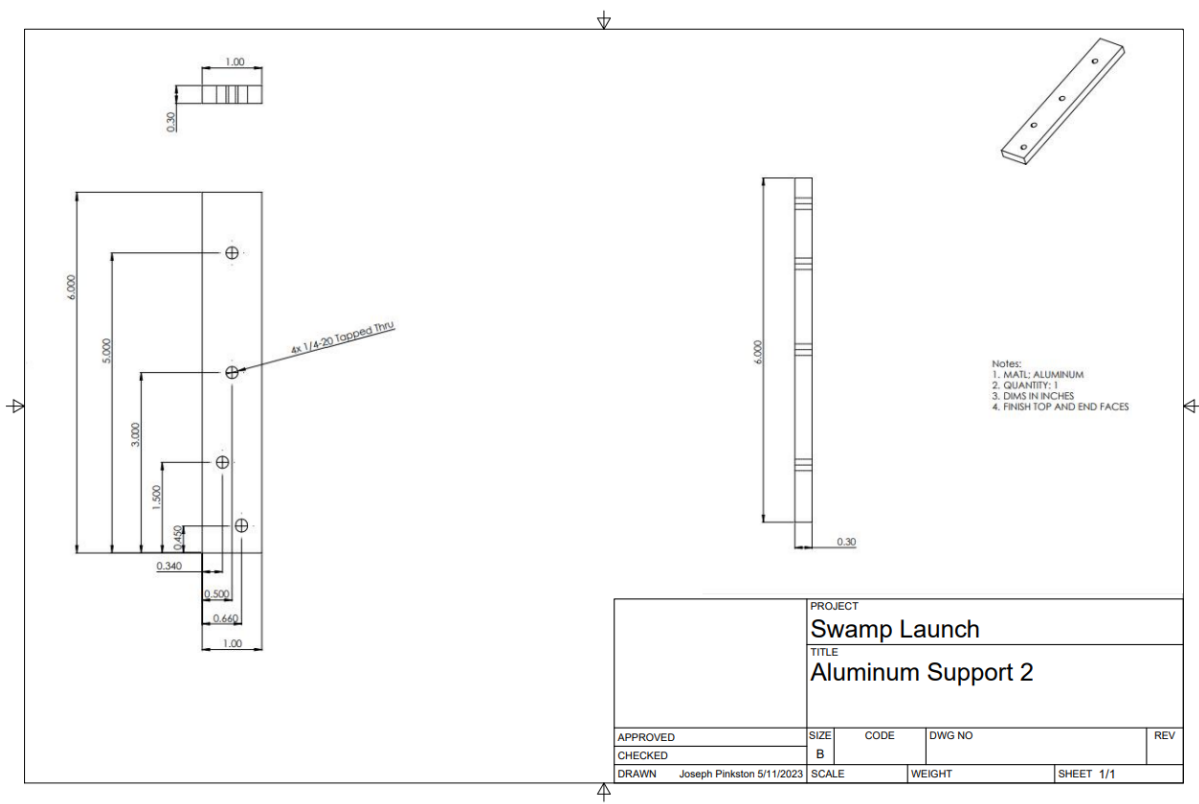
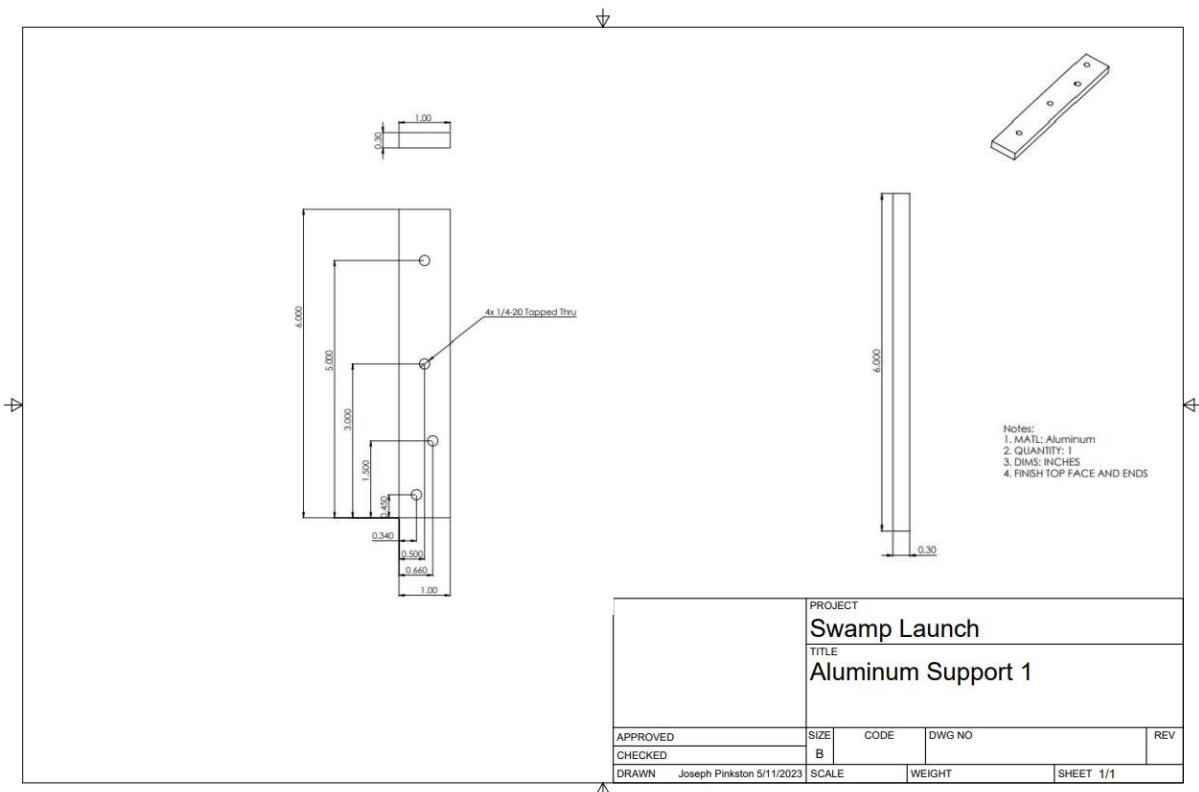


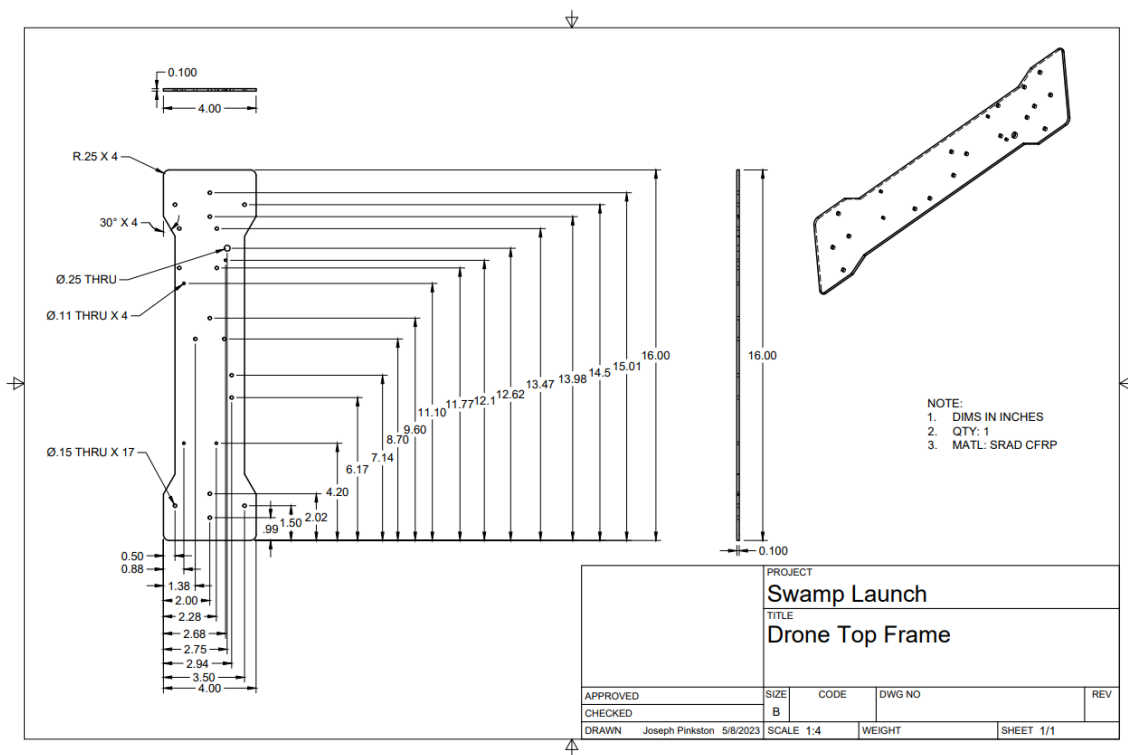
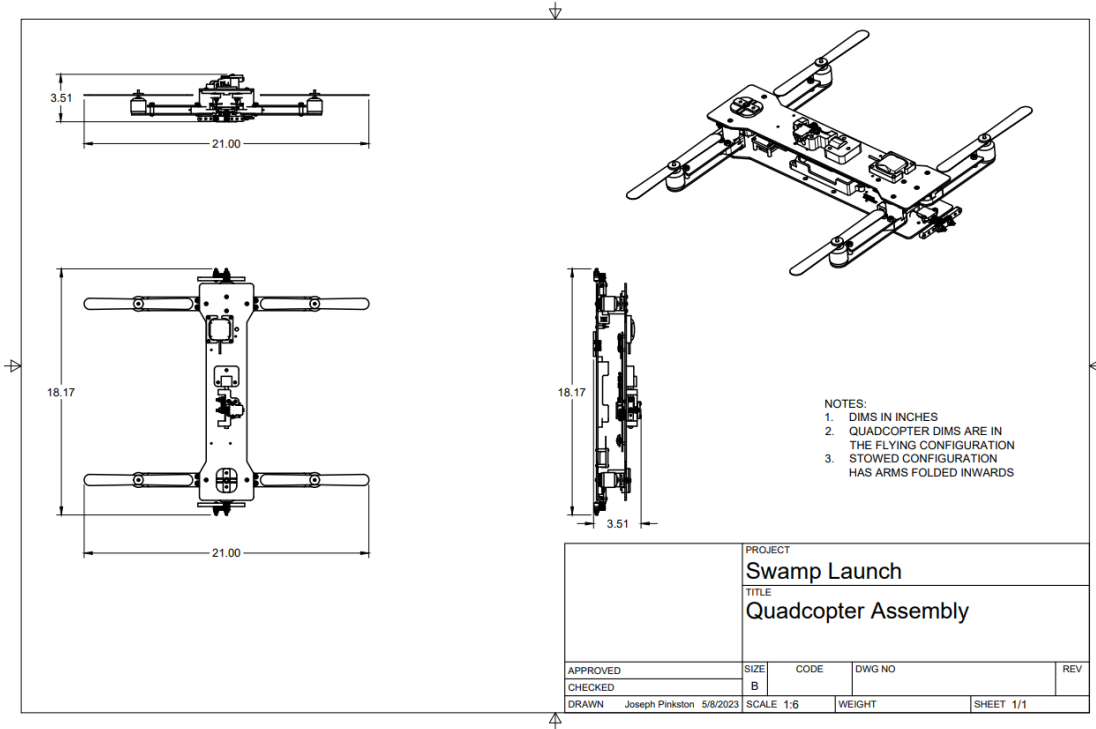


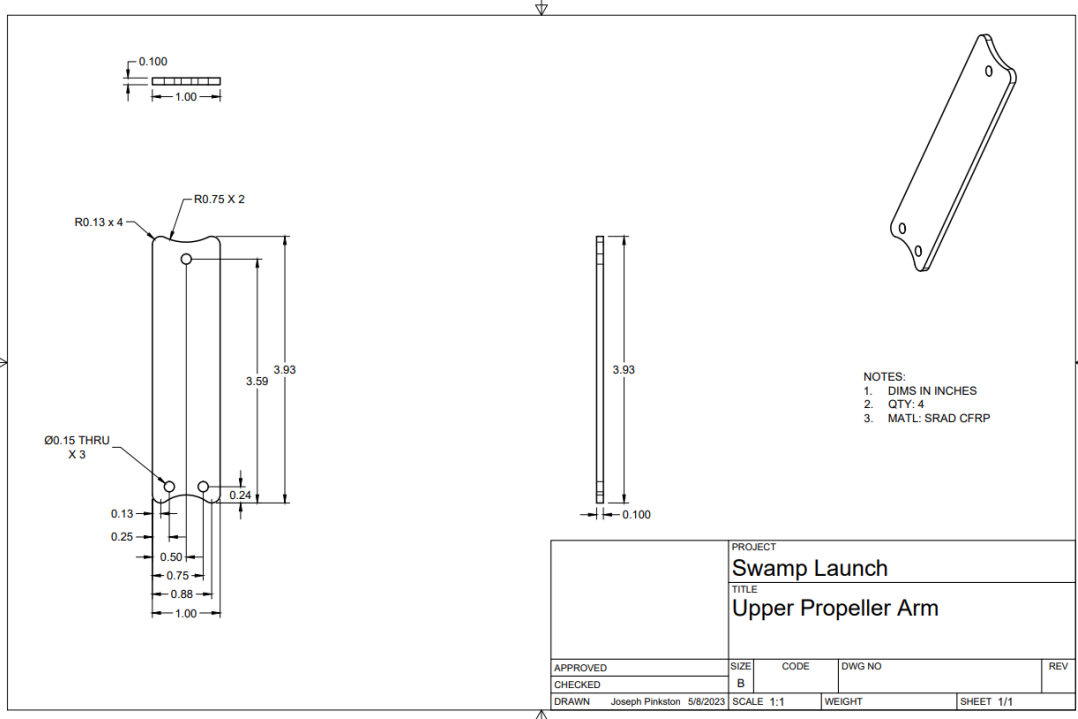
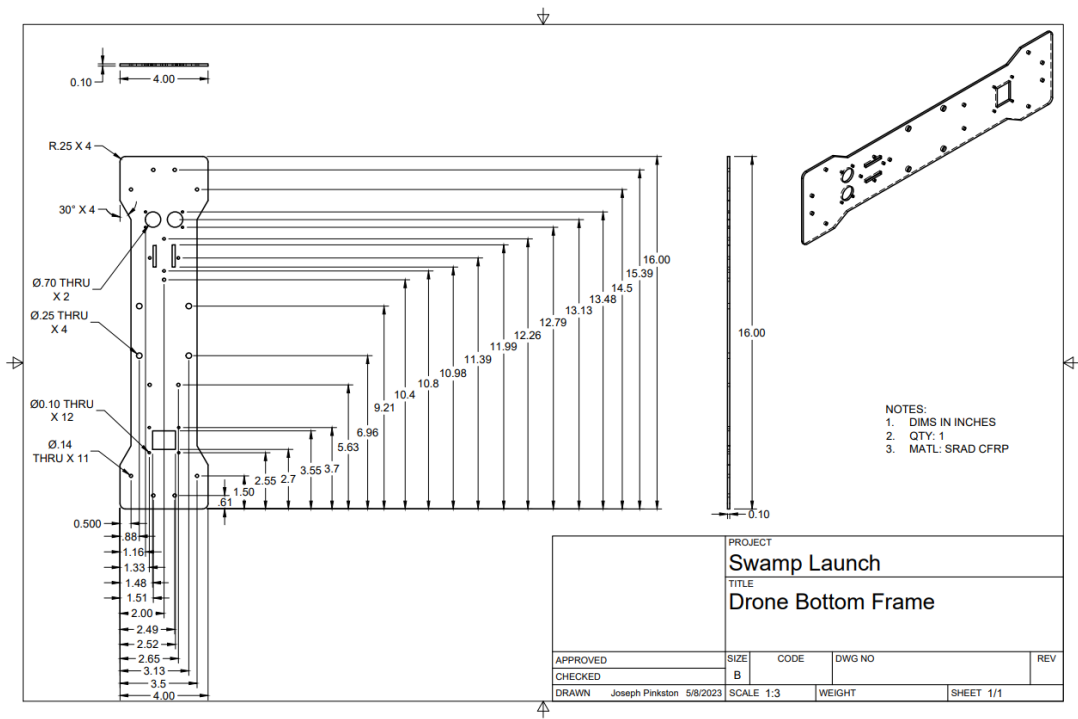


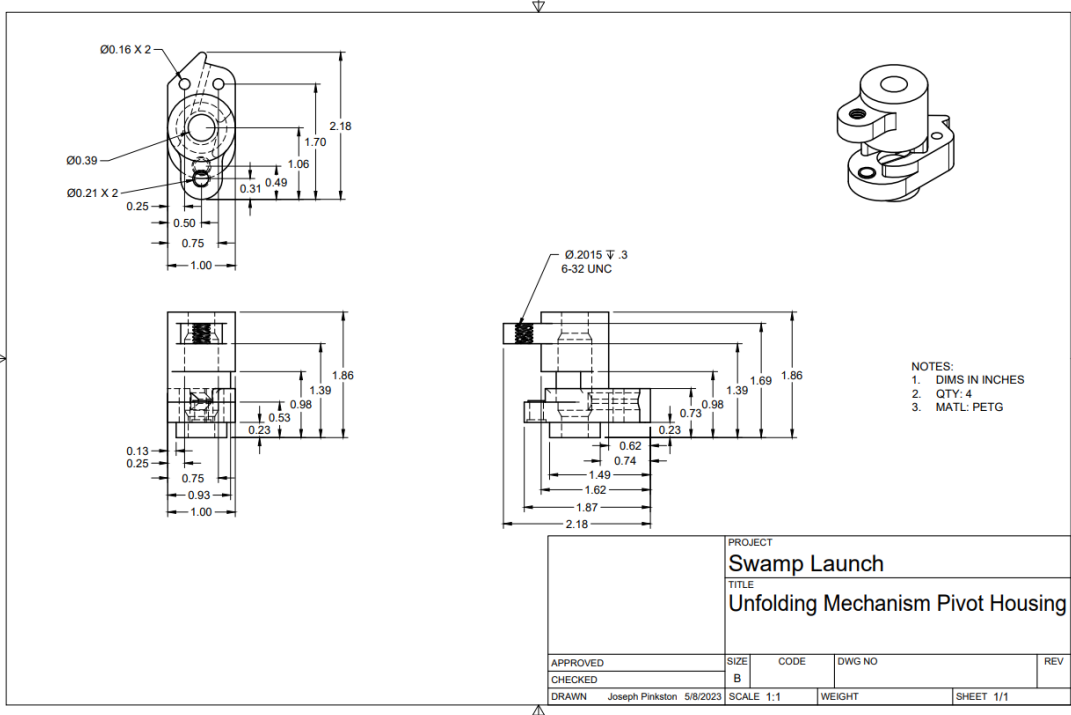
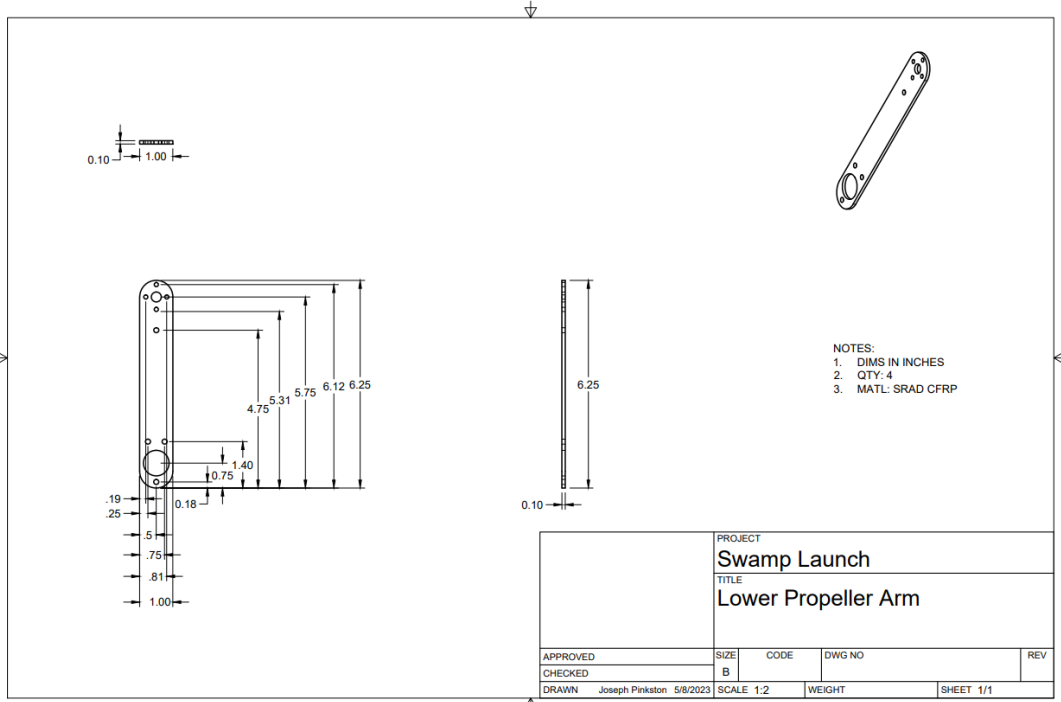


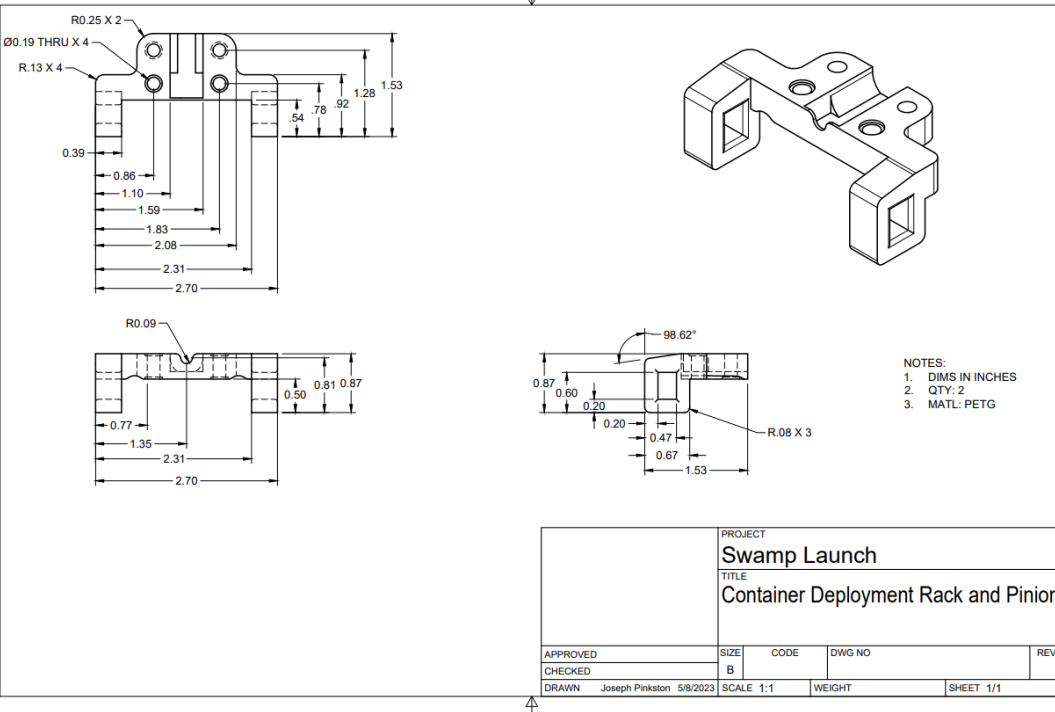
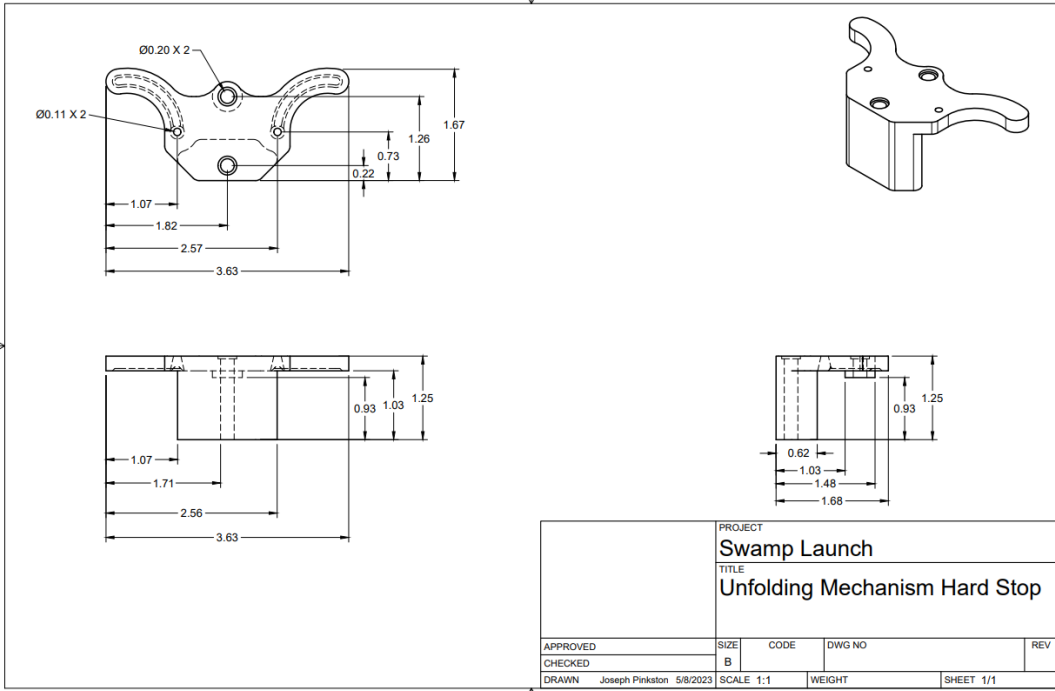


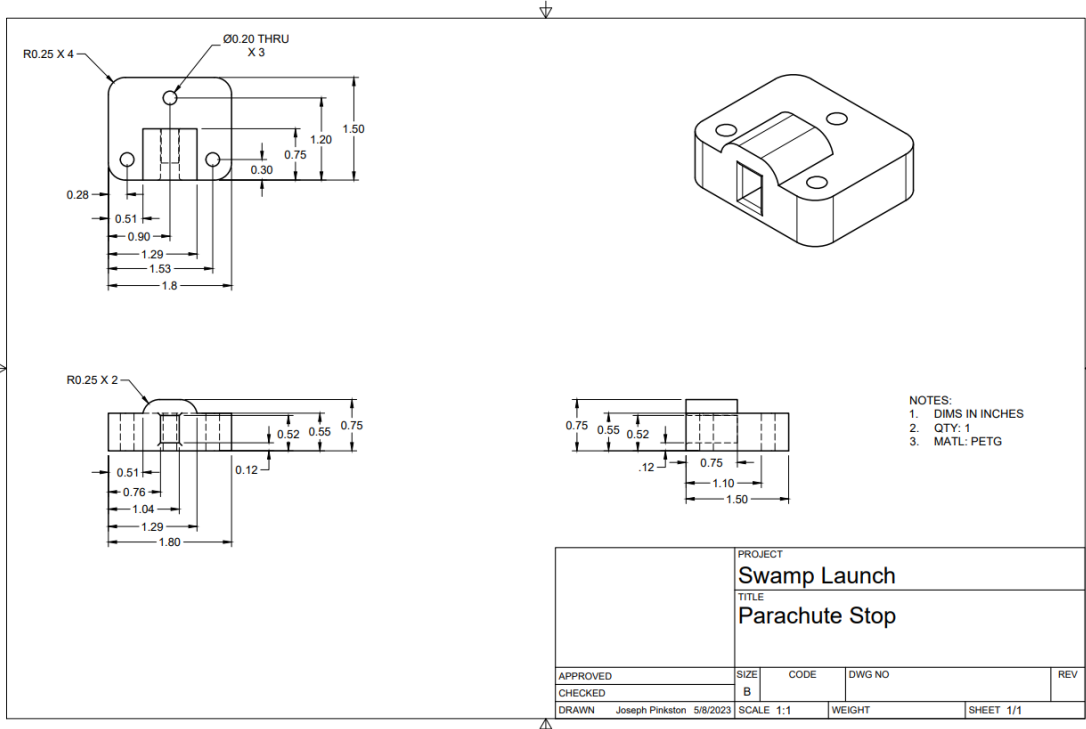
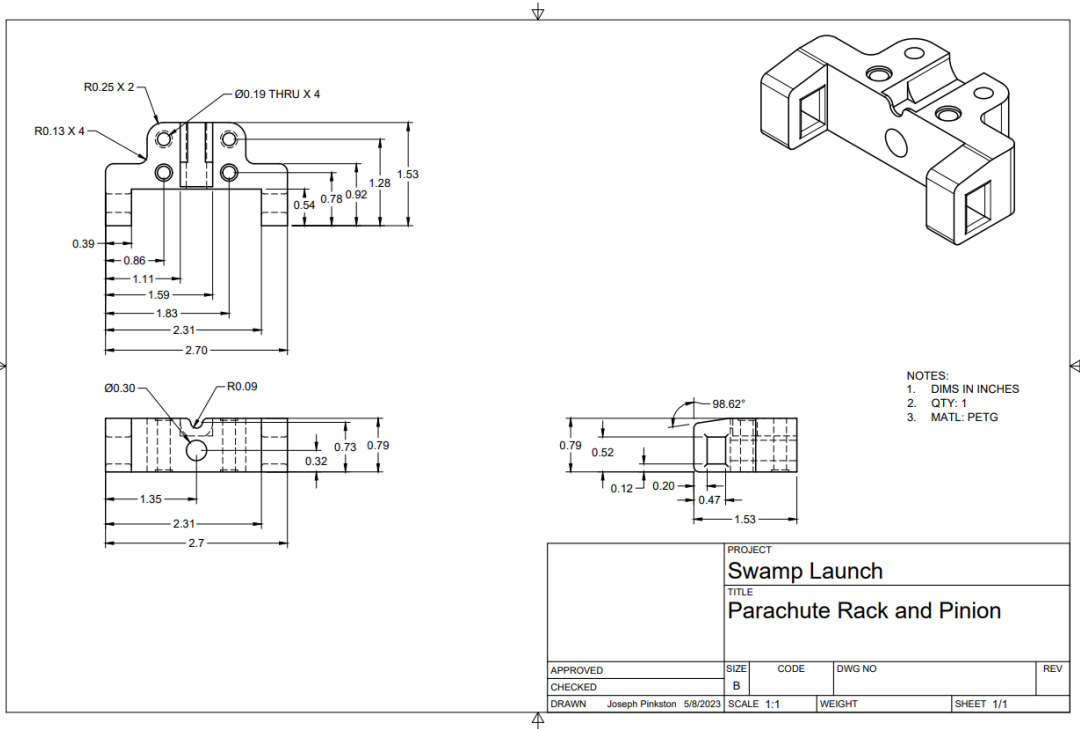


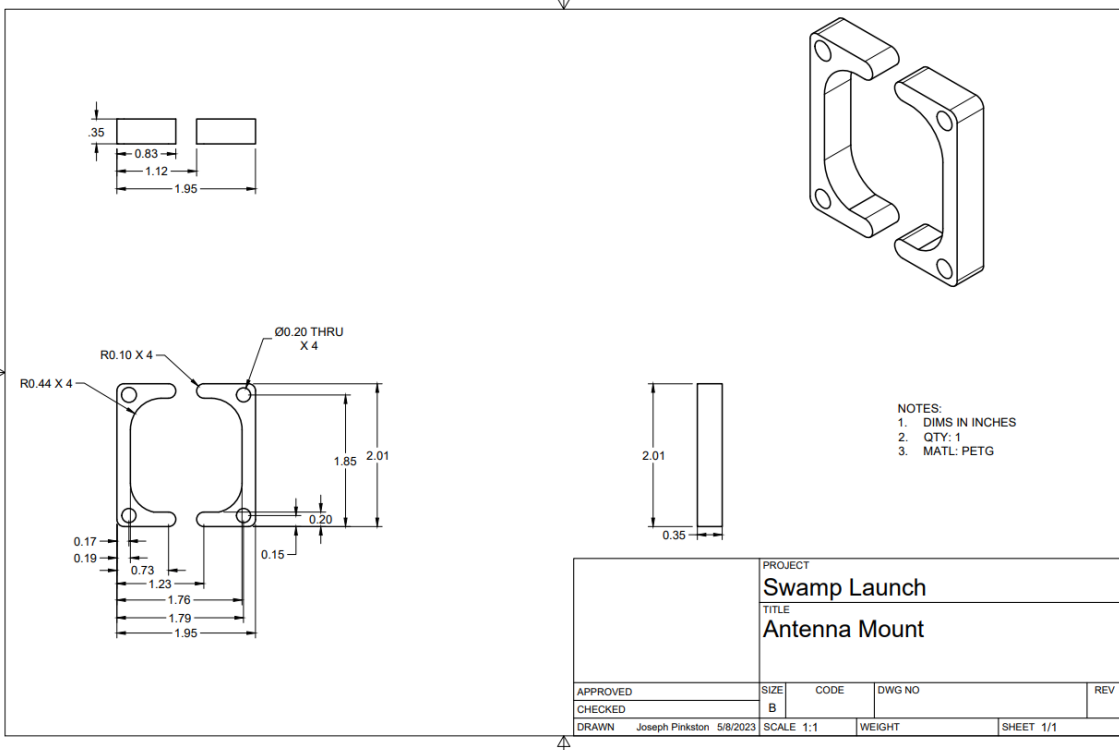
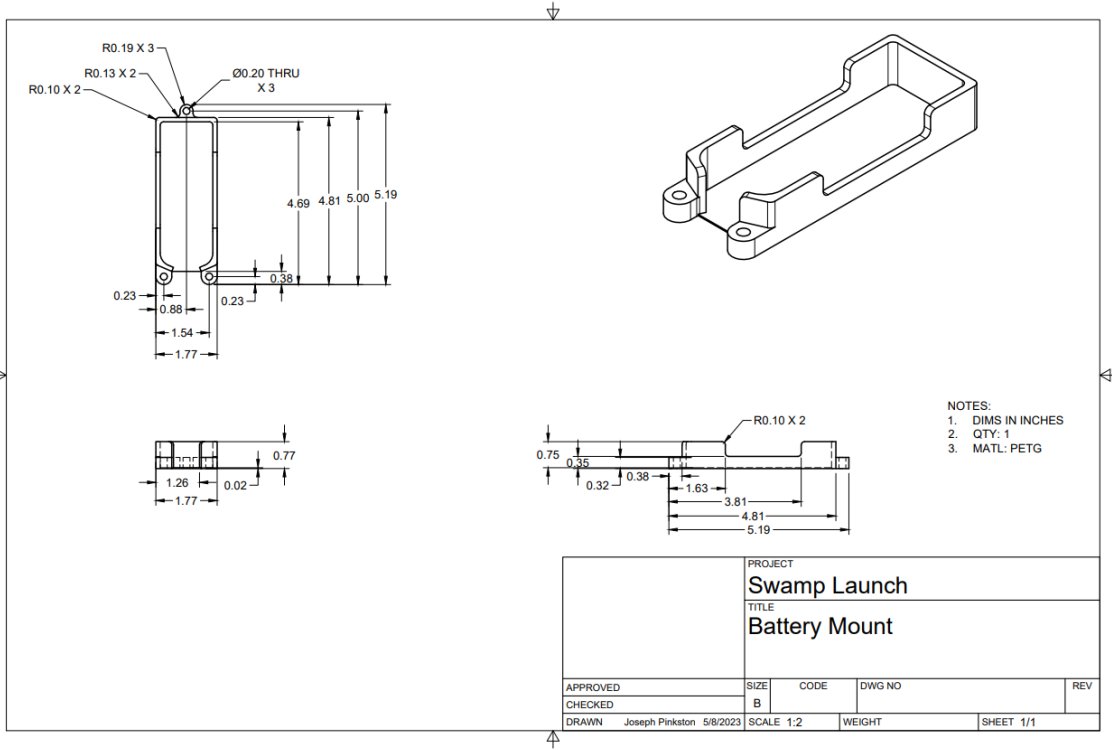














## Acknowledgments

The Swamp Launch IREC Team extends its thanks to our team advisor, Dr. Sean Niemi and our team mentor and flyer of record, Jimmy Yawn for their continuous support and guidance. The team would also like to thank Dr. Peter Ifju for allowing access to laboratory space and donating materials, Dr. Mike Griffis for his advice on payload design, and Kirsten Bowers for her mentorship and encouragement. Additionally, Swamp Launch thanks the Department of Mechanical and Aerospace Engineering at the University of Florida for their support of the team, along with all of our external sponsors: Blue Origin, Aerojet Rocketdyne, Autodesk, and Hands-On Gainesville.

## References

- [1] Z. Howard, "How To Calculate Fin Flutter Speed," Jul. 19, 2011
- [2] The Dogbone Connection: Part II - AISC, [https://www.aisc.org/globalassets/modern-steel/archives/1996/08/1996v08\\_dogbone.pdf](https://www.aisc.org/globalassets/modern-steel/archives/1996/08/1996v08_dogbone.pdf) (accessed May 12, 2023).
- [3] Petg techsheet - Prusament, [https://prusament.com/media/2020/01/PETG\\_TechSheet\\_ITA.pdf](https://prusament.com/media/2020/01/PETG_TechSheet_ITA.pdf) (accessed May 12, 2023).
- [4] R. G. Budynas and J. K. Nisbett, "Screws, Fasteners, and the Design of Nonpermanent Joints," in *Shigley's Mechanical Engineering Design*, New York, NY: McGraw-Hill Education, 2020
- [5] MATLAB, *Drone Simulation and Control, Part 1: Setting Up the Control Problem*. (2019). [Streaming Video]. Available: <https://youtu.be/hGcGPUqB67Q>
- [6] American Elements, "Safety Data Sheet: Carbon Fiber, CAS #: 7440-44-0". <https://www.americanelements.com/printpdf/carbon-fiber-7440-440-/sds>.
- [7] American Welding Society, "Cylinders, Safe Storage, Handling, and Use: Fact Sheet No. 30 – 04/14". [https://app.aws.org/technical/facts/FACT-30\\_2014.pdf](https://app.aws.org/technical/facts/FACT-30_2014.pdf)
- [8] Soller Composites, "Safety Data Sheet: 820 Resin/Bisphenol-A Epoxy Resin Blend". <https://www.sollercomposites.com/MSDS/820%20Resin.pdf>